TECHNICAL REPORT STANDARD TITLE PAGE

1. Report No. TX - 01 1780-5	**2. Government Accession No.**	**3. Recipient's Catalog No.**
4. Title and Subtitle Validation of Software Developed for Determining Design Modulus from Seismic Testing		**5. Report Date** November 2004
		6. Performing Organization Code
7. Authors I. Abdallah, D. Yuan and S. Nazarian		**8. Performing Organization Report No.** Research Report 1780-5
9. Performing Organization Name and Address Center for Transportation Infrastructure Systems The University of Texas at El Paso, El Paso, Texas 79968-0516		**10. Work Unit No.**
		11. Contract or Grant No. Project No. 0-1780
12. Sponsoring Agency Name and Address Texas Department of Transportation Office of Research and Technology Implementation P.O. Box 5080, Austin, Texas 78763-5080		**13. Type of Report and Period Covered** Final Report
		14. Sponsoring Agency Code

15. Supplementary Notes
Research Performed in Cooperation with TxDOT
Research Study Title: Design Modulus Values Using Seismic Data Collection

16. Abstract
The major outcome of this study is an algorithm for predicting the design modulus of each layer given the seismic modulus and the nonlinear parameters of each pavement layer. The algorithm developed has been incorporated in a software package called SMART (Seismic Modulus Analysis and Reduction Tool). In this report the results from the validation program carried out are addressed. More than a dozen sites were visited. The results from this validation indicate that the program is capable of providing reasonable values to design engineers. The procedure is particularly attractive in the situations where pavement layers are thin, depth to bedrock is shallow or when the water table is close to the pavement surface.

17. Key Words Falling Weight Deflectometer, Seismic Pavement Analyzer, Seismic Nondestructive Testing	**18. Distribution Statement** No restrictions. This document is available to the public through the National Technical Information Service, 5285 Port Royal Road, Springfield, Virginia 22161		
19. Security Classified (of this report) Unclassified	**20. Security Classified (of this page)** Unclassified	**21. No. of Pages** 142	**22. Price**

Form DOT F 1700.7 (8-69)

VALIDATION OF SOFTWARE DEVELOPED FOR DETERMINING DESIGN MODULUS FROM SEISMIC TESTING

by

Imad Abdallah, MSCE
Deren Yuan, PhD
and
Soheil Nazarian, PhD, PE

Research Project 0-1780

Conducted for

Texas Department of Transportation

Research Report 1780-5

November 2004

The Center for Transportation Infrastructure Systems
The University of Texas at El Paso
El Paso, TX 79968-0516

The contents of this report reflect the view of the authors, who are responsible for the facts and the accuracy of the data presented herein. The contents do not necessarily reflect the official views or policies of the Texas Department of Transportation or the Federal Highway Administration. This report does not constitute a standard, specification, or regulation.

The material contained in this report is experimental in nature and is published for informational purposes only. Any discrepancies with official views or policies of the Texas Department of Transportation or the Federal Highway Administration should be discussed with the appropriate Austin Division prior to implementation of the procedures or results.

NOT INTENDED FOR CONSTRUCTION, BIDDING, OR PERMIT PURPOSES

Imad Abdallah, MSCE
Deren Yuan, PhD
Soheil Nazarian, PhD, PE (69263)

Acknowledgments

The authors would like to express their sincere appreciation to Mark McDaniel of the TxDOT Construction Division, Joe Thompson of the Dallas District and John Rantz of Lubbock District for their ever-present support.

We are also grateful to a large number of TxDOT district personnel who assisted us with planning and site selection, field testing, installing trenches and retrieving materials.

A special salute to those maintenance crews who repaired the deep holes we left in their pavements!!

We would also like to thank the staff of the Engineering Research and Development Center of the Army Corps of Engineers for providing us with sites in Vicksburg, MS.

Executive Summary

Nondestructive testing (NDT) methods are typically used to measure the variations in the modulus of different pavement layers. The critical strains necessary to estimate the remaining lives of a pavement system are then determined from the estimated moduli. The Falling Weight Deflectometer (FWD) and the Seismic Pavement Analyzer (SPA) are two of the NDT devices used for this purpose.

The Falling Weight Deflectometer applies an impulse load to the pavement and measures the surface deflection with seven sensors. Moduli of different pavement layers can then be backcalculated from these deflections. The shortcomings of this method are the uncertainties associated with the backcalculation procedure.

The Seismic Pavement Analyzer is based on generating and detecting stress waves in a layered system. The elastic moduli of different layers are obtained from an inversion process. The SPA imparts small external loads to the pavement; therefore, seismic moduli are linear elastic moduli. To incorporate in pavement design and analysis, seismic moduli of different layers have to be adjusted to represent moduli at strain and stress levels that are close to those applied by truck traffic. To do so, the nonlinear and viscoelastic behaviors of different layers should be accurately determined. These nonlinear parameters vary widely for different types of granular base and subgrade materials. The nonlinear parameters of each pavement layer can be preferably obtained from laboratory testing. However, adequate published information is available to be used as a first approximation.

The major objective of this study is to develop an algorithm for predicting the design modulus of each layer given the seismic modulus and the nonlinear and/or viscoelastic parameters of each pavement layer. This is the last document produced as a part of this project. In the first document, the feasibility of the concept was demonstrated, and several options to be pursued further were provided. In the second document, it was demonstrated that the design modulus could be determined reasonably accurately by combining the seismic moduli with the nonlinear parameters of the base and subgrade determined from the laboratory tests. It was also demonstrated that a simple model based either on the plasticity index (PI) or the type of the material might be used as a first approximation. That document also contained a comprehensive discussion on the most feasible method for incorporating their methodology in the day-to-day operation of the Texas Department of Transportation (TxDOT).

In the third document, the work presented in the second report was further expanded to determine the feasibility of backcalculating the nonlinear parameters of the base and subgrade given the seismic modulus of each layer and the deflection basin measured at the same location. An algorithm has been developed for this purpose. In the algorithm, a material model that relates the design modulus with seismic modulus was selected. A so-called equivalent linear structural model was also adopted. An equivalent linear model is based on an elasto-static layered system modified to incorporate the material model through an iterative process. An optimization algorithm was developed to derive the nonlinear parameters of pavement materials from the FWD deflections and the seismic moduli.

The efforts towards combining all algorithms in a software package called SMART (Seismic Modulus Analysis and Reduction Tool) are described in the fourth report. That report also contains a user's manual for the SMART.

The validation of SMART is described in this report. More than a dozen sites were visited. The results from this validation indicate that the program is capable of providing reasonable values to design engineers. The procedure is particularly attractive in the situations where the depth to bedrock is shallow or when the water table is close to the pavement surface.

Implementation Statement

With the initiation of NCHRP project 1-37A, which aims towards a nation-wide mechanistic pavement design procedure, this project may have significant impact. To develop a mechanistic pavement design that can contain performance-based specifications, the same engineering properties that are used to design a pavement should be used to determine the suitability of a material for construction and should be specified as criteria for accepting the material placed at the site. The only practical and available method at this time is based on seismic testing. Furthermore, it seems that with proper laboratory testing technique and proper simulation one can develop remaining life models that are more realistic.

Some of the software and protocols being developed can also be applied in pavement design with the FWD.

Table of Contents

List of Figures

List of Tables

Chapter 1

Introduction

PROBLEM STATEMENT

Nondestructive testing (NDT) methods are typically used to measure the variations in the modulus of different pavement layers. The critical strains necessary for the estimation of the remaining life of a pavement system are determined from the estimated moduli. The Falling Weight Deflectometer (FWD) and the Seismic Pavement Analyzer (SPA) are two of the NDT devices used for this purpose.

The Falling Weight Deflectometer applies an impulse load to the pavement and measures the surface deflection with seven sensors. Moduli of different pavement layers can then be backcalculated from these deflections. The shortcomings of this method are the uncertainties associated with the backcalculation procedure.

The Seismic Pavement Analyzer is based on generating and detecting stress waves in a layered system. The elastic moduli of different layers are obtained from an inversion process. The SPA imparts very small external loads to the pavement; therefore, seismic moduli are linear elastic moduli. To incorporate in pavement design and analysis, seismic moduli of different layers have to be adjusted to represent moduli at strain and stress levels that are close to those applied by traffic loads. To do so, the nonlinear and viscoelastic behaviors of different layers should be accurately determined.

These nonlinear parameters vary widely for different types of granular base and subgrade materials. The nonlinear parameters of each pavement layer are preferably obtained from laboratory testing. However, in the absence of laboratory testing, adequate published information is available to be used as a first approximation.

OBJECTIVE AND APPROACHES

The major objective of this study is to develop an algorithm for predicting design modulus of each layer given its seismic modulus and the nonlinear and/or viscoelastic parameters. The algorithm developed under this project has been incorporated in a software package called SMART (Seismic Modulus Analysis and Reduction Tool). In Research Reports 1780-1 (1999), 1780-2 (2002) and 1780-3 (2004), the progression of developing the algorithms used in SMART is documented. TxDOT report 1780-4 (2004) is the user's guide for SMART. In this report the validation procedure and results of the validation are addressed. More than a dozen sites were visited where data was collected and materials retrieve for laboratory testing. The results from this validation indicate that the program is capable of providing reasonable values to design engineers. The procedure is particularly attractive in the situations where the depth to bedrock is shallow or when the water table is close to the pavement surface.

ORGANIZATION

Chapter 2 contains a review of relevant literature regarding the FWD and SPA as well as a general description of the methods for the interpretation of data from the two devices. The different pavement analysis algorithms used by the SMART program is presented. The two most common failure modes of the pavement and remaining life of the pavement are also described in that chapter.

Chapter 3 depicts the features and overall flow of SMART. Snapshots taken of SMART help describe the execution and operation of the program. That chapter can be used as a quick guide to start utilizing SMART.

The validation procedure used to verify the viability of using seismic data to calculate design modulus values is presented in Chapter 4. Each step of the validation starting from field testing to laboratory test and data analysis is outlined in that chapter. One of the test sites is used as an example to illustrate the entire process.

Chapter 5 contains the results of the validation process. A discussion of the analysis and results for all sites tested are also presented. The strengths and limitations of the algorithm based on the validation results are included.

The overall validation procedure and results are summarized and the relevant conclusions are drawn in Chapter 6.

Chapter 2

Background

INTRODUCTION

An ideal mechanistic pavement design process includes (1) determining pavement-related physical constants, such as types of existing materials and environmental conditions, (2) laboratory and field testing to determine the strength and stiffness parameters and constitutive model of each layer, and (3) estimating the remaining life of the pavement using an appropriate algorithm. Pavement design or evaluation algorithms can be based on one of many layer theory or finite element programs. The materials can be modeled as linear or nonlinear and elastic or viscoelastic. The applied load can be considered as dynamic or static. No matter how sophisticated or simple the process is made, the material properties should be measured in a manner that is compatible with the algorithm used. If a balance between the material properties and analytical algorithm is not struck, the results may be unreliable.

Brown (1996) discusses a spectrum of analytical and numerical models that can be used in pavement design. With these models, the critical stresses, strains and deformations within a pavement structure and, therefore, the remaining lives can be estimated. Many computer programs with different levels of sophistication exist. The focal point of all these models is the moduli and Poisson's ratio of different layers.

MATERIAL MODELS

The linear-elastic model is rather simple since the modulus is considered as a constant value independent of the state of stress applied to the pavement. As such, the modulus of each layer does not change with the variation in load applied to a pavement. Most current algorithms used in pavement analysis and design take advantage of this type of solution. The advantage of these models is that they can rapidly yield results. Their main limitation is that the results are rather approximate if the loads are large enough for the material to exhibit a nonlinear behavior. More sophisticated material models can of course be considered. The load-induced nonlinear behavior

may be of interest for the base, subbase and subgrade layers. The viscoelastic behavior of the AC layer has to be considered in many occasions.

Nonlinear Constitutive Model

The nonlinear constitutive model adopted for the base, subbase and subgrade layers by most agencies and institutions can be generalized as:

$$E = k_1 \sigma_c^{k_2} \sigma_d^{k_3} \tag{2.1}$$

where k_1, k_2 and k_3 are coefficients preferably determined from laboratory tests. In Equation 2.1, the modulus at a given point within the pavement structure is related to the state of stress. The advantage of this type of model is that it is universally applicable to fine-grained and coarse-grained base and subgrade materials. The accuracy and reasonableness of this model are extremely important because they are the keys to successfully combining laboratory and field results. Barksdale et al. (1997) have summarized a number of variations to this equation. Using principles of mechanics, all those relationships can be converted to the other with ease. The so-called two-parameter models advocated by the AASHTO 1993 design guide can be derived from Equation 2.1 by assigning a value of zero to k_2 (for fine-grained materials) or k_3 (for coarse-grained materials). As such, considering one specific model does not impact the generality of the conclusions drawn from a given model.

Using geotechnical engineering conventions, the term $k_1\sigma_c^{k2}$ corresponds to the initial tangent modulus. Since normally parameter k_2 is positive, the initial tangent modulus increases as the confining pressure increases. Parameter k_3 suggests that the modulus changes as the deviatoric stress changes. Because k_3 is usually negative, the modulus increases with a decrease in the deviatoric stress (or strain). The maximum feasible modulus from Equation 2.1 is equal to $k_1\sigma_c^{k2}$, i.e. the initial tangent modulus.

In all these models, the state of stress is bound between two extremes; when no external loads are applied and under external loads imparted by an actual truck. When no external load is applied the initial confining pressure, σ_{c_init}, is

$$\sigma_{c\_init} = \frac{1 + 2k_0}{3} \sigma_v \tag{2.2}$$

where σ_v is the vertical geostatic stress and k_o is the coefficient of lateral earth pressure at rest. The initial deviatoric stress, σ_{d_init} can be written as

$$\sigma_{d\_init} = \frac{2 - 2k_0}{3} \sigma_v \tag{2.3}$$

When the external loads are present, additional stresses, σ_x, σ_y and σ_z, are induced in two horizontal and one vertical directions under the application of an external load. A multi-layer elastic program can conveniently compute these additional stresses. The ultimate confining pressure, σ_{c_ult} is

$$\sigma_{c\_ult} = \frac{1+2k_0}{3}\sigma_v + \frac{\sigma_x + \sigma_y + \sigma_z}{3} \tag{2.4}$$

and the ultimate deviatoric stress, σ_{d_ult}, is equal to

$$\sigma_{d\_ult} = \frac{2-2k_0}{3}\sigma_v + \frac{2\sigma_z - \sigma_x - \sigma_y}{3} \tag{2.5}$$

Under actual truck loads, the modulus can become nonlinear depending on the amplitude of confining pressure, σ_{c_ult}, and deviatoric stress, σ_{d_ult}. In that case

$$E = k_1 \sigma_{c\_ult}^{\ k_2} \sigma_{d\_ult}^{\ k_3} \tag{2.6}$$

One of the purposes of this study is to relate seismic modulus with the load-induced nonlinear modulus while predicting k_2 and k_3 parameters considering state of stress under the external load imparted by a FWD or truck load. Ke et al. (2000) derived such a relationship, which is in the form of:

$$E = E_{seis}\left(\frac{\sigma_{c-ult}}{\sigma_{c-init}}\right)^{k_2}\left(\frac{\sigma_{d-ult}}{\sigma_{d-init}}\right)^{k_3} \tag{2.7}$$

where E is the resilient modulus at a given depth under FWD or truck load, E_{seis} is the seismic modulus of the layer, k_2 and k_3 are statically determined coefficients. $\sigma_{c\text{-}init}$ and $\sigma_{c\text{-}ult}$ are respectively initial and ultimate confining pressures. $\sigma_{d\text{-}init}$ and $\sigma_{d\text{-}ult}$ are the initial and ultimate deviatoric stresses, respectively. The derivation of Equation 2.7 is included in Report 1780-2 (2002).

One of the limitations of Equation 2.7 is that at very small or at very large deviatoric stresses the modulus tends to be infinity or zero, respectively. Many years of research (Kramer, 1996) have shown that below a certain strain level the modulus is constant and equal to the small-strain linear-elastic modulus of the material. Similarly, at higher strain levels, the modulus approaches a constant value. Therefore, a set of boundary limitations is applied. If in Equation 2.7 the strain is small enough that the modulus becomes greater than the seismic modulus measured in the field, the seismic modulus will be adopted as the modulus of the material. On the other hand, if at higher vertical strain levels the modulus becomes lower than 5% of the seismic modulus

measured in the field, 5% of seismic modulus will be adopted as the modulus of the material. As such, the upper and lower bounds of the modulus are:

$$E_{up} = E_{seis} \tag{2.8a}$$

$$E_{low} = 0.05E_{seis} \tag{2.8b}$$

Another variation to Equation 2.1 is model developed by the Georgia Department of Transportation (GADOT). In that study, Santha (1994) collected and tested a number of soil samples to determine parameters k from resilient modulus tests. He also obtained various construction parameters such as the moisture content, compaction, and percent saturation. He then developed regression equations for cohesive and granular materials that estimate parameters k from the construction parameters using the octahedral shear stress model:

$$M_R = k_1 P_a \left[\frac{\theta}{P_a}\right]^{k_2} \left[\frac{\tau_{oct}}{P_a}\right]^{k_3} \tag{2.9}$$

where $\theta = \sigma_1 + \sigma_2 + \sigma_3$ is the bulk stress, τ_{oct} is the octahedral shear stresses, P_a is the atmospheric pressure, and k_1, k_2 and k_3 are multiple regression constants evaluated from resilient modulus test data. According to Santha, for granular material the three k parameters are in the form of

$$\begin{aligned}\log(k_1) = {} & 3.479 - 0.07*MC + 0.24*MCR \\ & + 3.681*COMP + 0.011*SLT + 0.006*CLY \\ & - 0.025*SW - 0.039*DEN + 0.004*(SW^2/CLY) \\ & + 0.003*(DEN^2/S40)\end{aligned} \tag{2.10a}$$

$$\begin{aligned}\log(k_2) = {} & 6.044 - 0.053*MOIST - 2.076*COMP \\ & + 0.0053*SATU - 0.0056*CLY + 0.0088*SW \\ & - 0.0069*SH - 0.027*DEN + 0.012*CBR \\ & + 0.003*(SW^2/CLY) - 0.31*(SW+SH)/CLY\end{aligned} \tag{2.10b}$$

$$\begin{aligned}\log(k_3) = {} & 3.752 - 0.068*MC + 0.309*MCR \\ & - 0.006*SLT + 0.0053*CLY - 0.026*SH \\ & - 0.033*DEN - 0.0009*(SW^2/CLY) \\ & + 0.00004*(SATU^2/SH) - 0.0026*(CBR*SH)\end{aligned} \tag{2.10c}$$

and for cohesive materials,

$$\log(k_1) = 19.813 - 0.045 * MOIST - 0.131 * MC - 9.171 * COMP + 0.0037 * SLT + 0.015 * LL - 0.016 * PI - 0.021 * SW - 0.052 * DEN + 0.00001 * (S40 * SATU) \quad (2.11a)$$

$$\log(k_3) = 10.274 - 0.097 * MOIST - 1.06 * MCR - 3.471 * COMP + 0.0088 * S40 - 0.0087 * PI + 0.014 * SH - 0.0246 * DEN \quad (2.11b)$$

where MC is moisture content, MOIST is optimum moisture content, MCR is the ratio of MC and MOIST, COMP is compaction, SATU is percent saturation, S40 is percent passing sieve No. 40, CLY is percent of clay, SLT is percent of silt, SW is percent swell, SH is percent shrinkage, DEN is maximum dry unit weight, CBR is California Bearing Ratio, LL is liquid limit, and PI is plastic limit index.

Although these equations were generated based on test sites in Georgia they can be used in the absence of resilient modulus test for determining k_2 and k_3 values.

Nonlinear Plasticity Index Model

Ishibashi and Zhang (1993) combined the effects of the confining pressure and plasticity index on modulus behavior in the form

$$\frac{E}{E_{seis}} = K(\gamma, PI)(\sigma'_m)^{m(\gamma,PI)-m_0} \quad (2.12)$$

where PI is the plasticity index of the base or subgrade material and γ is the shear strain and

$$K(\gamma, PI) = 0.5\left\{1 + \tanh\left[\ln\left(\frac{0.000102 + n(PI)}{\gamma}\right)^{0.492}\right]\right\} \quad (2.13)$$

$$m(\gamma, PI) - m_0 = 0.272\left\{1 - \tanh\left[\ln\left(\frac{0.000556}{\gamma}\right)^{0.4}\right]\right\}\exp(-0.0145PI^{1.3}) \quad (2.14)$$

$$n(PI) = \begin{cases} 0.0 & for PI = 0 \\ 3.37\times10^{-6} PI^{1.404} & for 0 < PI \le 15 \\ 7.0\times10^{-7} PI^{1.976} & for 15 < PI \le 70 \\ 2.7\times10^{-5} PI^{1.115} & for PI > 70 \end{cases} \quad (2.15)$$

Several parameters affect the modulus of bituminous materials. The most important parameters are the rate of the loading (i.e., frequency of loading) and temperature. The typical frequency range at which asphalt concrete (AC) moduli measured with seismic methods is about 10 kHz to 25 kHz; whereas, the actual traffic load has a dominant frequency of about 10 Hz to 30 Hz. Aouad et al. (1993) clearly demonstrated the importance of considering the impact of frequency on modulus.

Viscoelastic Model

The AC modulus is strongly dependent on temperature. Aouad et al. (1993), Li and Nazarian (1994) and several other investigators have studied the variation in modulus with temperature. The relationship suggested by Li and Nazarian (1994) for adjusting the modulus of AC to a reference temperature of 77° F (25° C) was used here. That relationship is in the form of

$$E_{77^\circ F} = \frac{E_t}{1.35 - 0.0078(t-32)} \tag{2.16}$$

where E_{25} and E_t are the moduli at 77° F and temperature t (in Fahrenheit).

Using the principals of viscoelastic and time-temperature superposition, Witczak and his colleagues have provided a relationship that can be used to adjust the moduli for frequency and temperature through the so-called master curve. The new Mechanistic Pavement Design Guide encourages the use of the master curve. Witczak et al. (1999) describe the newer methodology proposed in the development of the master curve. A typical distribution of complex modulus with time and temperature of an asphalt concrete mixture is shown in Figure 2.1. The general practice has been that the testing is performed at various temperatures at similar loading times (see Figure 2.1a, then a data is shifted based on a reference temperature using a time-temperature shift factor (see Figure 2.1b) and finally a master curve is generated at the reference temperature using a curve fitting technique (see Figure 2.1c). The master curve is then developed based on the assumption that asphalt concrete is a thermo-rheoloigcally simple material. The results presented in Figure 2.1 are shifted horizontally to develop a master curve.

A sigmoidal function proposed by Ferry (1970) can be used to generate a master curve. The sigmoidal function is in the form of:

$$\log(E^*) = \delta + \frac{\alpha}{1 + e^{\beta + \gamma \log t_r}} \tag{2.17}$$

where E* = dynamic modulus, t_r = loading period, δ = Minimum value of dynamic modulus, $\delta + \alpha$ = Maximum value of dynamic modulus and β, γ = sigmoidal function shape parameter.

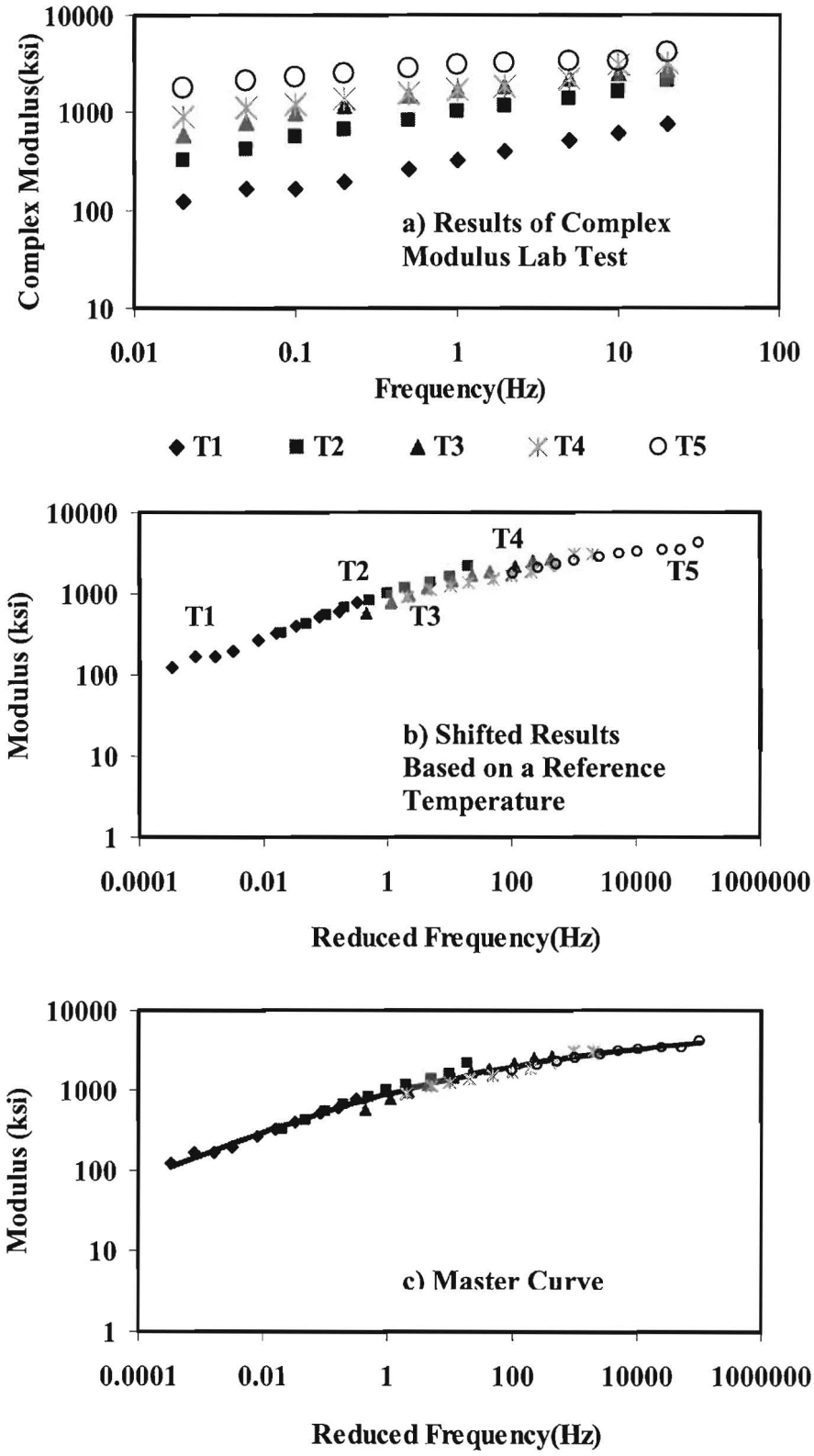

Figure 2.1 - Master Curve Concept

Mirza and Witczak (1995) have proposed the following relationships for obtaining values of the sigmoid parameters in the absence of lab tests:

$$\delta = -1.249937 + 0.02932\rho_{200} - 0.001767\rho_{200}^2 - 0.002841\rho_4 - 0.058097V_a - \frac{0.802208V_{beff}}{V_{beff} + V_a} \quad (2.18)$$

$$\alpha = 3.871977 - 0.0021\rho_4 + 0.003958\rho_{38} - 0.000017\rho_{38}^2 + 0.005470\rho_{34} \quad (2.19)$$

$$\beta = -0.603313 - 0.393532\log(\eta_t) \quad (2.20)$$

$$\gamma = 0.313351 \quad (2.21)$$

where ρ_{200} is percent passing on the 0.075mm sieve, ρ_4 is cumulative percent retained on the 4.76 mm sieve, V_a is percent air voids in the mix by volume, V_{beff} is percent effective bituminous content by volume, ρ_{38} is cumulative percent retained on the 9.5 mm sieve, ρ_{34} in cumulative percent retained on the 19 mm sieve, η_t is viscosity of the binder at a reference temperature.

Once the master curve is established, either from lab testing or the regression relationships presented in Equations 2.18 through 2.21, the design modulus can be readily determined from the design vehicular speed and the design temperature as recommended in the 2002 AASHTO Design Guide

Saeed and Hall (2001), based on tests on a half a dozen specimens have shown that the seismic modulus and the master curve from complex modulus correlate well. An example from one site is shown in Figure 2.2. Typical results from one material when the seismic and complex moduli are combined are shown in Figure 2.3. The process of defining the design modulus is marked on the figure as well. First a reference temperature is defined for the regional. A design frequency is then determined based upon the vehicular speed. The desired modulus based on these two input parameters can be readily defined.

ANALYSIS OPTIONS

The analysis algorithm can be either a multi-layer linear system, or a multi-layer equivalent-linear system, or a finite element code for a comprehensive nonlinear dynamic system. A multi-layer linear system is the simplest simulation of a flexible pavement. In this system, all layers are considered to behave linearly elastic. WESLEA (Van Cauwelaert et al., 1989) and BISAR (De Jong et al., 1973) are two of the popular programs in this category.

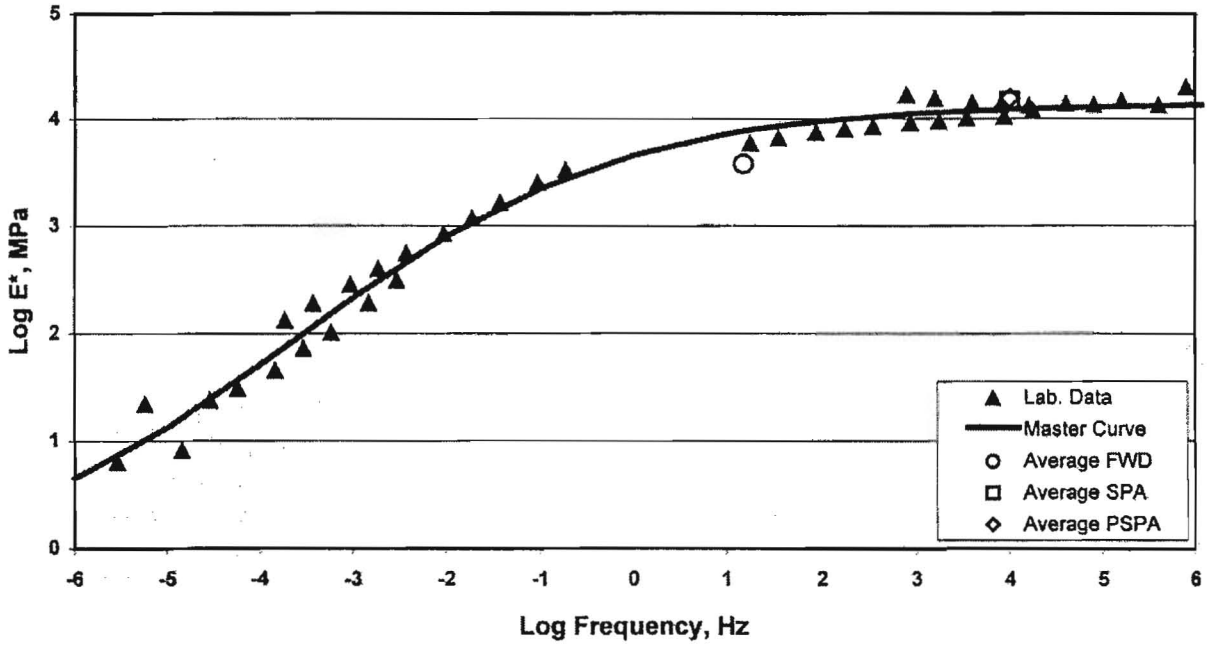

Figure 2.2 - Master Curve from Complex Modulus Compared with Moduli measured from Different NDT Tests (from Saeed and Hall, 2001)

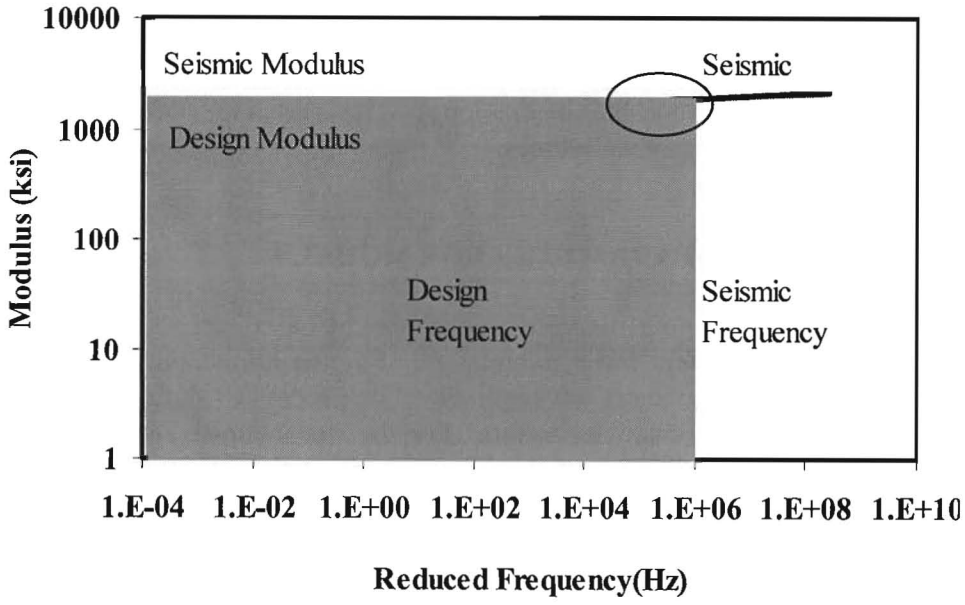

Figure 2.3 - Master Curve Concept for defining Seismic Modulus

The equivalent-linear process is based on the static linear elastic layered theory. Nonlinear constitutive models, such as the one described in Equation 2.1, can be implemented in them. An iterative process has to be employed in this process. To implement the algorithm, nonlinear layers are divided into several sublayers. One stress point is chosen for each nonlinear sublayer. An initial modulus is assigned to each stress point. The stresses and strains are calculated for all stress points using a multi-layer elastic computer program. The confining pressure and deviatoric stress can then be calculated for each stress point using Equations 2.2 through 2.5. A new modulus can then be obtained from Equation 2.7. The assumed modulus and the newly calculated modulus at each stress point are compared. If the difference is larger than a pre-assigned tolerance, the process will be repeated using updated assumed moduli. The above procedure is repeated until the modulus difference is within the tolerance and, thus, convergence is reached. Finally, the required stresses and strains are computed using final moduli for all nonlinear sublayers. Ke et al. (2001) describes the development of the equivalent-linear process. This method is relatively rapid; however, the results are approximate. In a linear-elastic layered solution, the lateral variation of modulus within a layer cannot be considered. To compensate to a certain extent for this disadvantage, a set of stress points at different radial distances are considered.

The all-purpose finite element software packages, such as ABAQUS, can be used for nonlinear models. These programs allow a user to model the behavior of a pavement in the most comprehensive manner and to select the most sophisticated constitutive models for each layer of pavement. The dynamic nature of the loading can also be considered. The constitutive model adopted in nonlinear models is the same as that in the equivalent-linear model, as described in Equation 2.7.

The goal with all these models is of course to calculate the critical stresses and strains and finally the remaining life. We will concentrate on the tensile strain at the bottom of the AC layer and compressive strain on top of the subgrade. These two parameters can be incorporated into a damage model (e.g. the Asphalt Institute models) to estimate the remaining lives due to a number of modes of failure (e.g. rutting and fatigue cracking). These equations are well known and can be found in Huang (1994) among other sources.

APPROPRIATE MODULUS PARAMETER FOR MODELS

The structural model and the input modulus values should be considered together. Different structural models require different input parameters. For the equivalent-linear and nonlinear models, all three nonlinear parameters are required. The process of defining these parameters can be categorized as material characterization. For the linear model, a representative linear modulus has to be determined. The process of approximating the modulus is called the design simulation.

One significant point to consider has to do with the differences and similarities between material characterization and design simulation. In material characterization, one attempts to determine the engineering properties of a material (such as modulus or strength). The material properties measured in this way, are fundamental material properties that are not related to a specific

modeling scenario. To use these material properties in a certain design methodology, they should be combined with an appropriate analytical or numerical model to obtain the design output. In the design simulation, one tries to experimentally simulate the design condition, and then estimate some material parameter that is relevant only to that condition. Both of these approaches have advantages and disadvantages. In general, the first method should yield more accurate results but at the expense of more complexity in calculation and modeling during the design process.

NONDESTRUCTIVE TESTING METHODS

Nondestructive testing techniques are widely used to obtain field stiffness parameters of pavement materials. Several nondestructive testing (NDT) and evaluation devices are available. Two nondestructive testing devices, Falling Weight Deflectometer (FWD) and Seismic Pavement Analyzer (SPA), are utilized in this study.

The Falling Weight Deflectometer is the most popular NDT device. The FWD applies an impulse load to the pavement, so that the pavement deflections can be measured at seven or more points. The deflections obtained from the seven sensors are input into a backcalculation program to determine the layer modulus of the pavement.

The Seismic Pavement Analyzer is becoming a popular NDT device. This trailer-mounted nondestructive testing device operates on the principle of generating and detecting stress waves in a layered medium Nazarian et al. (1993). The SPA uses more transducers than the FWD with higher frequencies and more sophisticated interpretation techniques. The measurement is rapid. A complete testing cycle at one point takes less than one minute (lowering sources and receivers, making measurements, and withdrawing the equipment). Pavement properties estimated by the SPA are the small strain moduli of different layers.

The advantages and disadvantages of deflection-based and seismic-based methods are summarized in Table 2.1. The SMART software developed under this project uses only data collected from seismic methods. The FWD will only be used for validation.

Table 2.1 Advantages and Disadvantages of Methods Used to Obtain Moduli

Test Method	Major Advantage	Major Weaknesses
FWD	Imposes loads that approximate wheel loads	The state-of-stress within pavement strongly depends on moduli of different layers, and hence is unknown.
SPA	Measures a fundamentally-correct parameter (i.e., linear elastic modulus)	State-of-stress during seismic tests differs from the state-of-stress under actual loads

TEMPERATURE CORRECTION

The modulus of the asphalt concrete (AC) layer is sensitive to changes in temperature of the asphalt. The means of adjusting the seismic modulus with temperature was introduced before. The shape of a deflection basin is also impacted by the temperature. Two procedures were used to adjust the deflection basin for temperature.

Scullion (1987) developed a shift factor based on deflections collected through out the day at a number of sites adjusted to a fixed temperature. Along with the shift factors a climatic classification of the state of Texas was devised. Texas was divided into five zones and with that a mean temperature value was assigned to each zone for each of the 12 month. The mean temperature and the shift factor could then be used to adjust the deflection immediately under the load using:

$$d_{0(adj)} = d_0 + Factor\left(Temp_{\text{Standard}} - Temp_{Measured}\right) \tag{2.22}$$

where $d_{0(adj)}$ is the adjusted deflection under the load, d_0 is the measured deflection under the load, *Factor* is the shift factor dependent on the thickness of AC layer (0.05 for thickness of AC layer is less than 3in., or 0.12 for thickness of AC layer is greater than 3in.), $Temp_{Standard}$ is the standard temperature that can be obtained from Figure 2.4 and $Temp_{Measured}$ is the measured temperature.

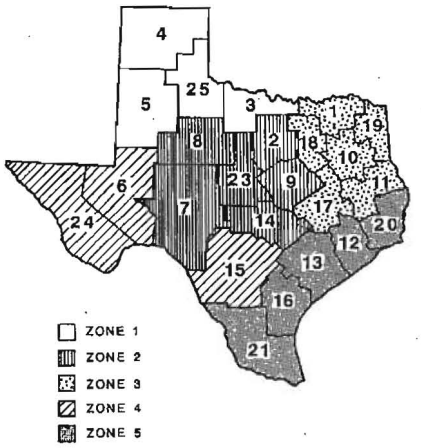

Mean Standard Temperature Values (°F)

Zone	Dec	Jan	Feb	Mar	Apr	May	Jun	Jul	Aug	Sep	Oct	Nov
1	48	40	39	66	87	92	103	116	104	82	49	60
2	65	72	53	76	100	99	86	118	112	93	61	61
3	56	46	66	78	89	95	100	114	89	90	70	70
4	55	76	82	96	103	105	114	112	108	106	98	67
5	66	74	71	77	95	94	93	110	118	99	93	63

Figure 2.4 - Standard Mean Temperature Based on Zones for Texas (from Scullion, 1987)

(Lukanen et al. 2000) developed a set of equations for temperature adjustment. In this procedure, the deflections are adjusted using the difference between the deflection under the load plate and the deflection at some offset sensor distance, as shown below:

$$Delta12 = d(0) - d(12) \quad (2.23a)$$
$$Delta24 = d(0) - d(24) \quad (2.23b)$$
$$Delta36 = d(0) - d(36) \quad (2.23c)$$
$$Delta60 = d(0) - d(60) \quad (2.23d)$$

The resulting equations for temperature adjustment are categorized by the AC thickness. For AC layer thickness of less than 4 in.:

$$d(0) = d(24) + Delta24 \ \ 10\text{^}((-0.000146 + 6.6E^{-5} h_t) * (T_m \ \ T_r)) \quad (2.24a)$$

for AC layers from 4 in. to 8 in.

$$d(0) = d(36) + Delta36 \ \ 10\text{^}((-0.00064 + 5.78E^{-5} h_t) * (T_m \ \ T_r)) \quad (2.24b)$$

and for the AC layer thickness greater than 8 in.:

$$d(0) = d(60) + Delta60 \ \ 10\text{^}((-0.000303 + 4.47E^{-5} h_t) * (T_m - T_r)) \quad (2.24c)$$

where $d(0)$ is the deflection adjusted to reference temperature, H_t is the thickness of asphalt layer (in mm), T_m is the measured (or estimated) mid-depth temperature (in °C), and T_r is the reference mid-depth temperature to adjust to (in °C). The adjusted deflections for the other spacings are functions of the deflection at a distance of 36 in. from the load. These regression equations can be used for that purpose:

$$log(delta12) = 3.45 - 1.59\, log(ac) + 0.489\, log(\Theta) + 0.449 \log(defl36) - 0.0275\, T + 0.012 T \log(ac) \log(\Theta) \quad (2.25a)$$

$$log(delta24) = 3.30 - 1.32\, log(ac) + 0.514\, log(\Theta) \log(defl36) - 0.00622\, T \log(\Theta) \log(defl36) + 0.00838\, T \log(ac) \log(\Theta) \quad (2.25b)$$

$$log(delta36) = 3.05 - 1.13\, log(ac) + 0.502\, log(\Theta) \log(defl36) - 0.00487\, T \log(\Theta) \log(defl36) + 0.00677\, T \log(ac) \log(\Theta) \quad (2.25c)$$

$$log(delta60) = 2.67 - 0.770\, log(ac) + 0.650\, log(delta36) + 0.00290\, T\, log(ac) \quad (2.25d)$$

where ac is the total thickness of the HMA (in mm), Θ is the latitude of the pavement section, $defl36$ is the deflection (normalized to 40 kN) at 36 in. from the center of the load plate (in microns) and T is the temperature at the mid-depth of the HMA (in °C).

These three sets of equations can be used to predict the deflections for all sensor locations. However, because deflections directly under and close to the load are most sensitive to temperature, adjusted deflections farther away from the center sensor will not be considered as necessary information.

A close examination of the models presented above indicates that for some thin asphalt layers, placed over a soft subgrade, and low latitudes, the models are not applicable. In these cases, the deflections would increase with a decrease in temperature. This situation was unfortunately pertinent to several of our case studies. In these cases, we did not adjust the deflection basin for temperature.

Chapter 3

Description of SMART

INTRODUCTION

The main purpose of the software package SMART (Seismic Modulus Analysis and Reduction Tool) is to use seismic moduli and well-substantiated nonlinear relationships to provide representative moduli for pavement design and analysis. SMART incorporates seismic moduli in a constitutive model recommended by a National Cooperative Highway Research Program (NCHRP) research project to determine the pavement responses in terms of the stress and strain developed within the pavement structures. Research Report 1780-4 (2002) contains the users' manual of SMART. The main features of the program are briefly described in this chapter.

SMART is a windows-based program. The main modules of the program are presented in Figure 3.1. The program contains four main modules; a) main menu, b) pavement property information and analysis, c) results, and d) online help. The flow of execution starts from the main menu, proceeds to pavement property information and analysis module and end with the results module. The online help module offers detailed explanation of all features in each of the SMART menus.

MAIN MENU

The main menu is shown in Figure 3.2. This menu controls access to different aspects of the program. The options available in the main menu are:

1. Analysis
2. Results
3. Help
4. Optional features

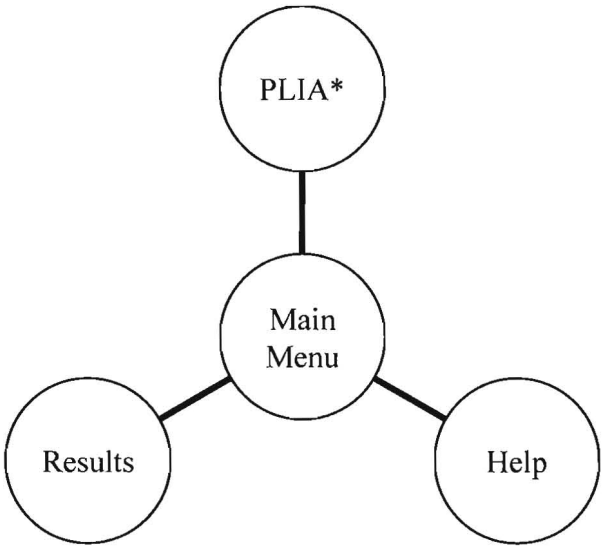

* Pavement Layer Information/Analysis

Figure 3.1 - Modules of SMART

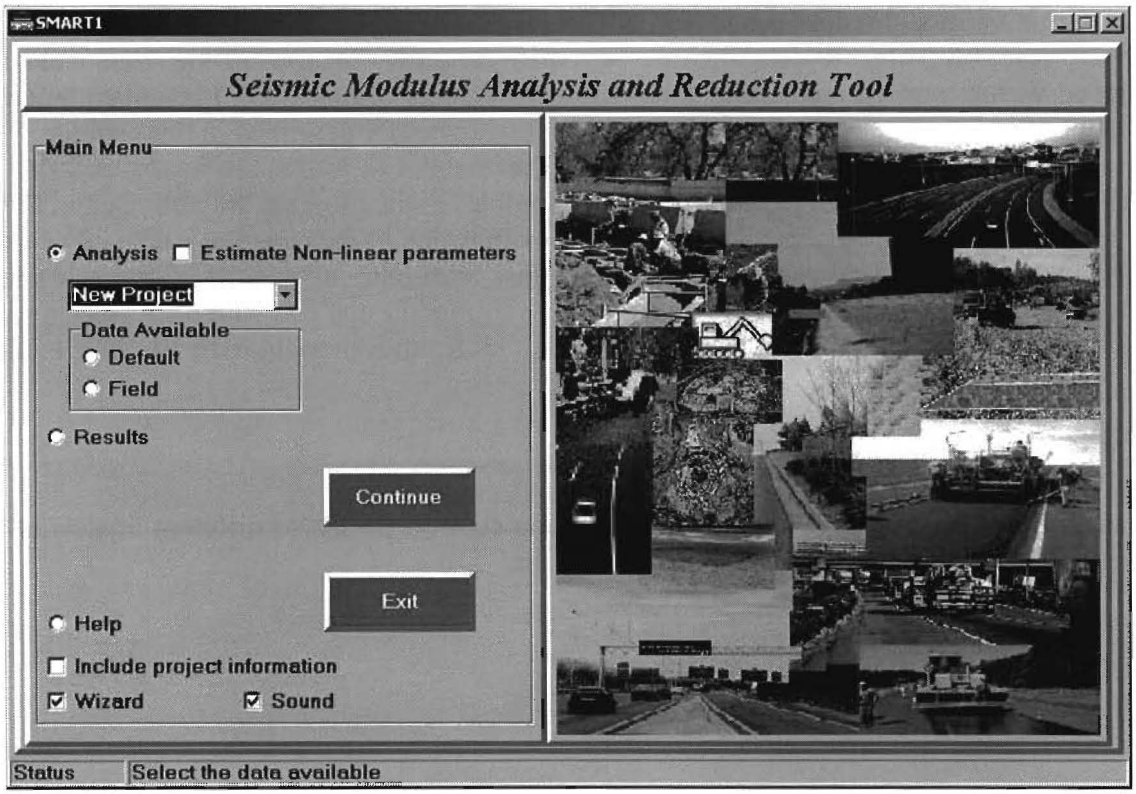

Figure 3.2 - Main Menu of SMART

Analysis: Analysis is the first option that the users select in the main menu. It allows the user to be prompted for the required data necessary to conduct a given analysis.

Results: This menu option provides users with the flexibility to directly access previously-analyzed data without performing the analysis again.

Help: This option brings up the online help menu providing users access to detailed explanations and information on all features of the program.

Optional features: Three additional (optional) features are provided in the main menu. The first feature is the project information option. Project information is a menu that allows a user to provide header information for each project. The second feature is the wizard option which provides instructions for novice users. The last optional feature is the sound option. Sounds are incorporated into SMART to help users transition with the flow of execution.

USING SMART

To start using SMART, a user first selects the analysis option. The user is then prompted to make a selection of either working with a new project or opening an existing one. The existing project option enables the user to select and rerun a previously-defined project. By selecting a new project, the user is prompted for the necessary data. At this point, the user can choose to use either a) default data or b) actual field data. The default data consists of a set of typical values which can be used during the design stages. These values are only recommendations and can be modified by users. Alternatively, the seismic data collected in the field can be retrieved. SMART provides the user with an option to link with a seismic reduction program.

Analysis with Default Data

The analysis with default data option provides a preliminary analysis without the need for complete field data. Users might have partial seismic data (e.g. modulus of AC from PSPA), in which case these values can be substituted in for the default values. When laboratory values are available, the user can substitute laboratory values as well. In the planning stages, .the built-in typical seismic values can be used to run the analysis

Figure 3.3 shows an example of the menu where the pavement structure is developed. For each layer, the user selects a) layer type, material type and constitutive model. Five layer types are available: a) overlay, AC, base, subbase and subgrade. After the layer is selected SMART will prompt the user to select a material type from a list of suitable options. Once the material type is selected, the user then selects a suitable constitutive model applicable to a given material. SMART has six models to select from: a) linear, b) viscoelastic, c) nonlinear (using resilient modulus test results), d) nonlinear (using the plasticity index test results), e) nonlinear (using estimated nonlinear parameters based on material quality) and f) nonlinear (using estimated nonlinear parameters based on index tests).

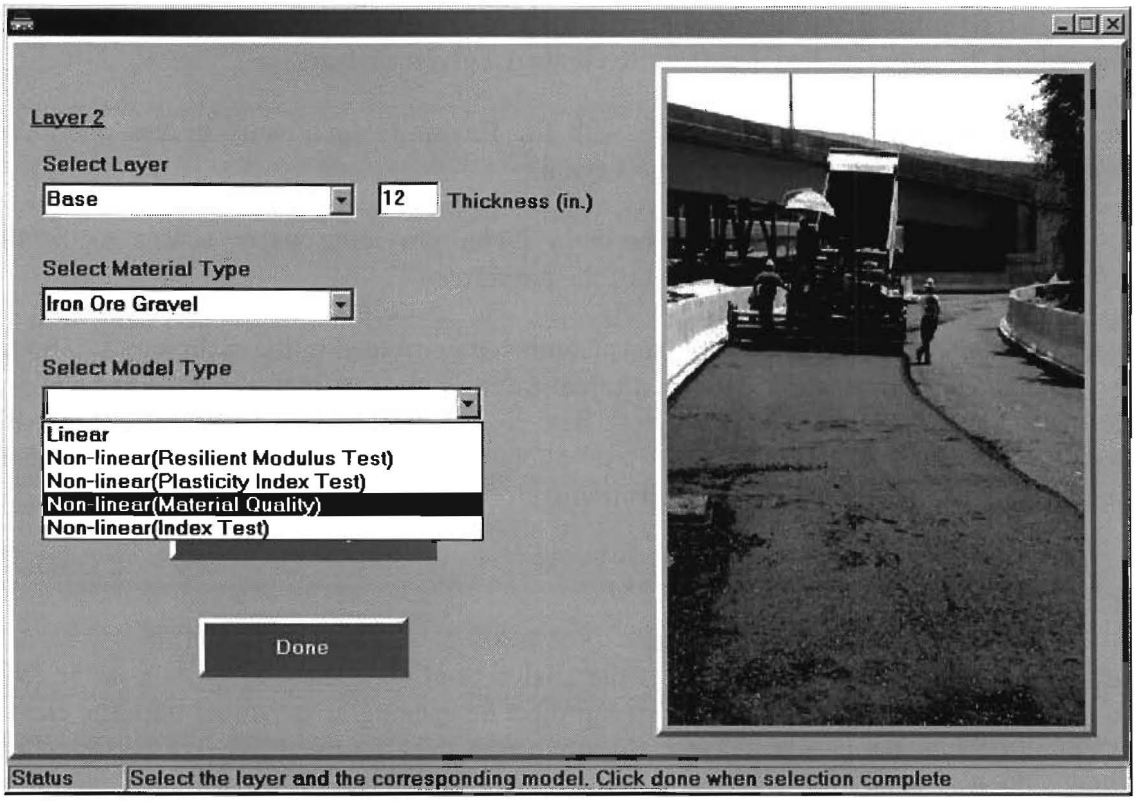

Figure 3.3 - Assembling Layer Property Information

The next menu provides a layer-by-layer summary of the information input (see Figure 3.4). The user can make any final changes to any parameter before performing the analysis. As depicted in Figure 3.4, the user can either enter the depth to rigid layer or select a semi-infinite layer. The first option allows users to consider shallow depth to rigid layer.

Analysis with Field Data

Analysis with field data allows the user to process seismic modulus and thickness values reduced with seismic inversion programs such as SASW for SPA. The goal would be to use reduced data from seismic test of an entire pavement section in SMART to obtain design modulus values.

SMART provides two options to incorporating reduced seismic data: a) reduce the data using SASW program and b) retrieve reduced data. If the field data has not been reduced the first option is used, where SMART links up to SASW for SPA. Once the data has been reduced and saved using SASW, it can be retrieved and analyzed using SMART. The second option retrieves reduced data by any seismic reduction software as long as the format of the output file is compatible. The format of the output file is available in the online help menu.

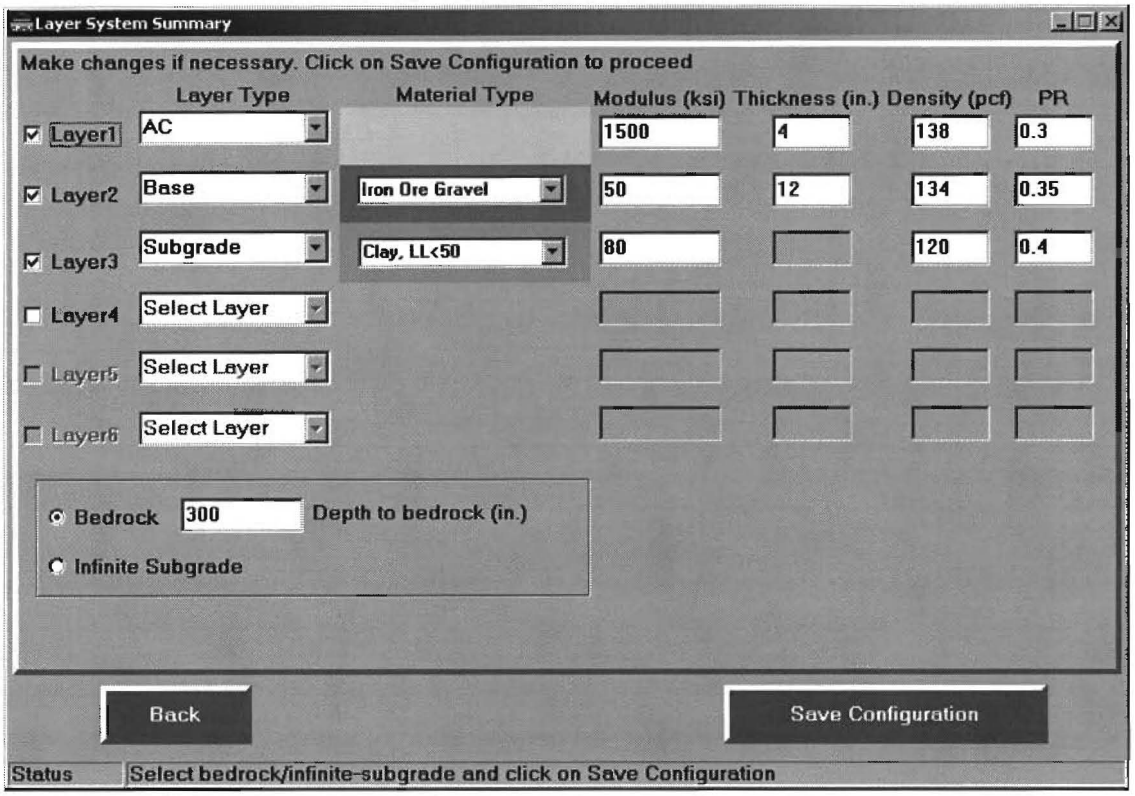

Figure 3.4 - Summary of Layer Properties

Upon selection of the data file, SMART reads and interprets the file containing seismic data and prompts the user to select the analysis model and the constitutive material types for each layer. Figure 3.5 shows a snapshot of the menu where the model types are selected. Once the layer model types are selected the data from the reduced seismic file is read and summarized as shown in Figure 3.6. After reviewing all input data, the user initiates the analysis by selecting the run analysis button.

Viscoelastic Feature for Overlays and AC Layers

SMART program features three options for temperature and frequency adjustments for the AC layer modulus values. These options are listed as: a) simplified, b) master curve based on mix properties, c) master curve based on lab testing. The details of adjusting modulus values based on temperature for all three methods were described in Chapter 2. Figure 3.7 contains the menus used for temperature adjustment. Figure 3.7a is a snapshot of the simplified method where the user only inputs the field or testing temperature. When selecting the update button from the menu, the modulus value is calculated for a temperature of 77°F (25°C).

If the second or third options are selected, the temperature adjustment is based on the master curve. The main premise of temperature adjustment due to master curve is to calculate a modulus value at a given temperature based on a sigmoid curve. A sigmoid curve is a four-

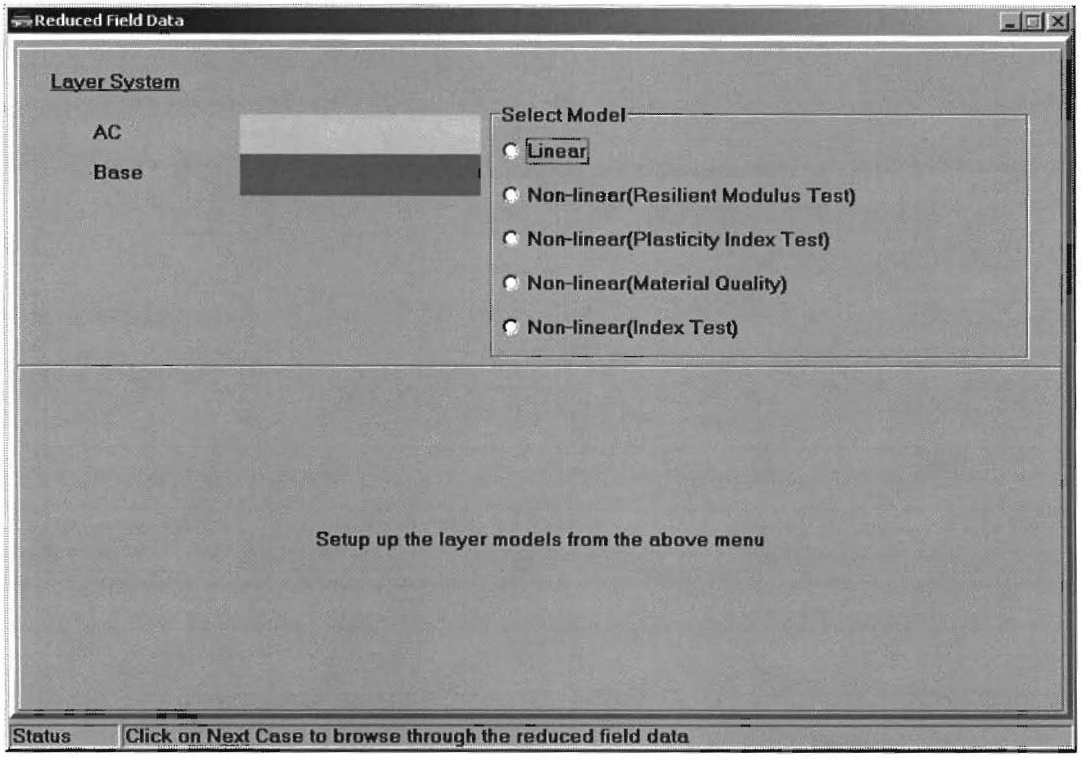

Figure 3.5 - Selecting Layer Models for Reduced Data File

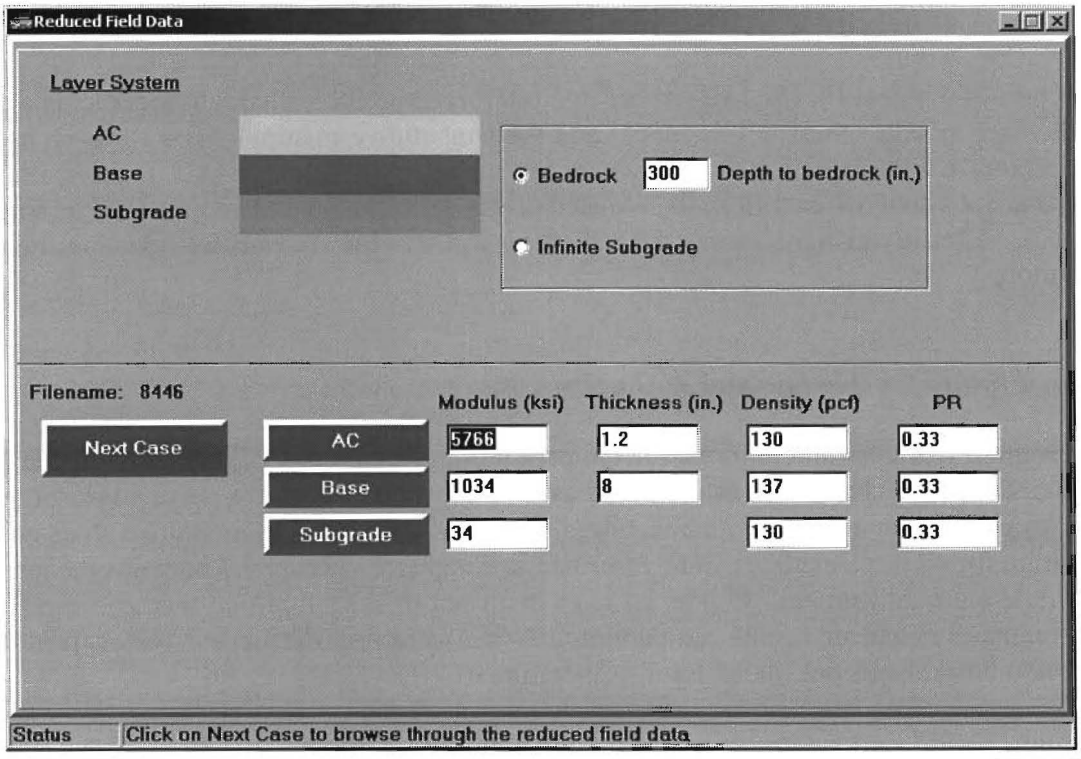

Figure 3.6 - Browsing through Reduced Datafile

a) Simplified Method

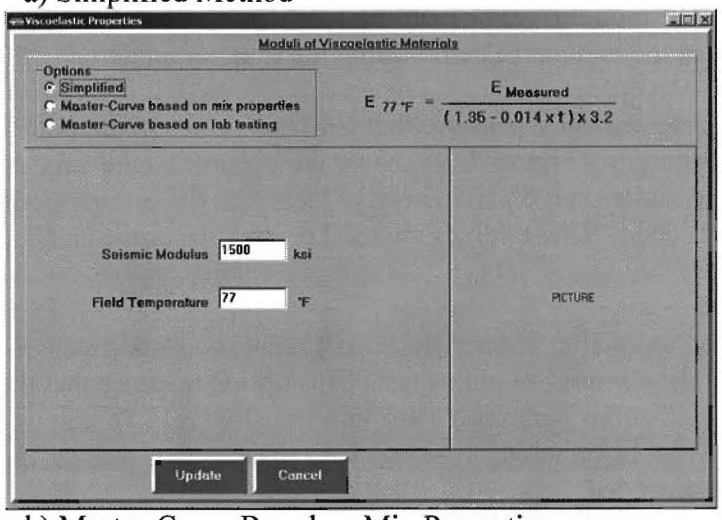

b) Master-Curve Based on Mix Properties

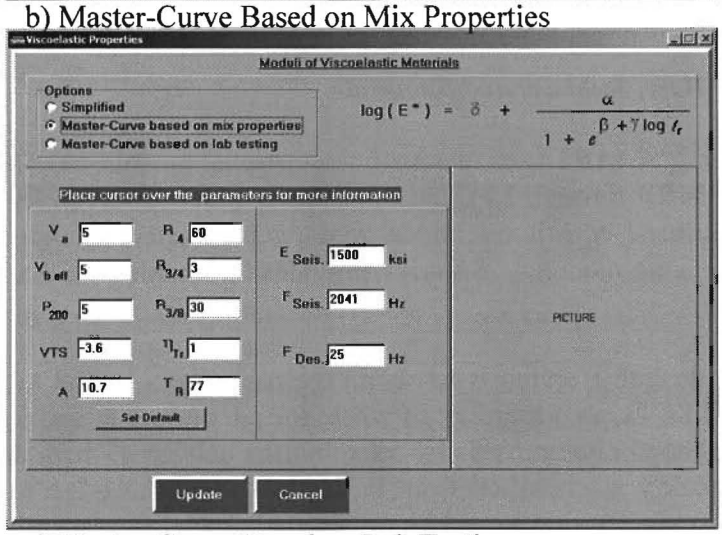

c) Master-Curve Based on Lab Testing

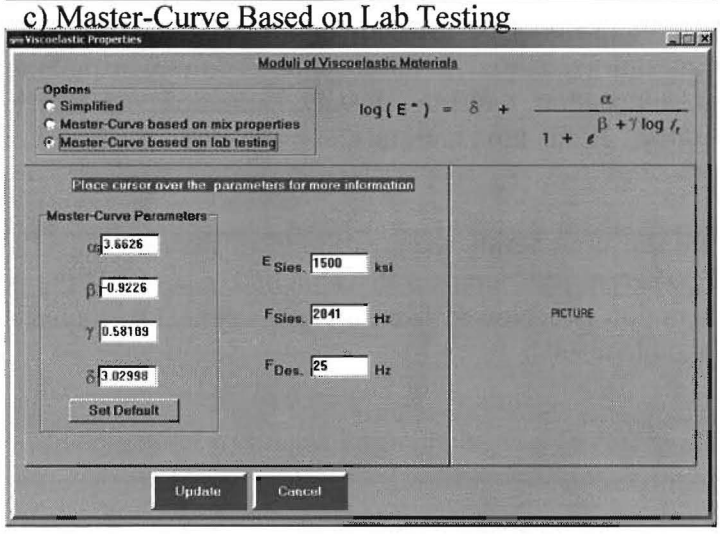

Figure 3.7 - Snapshots from SMART Viscoelastic Menus

parameter curve (α, β, γ, σ). As indicated in Chapter 2, by knowing the four parameters of the master curve, the adjusted modulus values can be calculated. The difference between the two master curve options is in the method of determining the four parameters.

The first method uses regression equations that are functions of material mix properties to calculate the curve parameters. Figure 3.7b shows the section where mix property values are provided to calculate the master curve parameters. Along with the mix properties, the design and testing frequencies are needed. These values are used to shift the curve and determine the design modulus value.

The second method for extracting master curve parameters as indicated in Chapter 2 is by laboratory testing using the complex modulus test. This option assumes that the laboratory test is performed and the master curve parameters are known. Figure 3.7c shows where the master curve parameters need to be entered. Along with parameters values, design and testing frequency values are also needed.

Nonlinear Feature for Base, Subbase and Subgrade

As discussed in Chapter 2, SMART uses two nonlinear material models: a) nonlinear constitutive model (refer to Equations 2.1 through 2.7), and b) plasticity index model (refer to Equations 2.12 through 2.15). The nonlinear constitutive model requires parameters k_2 and k_3 since parameter k_1 is calculated from seismic modulus. SMART provides three options from which parameters k_2 and k_3 can be obtained.

The first and the most desirable option is to obtain the parameters k_2 and k_3 from the resilient modulus tests. Figure 3.8a shows a snapshot of where the parameters k_2 and k_3 from lab test can be incorporated. The second alternative is by selecting the quality of the materials (see Figure 3.8b). The material quality is classified from basically good to average to poor. Based on literature and previous studies, preset k_2 and k_3 values are selected for each quality. This option is not recommended, and should only be used for preliminary analysis when values from the resilient modulus tests are not available. A third option is to obtain the parameters k_2 and k_3 from index tests such as compaction, moisture, density, saturation, etc. (see Equations 2.10 and 2.11). This option is disabled at this time until an extensive study for Texas condition is carried out.

The plasticity index nonlinear option only requires the PI of the material. Figure 3.8c shows a snapshot from SMART, where a user inputs a PI value of a material if the nonlinear plasticity option is selected. This option is borrowed from the geotechnical earthquake engineering field and should provide reasonable results.

Results

The results menu in SMART is either accessed from the main menu directly or automatically after an analysis is complete. As a reminder the main use of SMART is to determine design

a) Resilient Modulus Test

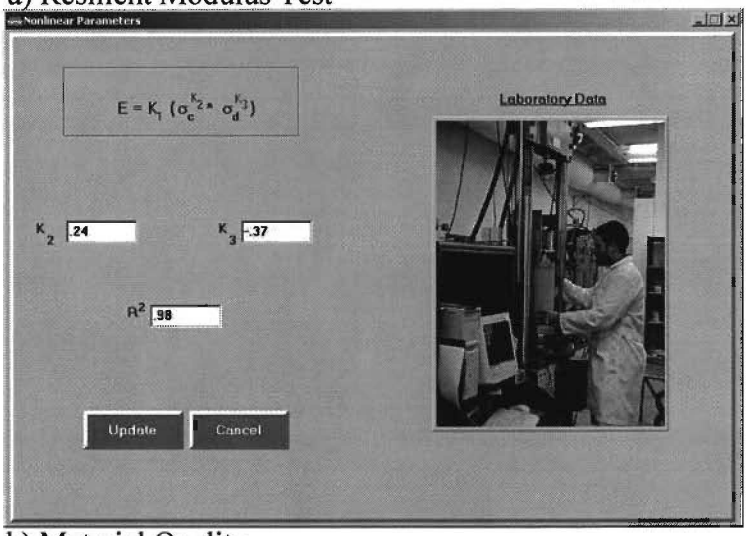

b) Material Quality

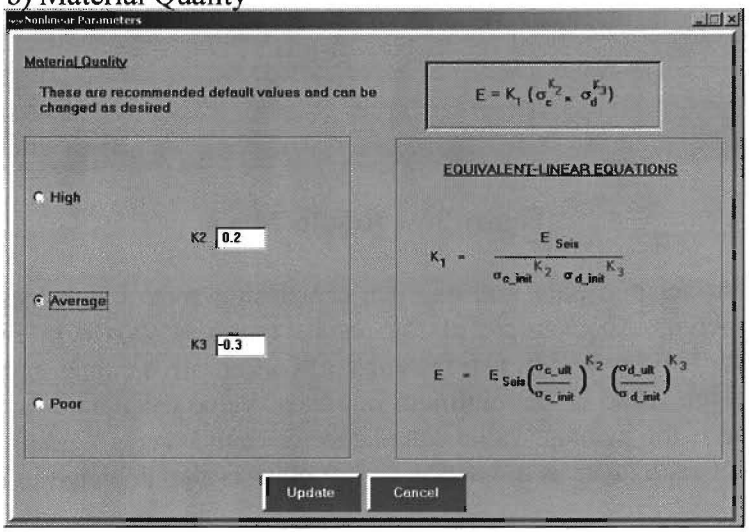

c) Plasticity Index Test

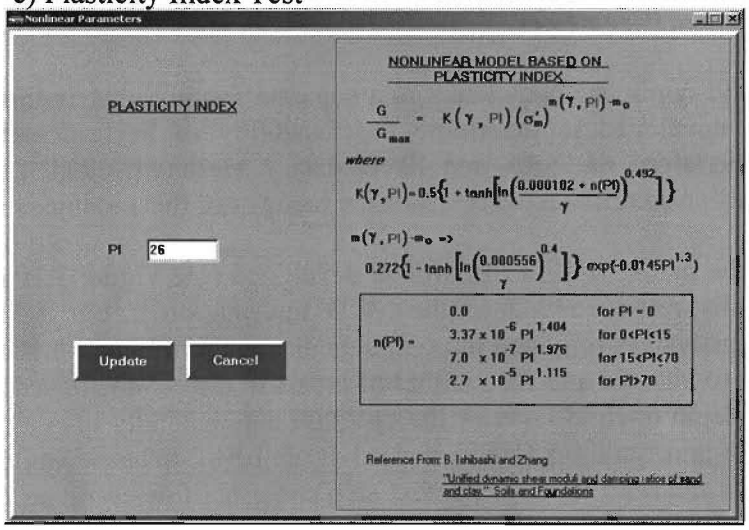

Figure 3.8 - Snapshot of Nonlinear Parameters Options

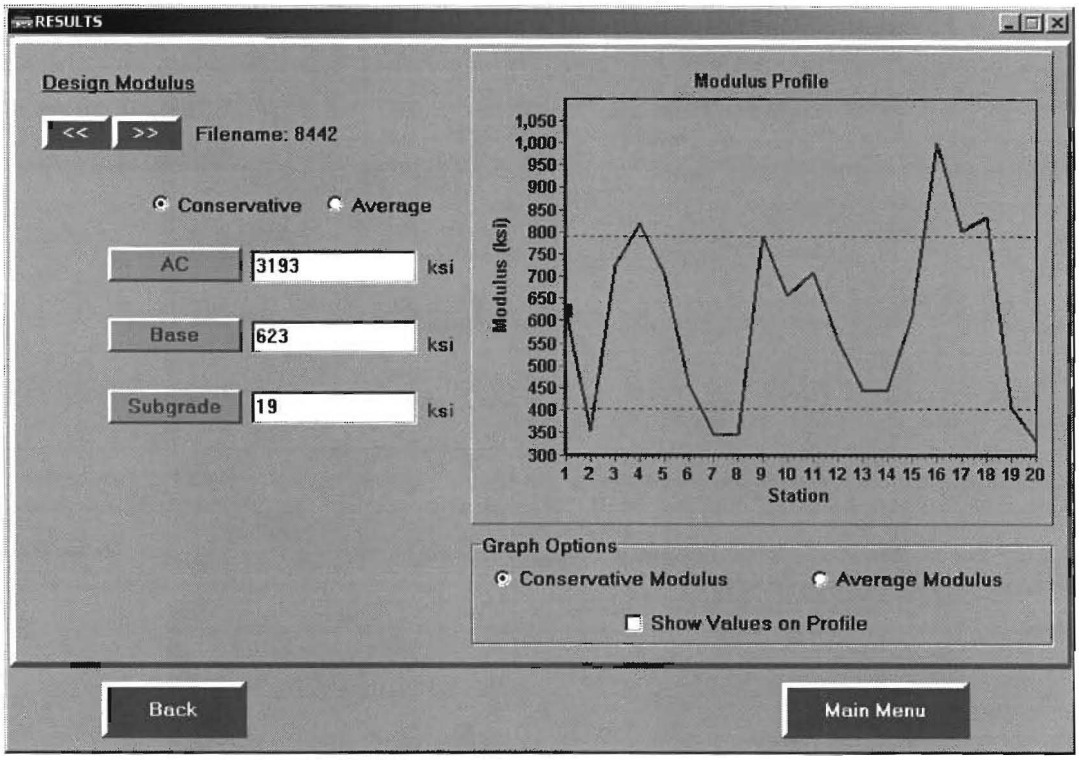

Figure 3.9 - Results Menu

modulus values from seismic data and as such the design modulus values are presented by SMART's results menu. An example of the results menu is shown in Figure 3.9. Design modulus of each layer is presented in two fashions: a) conservative values and b) average values. The conservative design value is the minimum nonlinear value calculated for each layer and the average design value is the average value calculated for each layer. A graph of the variation in the design modulus of each layer as a function of test point is also depicted in Figure 3.9.

Estimation of Nonlinear Parameters

The estimation of the nonlinear parameters is a separate module that is linked with SMART. This program was developed to determine the feasibility of backcalculating the nonlinear parameters k_2 and k_3 from the SPA and FWD data. Meshkani et al. (2001) contains the algorithm used in this program. An overview of the features of this module is included here.

A menu similar to the main menu in SMART is developed (see Figure 3.10a). The FWD data are then automatically retrieved. Once the FWD information is retrieved, all the required information for the analysis is provided through a menu shown in Figure 3.10b. The user selects the number of cases to analyze and the number of layers in the pavement section. The user also either specifies the depth to rigid layer or the program automatically uses a regression analysis developed by Rhode and Scullion (1990) and advocated by Michalak and Scullion (1995) to calculate the depth to the rigid layer. The next step consists of determining the seed values for the two nonlinear parameters for each layer based on the type and quality of the material.

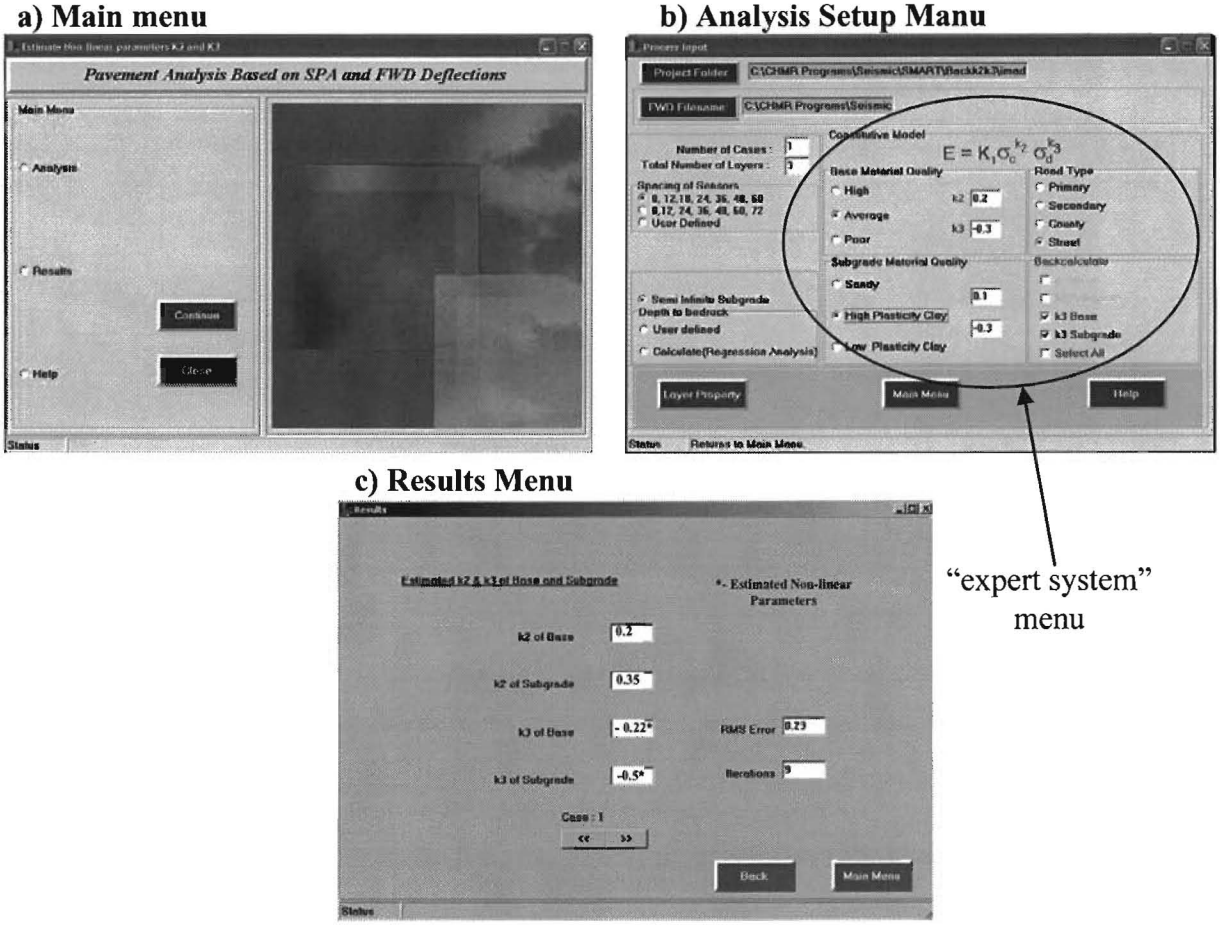

Figure 3.10 – Select Menus from Nonlinear Parameter Estimation Program

A simple "expert system" is built into the program based on studies by Meshkani et al. (2001) to provide recommendations to the user in terms of whether obtaining a reasonable backcalculated parameter is feasible or not. Meshkani et al. (2001) extensively demonstrated the limitations of backcalculating nonlinear parameters for thick and strong pavement structures.

Once the SPA data are retrieved, the results of the analysis are shown automatically in the results menu (see Figure 3.10c). The figure displays k_2 and k_3 values highlighting values the were backcalculated. Also presented in the result menu are the RMS error related to the mismatch between the measured and calculated deflection basins to assess the closeness of the two deflection basins. The values from this program can then be used to calculate the design modulus values of the pavement section being analyzed.

Chapter 4

Validation Process

INTRODUCTION

As in any other validation process, the ultimate goal is to compare the results from the proposed methodology to known and measurable parameters. In this project, the main goal was to determine the validity of using seismic moduli in the algorithms incorporated into SMART to determine the design moduli. Since determining the exact moduli of different pavement layers at a test site is close to impossible, an independent means of assessing the validity of the SMART was needed.

One independent way of assessing the validity of the proposed algorithm is the use of the FWD measurements. An FWD measures a response (seven deflections) of a pavement to a known load. Normally, the load and deflections can be input into a backcalculation program to determine the modulus of each layer. Given the uncertainty associated with the backcalculation process, we attempted to avoid it as a primary validation tool. A more straight forward means of validating the process is to estimate the seven deflections that would have been measured by the FWD using the seismic moduli. Seismic moduli and lab test results were input into SMART to determine the variation in modulus within each layer. Using the moduli suggested by SMART, the seven deflections were then calculated. The closeness between the measured deflection basins and those calculated from the output of SMART was used to determine the appropriateness of the suggested algorithms.

Figure 4.1 illustrates how the validation tasks are related. To obtain all the necessary information, the following main tasks had to be carried out:

a) field testing,
b) lab testing,
c) data analysis and
d) interpretation of results

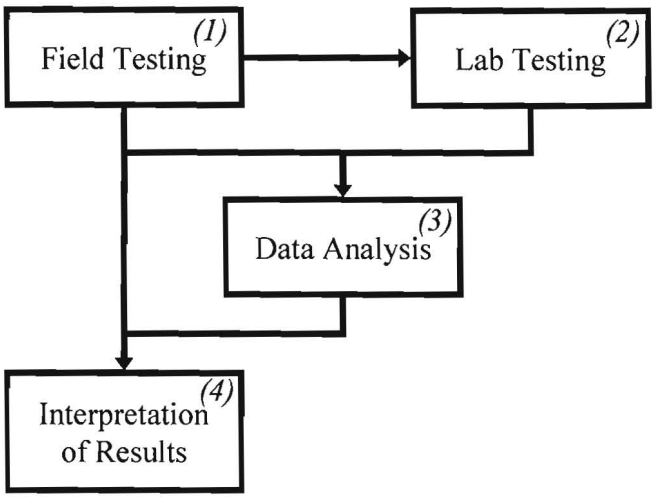

Figure 4.1 - Flowchart of Validation Process

The first task was field testing, which consisted of collecting seismic data, FWD deflections, and retrieving materials for lab testing. The second task was to perform resilient modulus tests on the specimens collected from the test site. The nonlinear parameters from the lab tests and the seismic field data were then used as input to SMART to obtain design modulus profile for each layer (Task 3). As a part of Task 3, the theoretical deflections from the calculated modulus profile were also determined. The final step consisted of comparing the theoretical and experimental deflections. As a secondary task, the moduli from the FWD backcalculation and from SMART were also compared.

The validation process started with the selection of a wide variety of test sites. A matrix of desirable sites, as presented in Table 4.1, was developed to ensure that all flexible pavement sections built in Texas are considered. The pavement sections were first categorized based on the subgrade type (i.e., clayey vs. sandy). Each category was further subdivided into the following four groups: a) thin AC with thin base, b) thin AC with thick base, c) thick AC with thick base, and d) thick-AC with thin base. The range of layer thickness for each pavement section is included in the table. To optimize the use of the resources available for this project, two of the pavement types were eliminated. Pavement sections with thick AC and thin base for both types of subgrades are not common in Texas and therefore not considered in the validation process. These two sections are shaded gray in Table 4.1.

FIELD TESTING

The data collection process consisted of conducting nondestructive tests with the FWD and SPA followed by a trenching operation where material was retrieved for lab testing. The NDT protocol at each site consisted of testing eleven locations each about 30 ft apart. As shown in Figure 4.2, five points were located before the trench, five after the trench, and the eleventh point in the vicinity of the trench. This allowed for the quantification of variations in the material properties along a site. Figure 4.2 also outlines the numbering scheme used in reporting the

Table 4.1 - Matrix of Pavement Sections Used for Validation

Layer Type	Subgrade Type							
Subgrade	Clayey				Subgrade			
Base	Thin (6in. To 8in.)		Thick (12in. To 18in.)		Thin (6in. To 8in.)		Thick (12in. To 18in.)	
AC	Thin (2in. To 4in.)	Thick (6in. To 8in.)	Thin (2in. To 4in.)	Thick (6in. To 8in.)	Thin (2in. To 4in.)	Thick (6in. To 8in.)	Thin (2in. To 4in.)	Thick (6in. To 8in.)

Note: shaded area was excluded as possible test section.

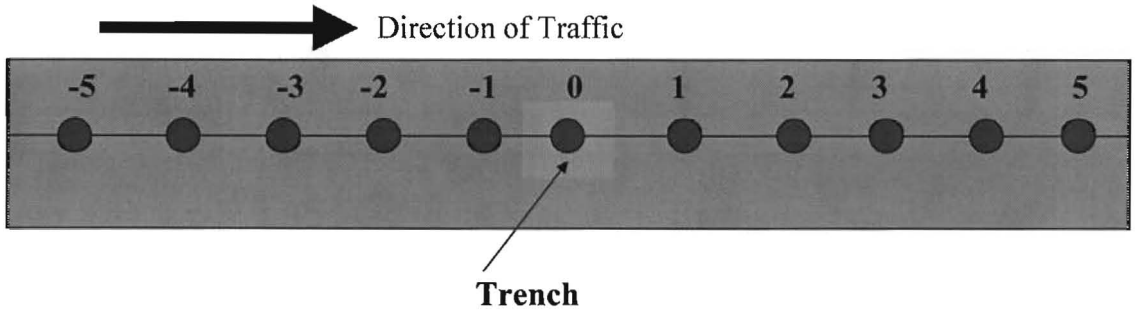

30 ft between each test point

Figure 4.2 - Layout of Test Locations at Each Site

properties along a site. In some of the sites, where trenching was not carried out, more or less than eleven points were tested as it will be discussed in Chapter 5.

NDT Test Equipment and Data Collection

Falling Weight Deflectometer (FWD)

FWD tests were carried out at four load levels at each test point. The measured load and deflections were saved into a file for further analysis. This process was repeated for each test point. The data associated with a load of 9000 lb was extensively used in this study because it simulates the load applied by a typical truck.

Seismic Pavement Analyzer (SPA)

The SPA lowers transducers and sources to the pavement and digitally records surface deformations induced by a large pneumatic hammer which generates low-frequency vibrations, and a small pneumatic hammer which generates high-frequency vibrations (see Figure 4.3). All measurements were performed either shortly before or shortly after the FWD tests at the same points. The main test used in this study is the SASW tests. The SASW method is a seismic method that can nondestructively determine modulus profiles of pavement sections. Detail on the SASW test process can be found in Nazarian et al. (1995).

a) FWD data Collection **b) SPA-SASW data Collection**

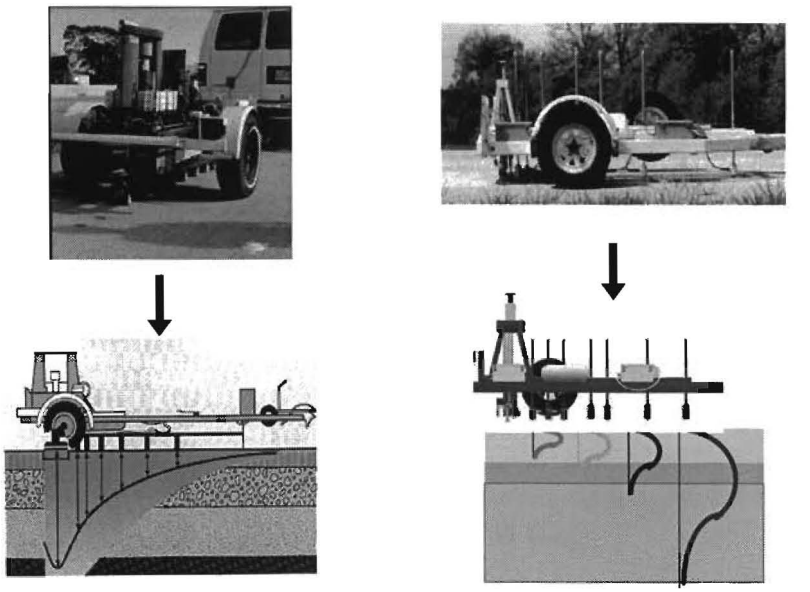

Figure 4.3 - FWD and SPA Data Collection Scheme

Trenching and Sample Collection

The materials necessary for the resilient modulus tests were retrieved from a trench dug in the pavement usually at the center test point. The procedure for collecting the soil samples consists of the following steps:

- Approximately a 3 ft by 12 ft section of AC was removed. This operation was carried out with no or little water to minimize changes to the moisture of base.
- At least five moisture and density tests were carried out on top of the exposed base layer using a nuclear-density device.
- About 600 lbs of the base material was carefully removed and bagged for lab testing.
- Several random specimens were retrieved so that the in-place moisture content of the base can be verified.

- The trench was thoroughly cleaned to the top of the subgrade by removing the excess base material from it.
- About 300 lb of the subgrade material was removed and bagged for lab testing.
- The pavement section was backfilled and repaired.

A few AC cores were also obtained to verify the thickness of the layer.

LABORATORY TESTING

The base specimens were prepared in 6-in. molds in six 2-in. lifts using a standard mechanical hammer following test method Tex-113-E. The material required for preparing a specimen was homogenized at the desired moisture content by adding the required water, thoroughly mixing, and storing for one day. Similar procedure was followed for the subgrade materials but the standard Proctor procedure was followed on 4 in. diameter 8 in. high specimens.

The resilient modulus of the subgrade and base materials were typically determined by applying various deviatoric stresses at different confining pressures in a repeated load triaxial test. The confining pressure was applied by subjecting the specimen to compressed air inside the acrylic cell surrounding the specimen. The pressure was monitored by a pressure gage.

Figure 4.4 shows the resilient modulus test in progress. A half-sine loading waveform with a loading duration of 0.1 seconds and rest period of 0.9 seconds is used. The axial deformations were measured along the middle one-third of the specimen with six non-contact proximetor sensors. The protocol developed by Nazarian et al. (1995) was followed. From the measured axial displacements at a particular deviatoric stress and confining pressure, the resilient modulus of the specimen was determined.

Figure 4.4 - Schematic of Resilient Modulus Test

The constitutive model used to describe the results of the resilient modulus tests is

$$M_R = k_1 \sigma_c^{k2} \sigma_d^{k3.} \quad (4.1)$$

σ_d and σ_c are the deviatoric stress and confining pressure, respectively. Parameters k_1 through k_3 are statistically-determined coefficients. Equation 4.1 is the same as Equation 2.1 described in Chapter 2.

DATA ANALYSIS

In this section, the results from a site located in Waco, Texas are included to clarify the analysis process. The site consisted of about 3 in. of AC over 17 in. of stiff base over a moist clayey subgrade. This site was selected because its results were generally representative of most sites. The site which was located on FM 933 was visited in August, 2001.

The procedure used to analyze the data and test the samples collected from the field is as follows:

- Conduct laboratory resilient modulus tests to determine nonlinear parameters k_2 and k_3 for the base and subgrade,
- Reduce SPA results to determine seismic modulus profile,
- Combine seismic moduli with laboratory-derived k_2 and k_3 to estimate design modulus using SMART,
- Calculate surface deflections from design modulus values using SMART and compare with those measured with the FWD,
- Reduce FWD data to determine effective modulus of each layer,
- Compare the variation in modulus within the base and subgrade with the backcalculated ones, and
- Predict nonlinear parameters k_2 and k_3 for base and subgrade by combining seismic moduli with FWD deflections. This part of the analysis process is included to verify the limitation of backcalculating nonlinear parameters with the two NDT devices.

Each item is elaborated below.

Resilient Modulus

The resilient modulus, as discussed earlier, is used to determine the nonlinear parameters k_2 and k_3 of the base and subgrade. Figure 4.5a demonstrates typical response from bases. As the confining pressure increases, the modulus also increases. Conversely, as the deviatoric stress increases, the modulus decreases. Similar results but for the subgrade are shown in Figure 4.5b for the clayey subgrade. As anticipated, the modulus does not vary much with the confining pressure. The k_2 and k_3 values from Equation 4.1 for the base are 0.50 and -0.30, and for the subgrade are 0.04 and -0.4, respectively.

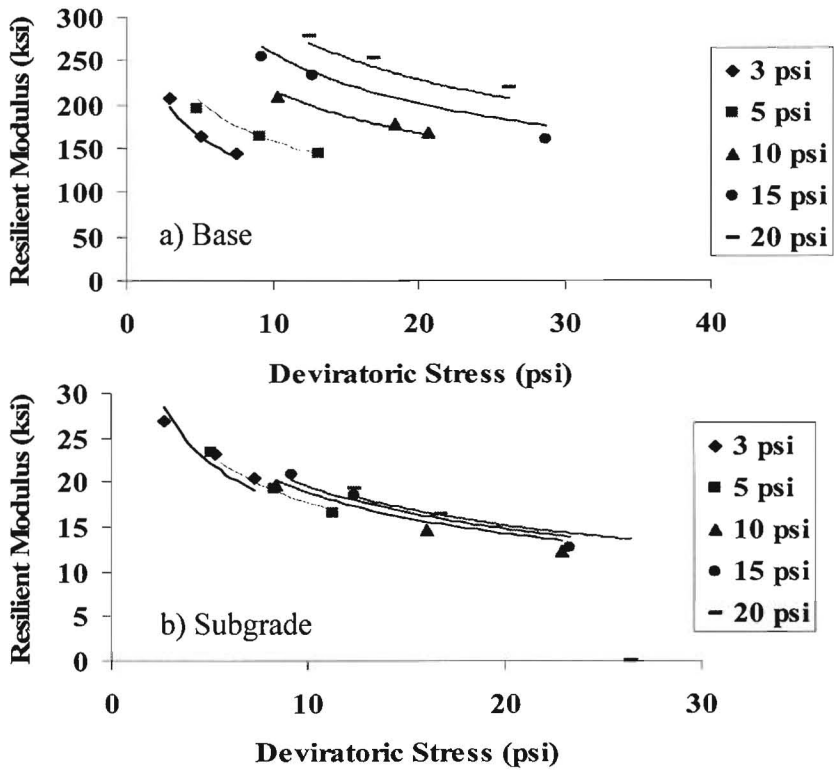

Figure 4.5 - Process for Estimating Nonlinear Parameters Based on Resilient Modulus Test

FWD Analysis

The backcalculation programs MODULUS and EVERCALC were used to estimate the design modulus values of the layers. Even though MODULUS is exclusively used by TxDOT, EVERCALC allows more flexibility over the depth to rigid layer. The FWD deflections measured in the field for FM 933 are presented in Table 4.2. The reported FWD deflections were normalized to 9000 lb using the following equation:

$$d_i^{Normalized} = d_i\left(\frac{9000}{Load_{Actual}}\right) \quad i = 1\,to\,7 \tag{4.2}$$

where d_i is the deflection at sensor i and $Load_{Actual}$ is the load at the time of the test.

The measured deflection bowl at the trench location is compared with the deflection bowls calculated from the two backcalculation programs in Figure 4.6. The backcalculated moduli from each program are also presented in Figure 4.6. The modulus of the AC was fixed since the AC layer was less than 3 in. thick. As shown in the figure, the two theoretical deflections bowls match the measured deflection bowl well with slightly different set of modulus values.

Table 4.2 - Measured FWD Field Data Normalized to 9000 lbs

Point	Deflections (mils)						
	Sensor Spacing						
	0 in.	12 in.	24 in.	36 in.	48 in.	60 in.	72 in.
-5	8.3	4.3	3.2	2.6	2.1	1.7	1.3
-4	7.4	4.2	3.4	2.7	2.3	1.9	1.5
-3	7.9	4.6	3.4	2.6	2.1	1.6	1.3
-2	8.0	4.2	3.0	2.4	1.8	1.5	1.2
-1	6.9	3.7	2.8	2.3	1.8	1.5	1.2
0	6.6	3.6	2.6	2.0	1.5	1.2	1.0
1	5.6	3.3	2.5	2.0	1.6	1.3	1.0
2	5.3	3.2	2.5	1.9	1.6	1.3	0.9
3	6.2	3.7	2.9	1.9	1.4	1.2	0.9
4	5.5	3.1	2.5	2.1	1.6	1.4	1.1
5	8.5	4.2	3.2	2.5	2.1	1.8	1.3
Mean	6.9	3.8	2.9	2.3	1.8	1.5	1.2
Std. Dev.	1.2	0.5	0.3	0.3	0.3	0.2	0.2
C.V.	16.9%	13.3%	11.5%	13.4%	15.5%	16.4%	16.5%

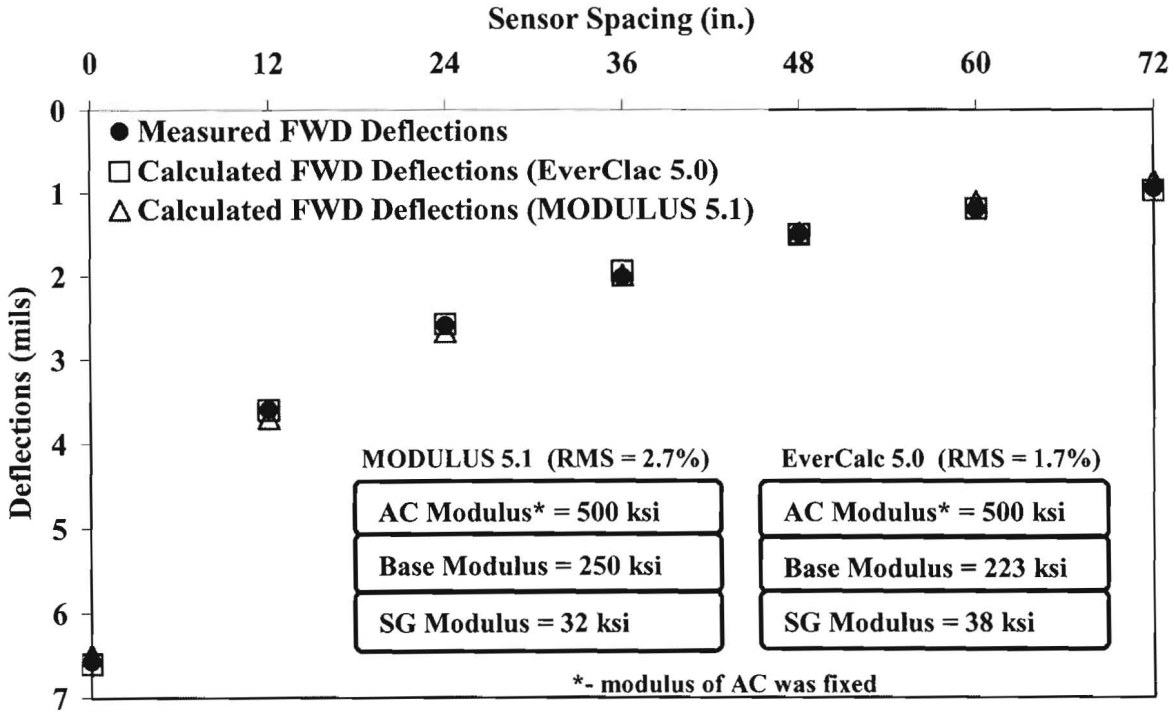

Figure 4.6 - FWD Analysis Process

The results of the FWD backcalculation from both MODULUS and EVERCALC for the remaining points tested at FM 933 are summarized in Table 4.3. The RMS errors, which reflect the closeness of fit between the measured and calculated deflection bowls, are small for all test points. The average base and subgrade moduli from MODULUS are 285 ksi and 27 ksi, respectively and from EVERCALC, 265 ksi and 34 ksi respectively.

Table 4.3 - Results of Backcalculated Design Modulus Values

POINT	Modulus (ksi) using MODULUS 5 .1				Modulus (ksi) using EVERCALC 5.0			
	AC	BASE	SUBGRADE	RMS	AC	BASE	SUBGRADE	RMS
-5	500	215	26	7.0%	500	211	30	4.2%
-4	500	311	22	6.5%	500	308	28	4.1%
-3	500	230	24	3.0%	500	204	30	1.5%
-2	500	206	28	5.1%	500	191	33	2.2%
-1	500	284	28	6.1%	500	276	34	3.6%
0	500	250	32	2.7%	500	223	38	1.7%
1	500	361	30	3.5%	500	330	38	1.6%
2	500	407	29	4.6%	500	355	38	4.5%
3	500	270	31	3.8%	500	229	39	5.2%
4	500	405	28	5.7%	500	396	36	3.7%
5	500	195	24	8.6%	500	196	28	5.8%
Avg.	500	285	27	5%	500	265	34	3%
Std. Dev.	-	77	3	2%	-	72	4	2%
COV	-	27%	12%	36%	-	27%	12%	44%

SPA-SASW Analysis

The reduction of the SASW data is a two step process (see Nazarian et al., 1995). The first step consists of constructing an idealized dispersion curve; variation in phase velocity with wavelength. Once a dispersion curve is determined, an inversion (backcalculation) algorithm is used to estimate the seismic modulus profile of the pavement section. This reduction scheme is performed for each test point.

The dispersion curve and seismic modulus profile at the trench location for FM 933 are presented in Figure 4.7. The measured and calculated dispersion curves are compared in Figure 4.7a. The calculated dispersion curve is generated by the inversion process using the seismic modulus profile depicted in Figure 4.7b. The RMS error and number of iterations in Figure 4.7b refer to the closeness of the fit between the measured and calculated dispersion curves. Table 4.4 present the results for all test points at FM 933. The average, standard deviation and coefficient of variation (COV) are also presented. The results from the seismic reduction process for all sites are presented in Appendix B.

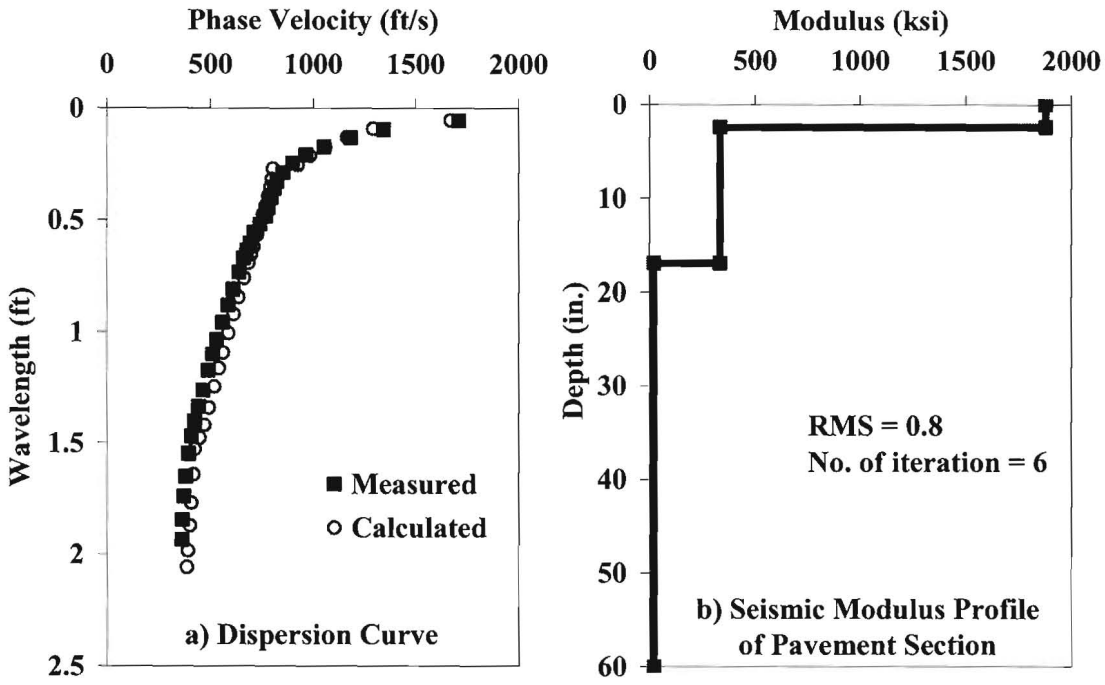

Figure 4.7 - SPA-SASW Data Reduction Processes

Table 4.4 - Results of SASW Data Reduction Process for FM 933

Point	AC		Base		Subgrade
	Modulus (ksi)	Thickness (in.)	Modulus (ksi)	Thickness (in.)	Modulus (ksi)
-5	2267	2.2	346	15.6	30
-4	2070	2.2	375	16.0	26
-3	2199	1.9	276	16.1	28
-2	2094	2.0	276	17.3	25
-1	2028	2.8	348	17.5	23
0	1878	2.4	335	16.9	20
1	2108	2.5	404	16.3	26
2	2133	2.7	385	16.7	32
3	2011	2.6	172	18.2	27
4	1978	2.6	448	16.4	29
5	2240	2.0	286	16.1	29
Avg.	2091	2.4	332	16.7	27
Std. Dev.	117	0.3	76	0.8	3.4
C.O.V.	6%	12%	23%	5%	13%

Analysis with SMART

The next stage in the validation process consisted of introducing the seismic moduli and the results from the laboratory tests (k_2 and k_3 values) into the SMART program. Figure 4.8 shows the overall data flow as used by SMART. The first stage demonstrates the process where SMART retrieves seismic data and nonlinear layer parameters to calculate the variation in design modulus within each pavement layer. In the second stage, seven deflections under a 9000 lb load from the moduli estimated by the SMART are calculated. Two sets of design modulus values (i.e. conservative and average) are also calculated with SMART.

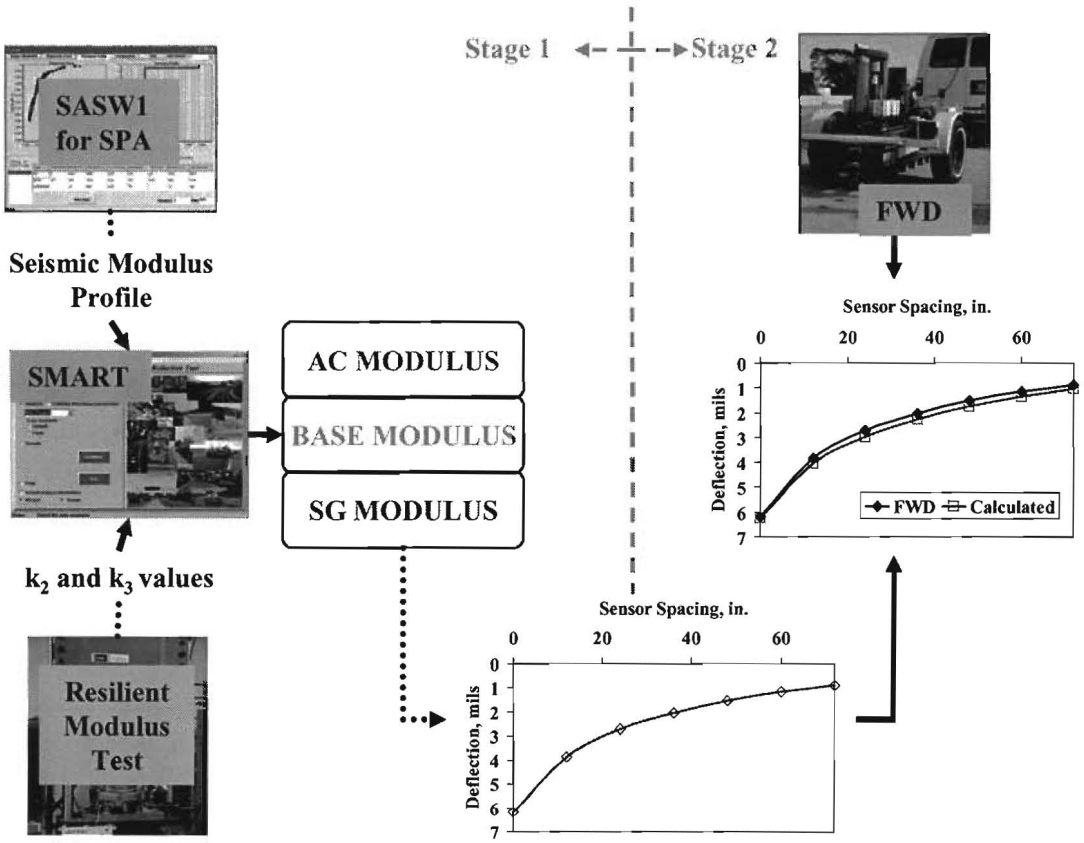

Figure 4.8 - SMART Analysis to Calculate FWD Deflections

Comparison of Deflections

Deflection basins measured with the FWD and those calculated from SMART using nonlinear and linear analyses at the trench point for FM 933 are compared in Figure 4.9. The measured deflections were adjusted to a temperature of 77°F using the temperature correction scheme proposed by Lukanen et al. (2000). At a few sites when the test temperatures were high (>120°F) and the AC layers were thin, the deflection correction scheme would yield unreasonable results (i.e. proposed deflections for Sensor 1 that were greater at 77°F than the test

temperature). In those few cases, the deflections were not adjusted for temperature. Appendix A provides the results of the FWD deflections for all test sites.

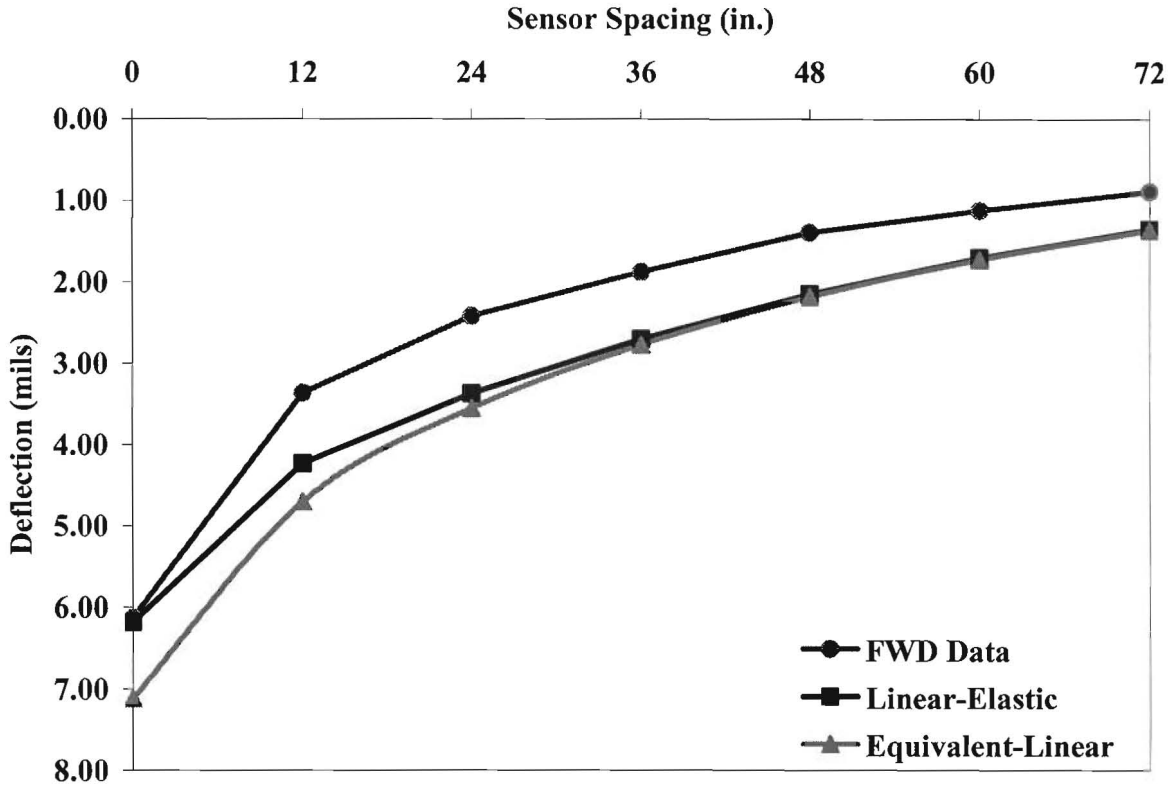

Figure 4.9 - Comparison of Deflection Bowls calculated with SMART to Measured FWD Deflections

The deflections from the linear and nonlinear models without considering depth to a rigid layer are compared in Figure 4.9. The deflections from the last four sensors compare quite well when either the linear or the equivalent-linear model is used. On the other hand, the deflections for the first three sensors from the equivalent linear analysis yield larger deflections as compared to the linear elastic solution. This should be the case since the nonlinear behavior of the layers is only prominent near the load. Farther from the load, the stresses are similar irrespective of the material model used.

In Figure 4.9, the shapes of the FWD and equivalent-linear deflection bowls are similar. However, the calculated and measured deflections are parallel to one another. This can occur because the depth to a rigid layer is ignored. Meshkani et al. (2001) showed that by varying the depth to a rigid layer, the calculated deflection bowl can be shifted to better fit the measured bowl. Also verified in the report is that varying the depth to rigid layer in that manner had no impact on the estimated critical strains and the remaining lives of a pavement. To demonstrate this concept, the deflection bowl was calculated by gradually moving the rigid layer closer to the surface.

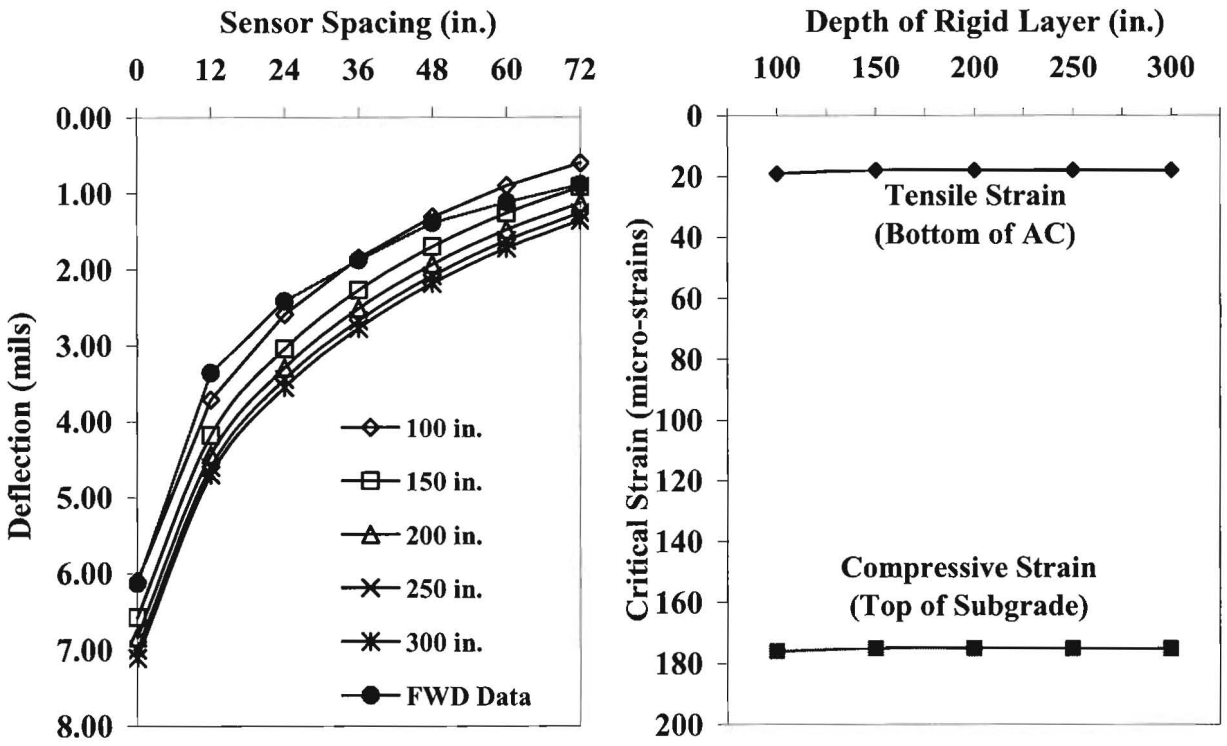

Figure 4.10 - Impact of varying Depth to Rigid Layer

The variation in the deflection bowl by varying the depth to rigid layer from 300 in. (standard option in SMART) to 100 in. is shown in Figure 4.10a. At a depth of 100 in., the calculated deflections agree well with the FWD measurements. Figure 4.10b shows the results of the critical strains with varying depths to rigid layer. The critical strains used to predict remaining life of the pavement do not change. To avoid any bias in the results, this process was not adopted for the validation process. The depth to rigid layer used in the analysis was maintained at a depth defined from the algorithm incorporated in MODULUS for estimating the depth to the rigid layer.

The calculated deflections for the equivalent-linear model for FM 933 site are shown in Table 4.5. The RMS errors with respect to the FWD measurements are also reported. The RMS error for all points except one (point 0) are less than 10%. Similar results are shown for the PI model in Table 4.6. In general, the PI model, which is thoroughly discussed in Research Report 1780-2 (Ke et al. 2002), yields results with slightly higher RMS errors. The subtle difference between the nonlinear model and the PI model is that the deflections near the load from the PI model are typically greater than those from the nonlinear model. As compared to the FWD deflections, the PI model over-predicts the deflections near the load; whereas the nonlinear model under-predicts them. These results are good indications of the applicability of the seismic methods to determine design values that can be used for pavement design and analysis. The average deflections for all test sites calculated from SMART are presented in Chapter 5.

Table 4.5 - Deflection Results from Equivalent-Linear Methods Using SMART

Location	Deflection, mils							RMS Error
	0 in.	12 in.	24 in.	36 in.	48 in.	60 in.	72 in.	
-5	6.18	3.85	2.72	2.03	1.52	1.16	0.89	9%
-4	6.25	4.05	2.97	2.28	1.74	1.35	1.05	8%
-3	7.15	4.31	2.96	2.19	1.63	1.23	0.95	7%
-2	6.99	4.28	3.03	2.29	1.74	1.35	1.05	3%
-1	6.14	4.00	3.02	2.39	1.88	1.49	1.18	2%
0	7.18	4.78	3.59	2.83	2.22	1.75	1.39	15%
1	5.80	3.78	2.84	2.20	1.70	1.33	1.04	4%
2	5.19	3.24	2.36	1.80	1.38	1.06	0.83	4%
3	8.09	4.51	2.93	2.14	1.60	1.22	0.95	6%
4	5.23	3.38	2.55	1.97	1.52	1.19	0.93	3%
5	6.80	4.10	2.83	2.09	1.56	1.18	0.91	8%
Average	6.5	4.0	2.9	2.2	1.7	1.3	1.0	6%
Std. Dev.	0.9	0.5	0.3	0.3	0.2	0.2	0.2	4%
COV	14%	11%	11%	12%	13%	15%	15%	60%

Table 4.6 - Deflection Results from PI Methods Using SMART

Location	Deflection (mils)							RMS Error
	0 in.	12 in.	24 in.	36 in.	48 in.	60 in.	72 in.	
-5	6.71	3.77	2.57	1.95	1.49	1.15	0.89	9%
-4	7.39	4.05	2.84	2.19	1.71	1.33	1.05	8%
-3	7.52	4.24	2.79	2.1	1.6	1.22	0.95	7%
-2	7.56	4.31	2.89	2.21	1.72	1.34	1.05	2%
-1	7.31	4.13	2.94	2.31	1.85	1.47	1.17	2%
0	8.74	4.97	3.49	2.74	2.18	1.74	1.38	15%
1	6.84	3.82	2.73	2.13	1.68	1.32	1.04	4%
2	5.73	3.21	2.26	1.74	1.35	1.06	0.83	5%
3	7.87	4.13	2.74	2.06	1.57	1.21	0.95	5%
4	6.33	3.38	2.45	1.91	1.5	1.17	0.92	4%
5	7.12	4.02	2.66	2.01	1.53	1.17	0.91	9%
Average	7.2	4.0	2.8	2.1	1.7	1.3	1.0	6%
Std .Dev.	0.8	0.5	0.3	0.3	0.2	0.2	0.2	4%
COV	11%	12%	11%	12%	13%	15%	15%	59%

Estimating Design Modulus Values

In the previous section, the deflections obtained from the seismic method were compared to deflections measured with the FWD. The calculated deflections were estimated from the variation in the modulus within each layer. Ke el al. (2000) contains an algorithm to obtain the variation in modulus within a layer. The variation in modulus in each layer calculated by SMART for the FM 933 at the trench location is contoured in Figure 4.11. The top layer was considered as a linear viscoelastic layer, and therefore its modulus is a constant value of 586 ksi. The variations in the modulus values within the base and subgrade layers under a standard dual-tandem axle are also shown in the figure. The modulus of the base layer varies from 200 ksi (located at the bottom of the base under the load) to 320 ksi (located away from the loading area). As for the subgrade the modulus varies from 14 ksi (located near the loaded area) to 20 ksi (located at the bottom of the subgrade). The critical stresses and strains obtained from the interface based on these results will vary significantly from those obtained from the linear analysis. It is therefore evident that considering the load-induced variation in modulus of each layer has a large impact on the estimated remaining life of a pavement.

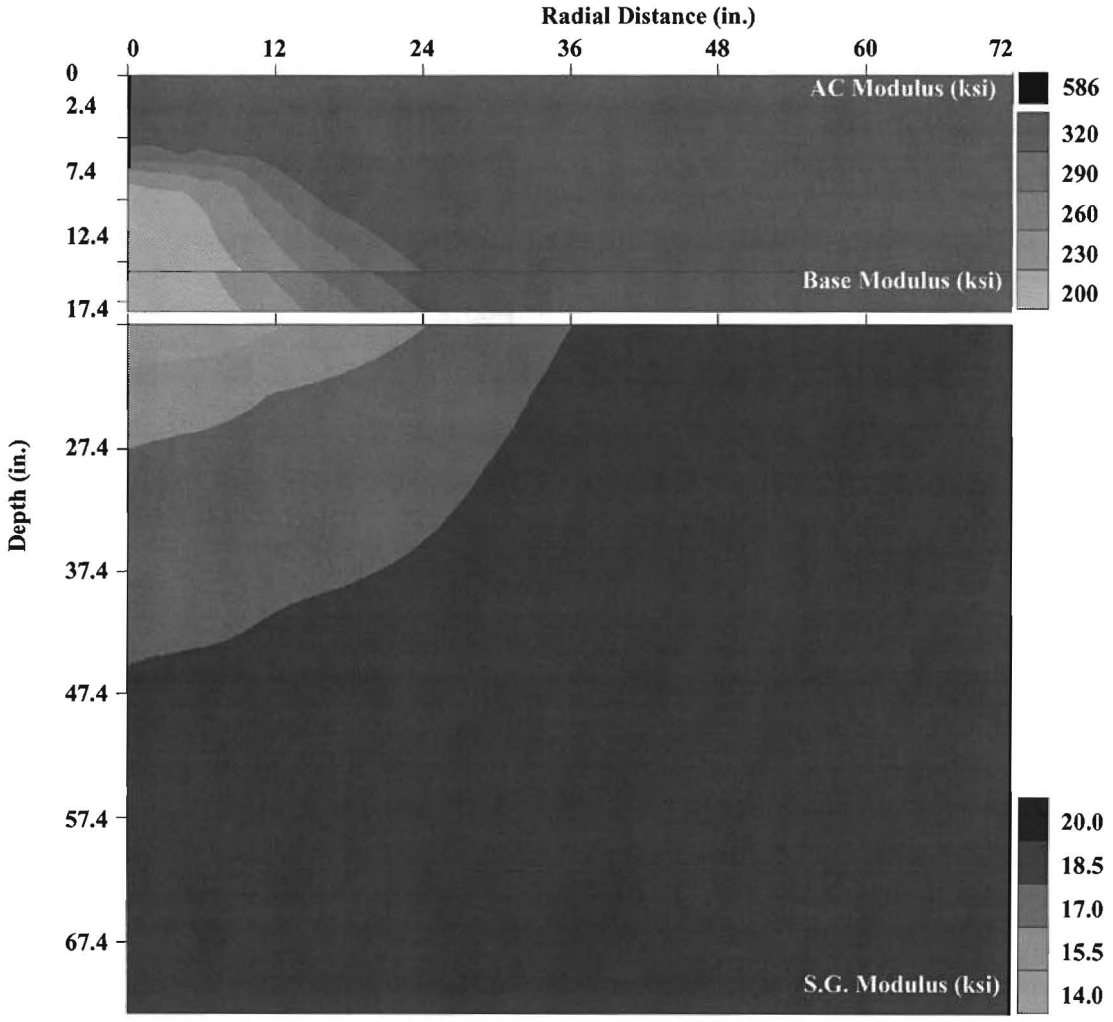

Figure 4.11 - Modulus Profiles Based on a Center Point of FM 933

Although the variation in modulus within each nonlinear layer can be used visually to appreciate the degree of load-induced nonlinearity in the layer, they may not be quantitative enough for engineering design. Therefore, graphs like those shown in Figure 4.11 have to be further summarized.

A schematic of the algorithm used by SMART to provide the design modulus for each layer is shown in Figure 4.12. Upon consultation with TxDOT Project Management Committee for this project, the minimum (conservative) and a weighted average modulus (average) under the load within a layer is provided as an output to the user. For the trench location at FM 933, the design moduli are schematically presented in Figure 4.12. Note that the design moduli are related to the load applied, the thickness of the layers, the nonlinear parameters of the base and subgrade and the viscoelastic behavior of the AC layer.

The modulus values for the entire site are presented in Table 4.7. The table contains both the conservative and average moduli. Users can decide which of the two modulus values to use based on the importance of the project and the required level of confidence of the project. For the FM 933, the minimum design modulus values for the base and the subgrade are about 20% to 30% less than the average values.

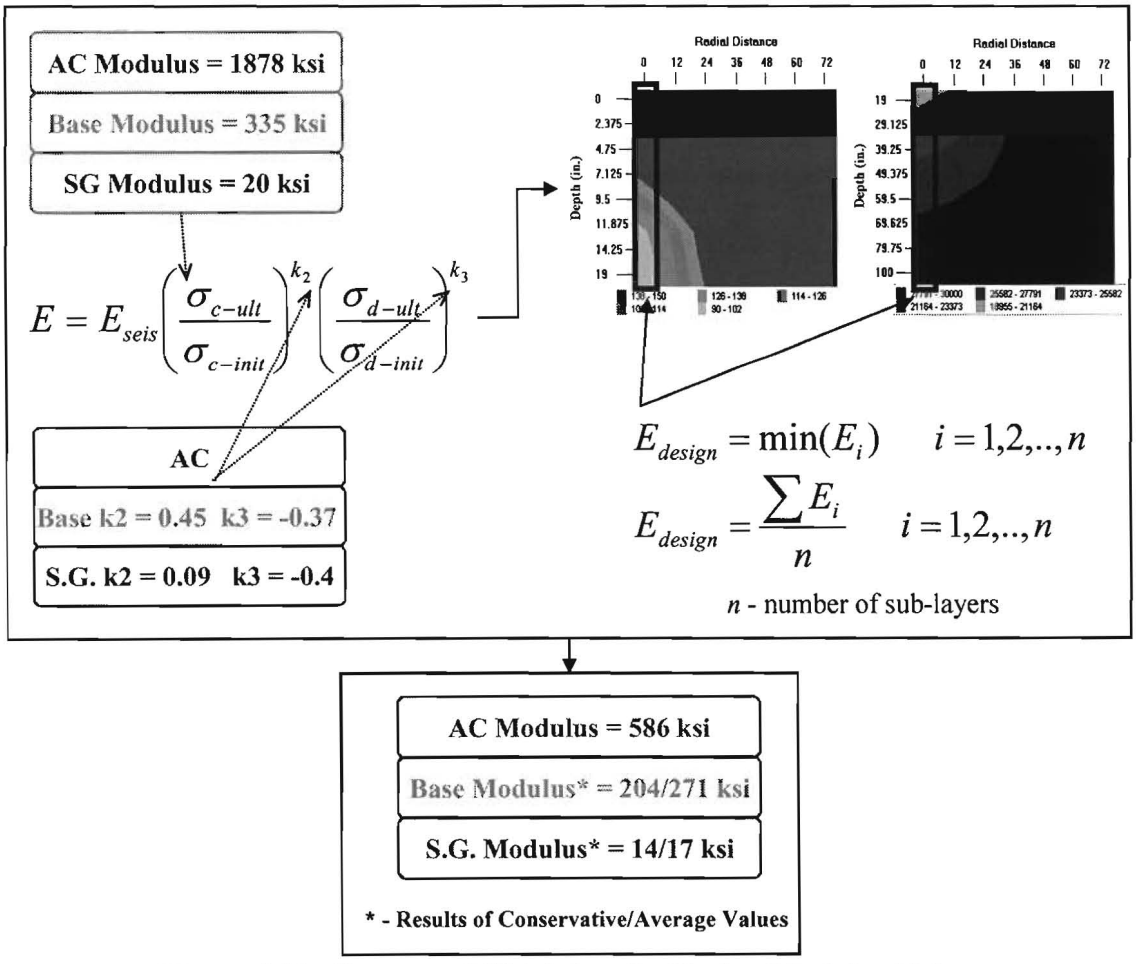

Figure 4.12 - Process of Obtaining the Design Modulus Values

Table 4.7 - Design Moduli from SMART for FM 933 Site

Point	Modulus (ksi)					
	Conservative			Average		
	AC	Base	Subgrade	AC	Base	Subgrade
-5	708	209	19	708	280	26
-4	646	228	17	646	306	22
-3	687	158	18	687	219	24
-2	654	163	16	654	222	21
-1	633	222	16	633	288	20
0	586	204	14	586	271	17
1	658	258	18	658	335	22
2	666	251	21	666	322	28
3	628	93	17	628	133	23
4	618	296	20	618	378	25
5	700	166	18	700	228	25
Avg.	653	204	18	653	271	23
Std. Dev.	37	57	2	37	68	3
COV	6%	28%	11%	6%	25%	13%

As a final summary, the moduli obtained from different tests and different stages of processing for the site are summarized in Table 4.8. The AC layer moduli from the two FWD analysis programs were maintained constant at 500 ksi, were the low-strain seismic modulus is about 2,100 ksi. After the viscoelastic behavior of that layer is considered, the design modulus of about 650 ksi is obtained. The modulus for the base layer from the FWD analysis is about 265 ksi to 290 ksi at this site which is extremely higher than typical base but representative of the site tested. The low-strain seismic modulus of the layer is also high and about 330 ksi. However, when the load-induced nonlinear behavior of the layer is considered, a minimum base modulus of about 204 ksi is estimated near the subgrade layer with an average modulus of about 270 ksi as the weighted average modulus of the layer. For the subgrade, the FWD deflections yield a modulus of about 27 ksi to 34 ksi, which is similar to the subgrade modulus of about 27 ksi low-strain seismic modulus estimated by the SPA. The load-induced nonlinear analysis with SMART yields a minimum modulus of about 18 ksi with an average modulus of 23 ksi. The significance of this case study is that the seismic analysis can yield moduli that can estimate the measured deflection basin with a reasonable closeness, at the same time it provides a means of incorporating the nonlinear behavior of the layer in a more rational manner.

Table 4.8 - Summary of Results from FM 933 Study

Layer	Modulus, ksi				
	FWD		SASW	SMART	
	Modulus	EVERCALC		Conservative	Average
AC	500	500	2091	653	653
Base	285	265	332	204	271
Subgrade	27	34	27	18	23

Estimation of Nonlinear Parameters of Base and Subgrade

As stated before, the nonlinear parameters of the base and subgrade were also estimated using the FWD deflections and the seismic modulus values. A detailed description of this algorithm can be found in Meshkani et al. (2001). This analysis was incorporated as a module in SMART.

The algorithm for extracting the nonlinear parameters of the base and subgrade are briefly sketched in Figure 4.13. The process begins with extracting the NDT information such as the FWD deflection and the seismic modulus profile at each point into the software. The algorithm then calculates a deflection bowl using the seismic moduli and seed values for k_2 and k_3. The calculated deflections are compared with the measured deflections. An error minimization routine is then used to reach at the most suitable nonlinear parameter. The program is capable of estimating up to four nonlinear parameters, two for each layer.

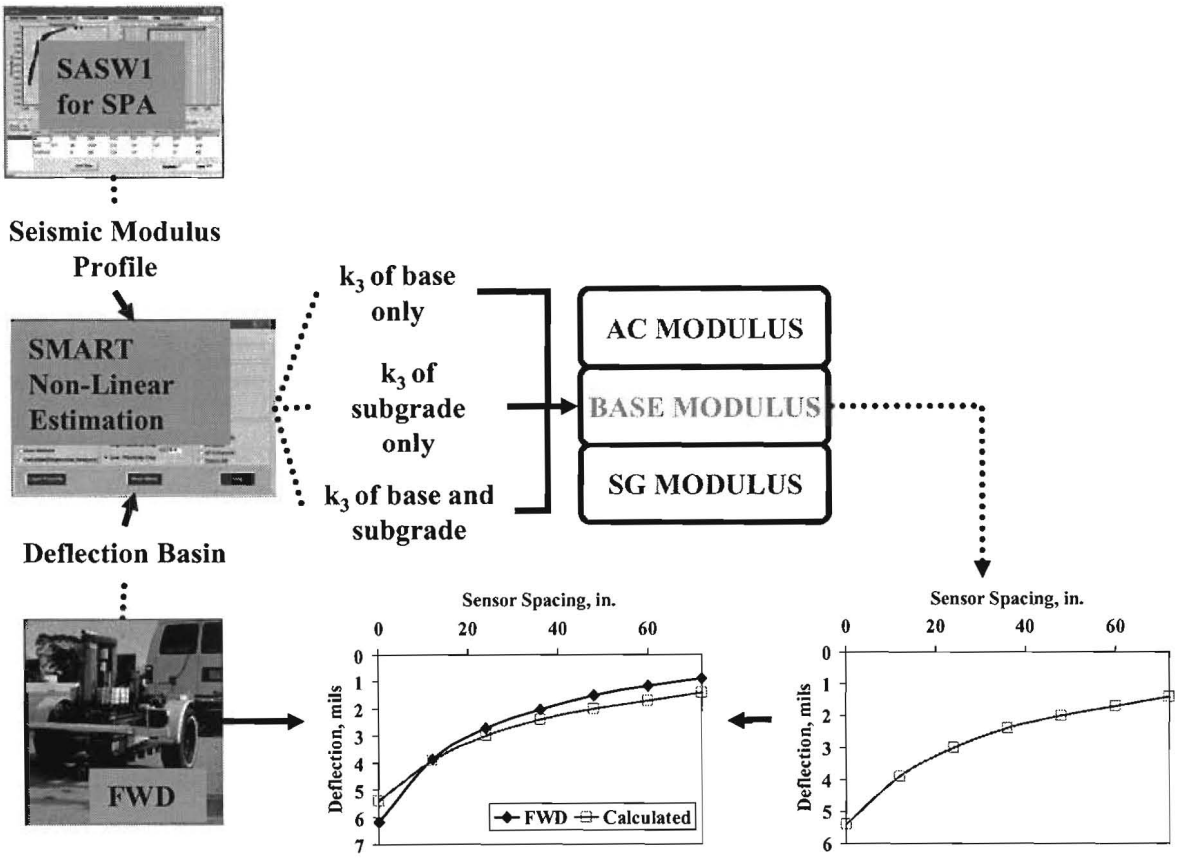

Figure 4.13 - Schematic Algorithm for Estimation of Nonlinear Parameters of Base and Subgrade

Meshkani et al. (2001) concluded that in most cases, the FWD deflection basins are not sensitive to the parameters k_2 of the base and subgrade. As such only k_3 for the base and subgrade were estimated. The extraction of nonlinear parameters was carried out in the following three fashions:

a) the k_3 of the subgrade was assumed as constant and the k_3 of the base was extracted,
b) the k_3 of the subgrade was extracted and the k_3 of the base was assumed as constant, and
c) both k_3 of the base and subgrade were extracted.

Values measured in the lab were assigned to those layer parameters that were not being extracted The variations in the deflection basins from the three backcalculation processes for the trench location at FM 933 site is presented in Figure 4.14. The calculated deflections seem to compare well with the measured deflections. Item c above was also repeated with the default values for k_2 values of base and subgrade. Again, a reasonably close comparison was obtained between the measured and calculated deflections.

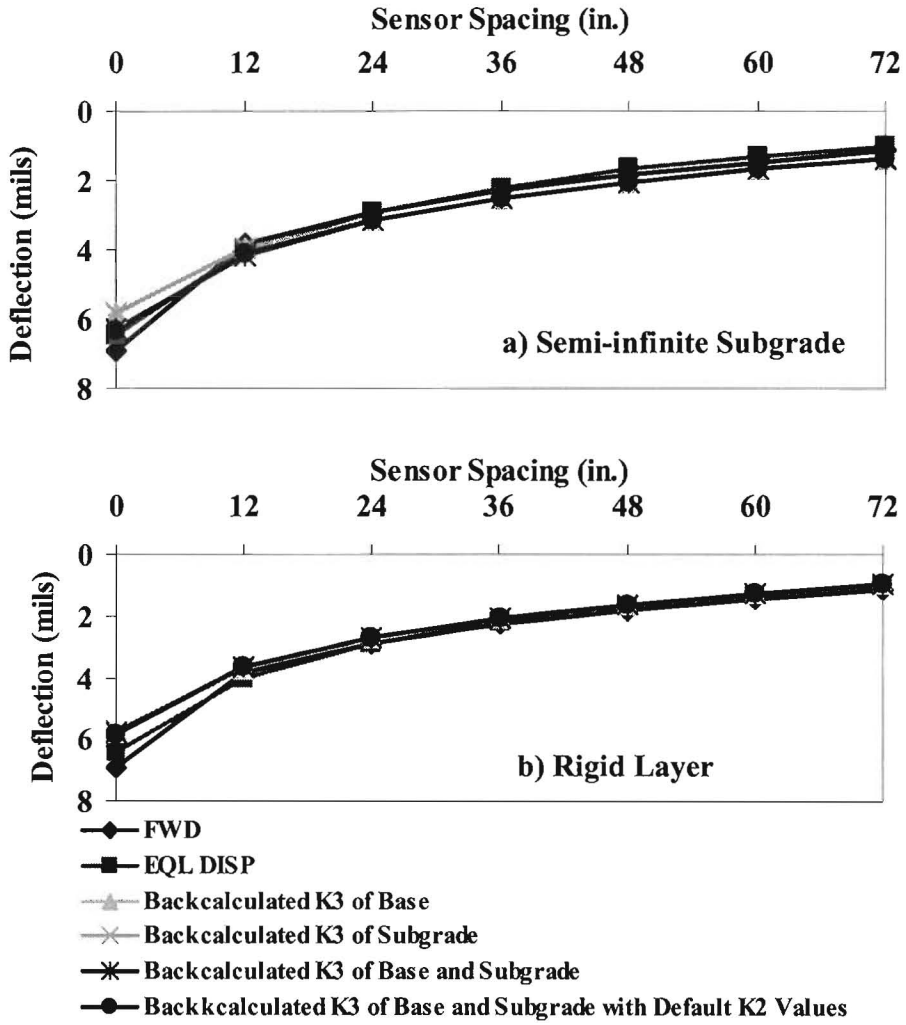

Figure 4.14 - Comparison of Calculated Defections with Measured FWD Deflections after Completion of Estimation of Nonlinear Parameters

The backcalculated nonlinear parameters along with the RMS error after the completion of the backcalculation process are presented in Table 4.9. The analysis was carried out in two ways by ignoring depth to the rigid layer and by considering it at the depth that MODULUS algorithm estimates its existence. When the depth to the rigid layer was not considered, the RMS error was about 4% in all cases; however, when the depth to the rigid layer was considered the error was reduced to about 1%. The estimated nonlinear parameters in some cases were somewhat close. In most cases, the returned parameter was close to the maximum or minimum values allowed for the parameters. In most cases, the parameters k_3 of the base was returned as -0.5 whereas the measured value was closer to -0.3. On the other hand the parameters k_3 of the subgrade was returned as either -0.3 or -0.5 whereas the measured values was -0.4

Table 4.9 - Estimation of Nonlinear Parameter k_3 for FM 933 Trench Point

a) With Semi-infinite Subgrade

Case	Base		Subgrade		No. of Iterations	RMS Error
	k_2	k_3	k_2	k_3		
Backcalculation for k_3 of Base	0.5	0	0.04	-0.4	11	3.91
Backcalculation for k_3 of Subgrade	0.5	-0.3	0.04	-0.3	11	3.85
Backcalculation for k_3 of Base & Subgrade	0.5	-0.5	0.04	-0.5	3	4.02
Backcalculation for k_3 of Subgrade with Default k_2 Values	0.4	-0.49	0.1	-0.5	3	4.01
Measured in Lab	0.5	-0.3	0.04	-0.40	--	--

b) With Rigid Layer at Depth of 100 in.

Case	Base		Subgrade		No. of Iterations	RMS Error
	k_2	k_3	k_2	k_3		
Backcalculation for k_3 of Base	0.5	-0.50	0.04	-0.40	11	1.16
Backcalculation for k_3 of Subgrade	0. 5	-0.3	0.04	-0.50	11	1.21
Backcalculation for k_3 of Base & Subgrade	0.5	-0.50	0.04	-0.3	11	1.18
Backcalculation for k_3 of Subgrade with Default k_2 Values	0.40	-0.50	0.1	-0.32	11	1.1
Measured in Lab	0.5	-0.3	0.04	-0.40	--	--

Chapter 5

Presentation of Results

INTRODUCTION

The validation process described in Chapter 4 was applied to a number of sites to determine the reasonableness of the program SMART. The detailed results from each step of the analysis are included in Appendices A through F. In this chapter the results are summarized, categorized and analyzed.

LOCATION OF SITES

The selected sites were located in six districts consisting of Beaumont, Dallas, Fort Worth, El Paso, Odessa and Waco. In addition, eight section of the so-called Forest Service Road (FSR) test track located in the facilities within the Engineering Research and Development Center (ERDC) of the Army Corps of Engineers in Vicksburg Mississippi were tested.

The site identification and pavement structure for all test sections are included in Table 5.1. For the most part, the focus of the study was on flexible pavements with granular bases over subgrade. However, in a few cases, pavements consisting of more than three layers with some treatment agents were tested. For the US 67, Dallas Site, a layer of select fill was placed as a fill layer, while the SH 73, Beaumont site contained a relatively thick subbase layer. Several of the Forest Service Road sites at ERDC were simply an AC layer over subgrade.

Originally, the goal was to focus on newly-constructed sites. However, only two sites, Waco and Dallas, fit that category. The other Texas sites were tested in conjunction with other research projects or forensic activities. The condition of each site is briefly described in Table 5.1.

As indicated before, the detailed results of the analyses at each point tested for each site can be found in appendices A through F. In most cases eleven test points were considered as discussed

Table 5.1 - Test Sites Used in Validation Process

District	Site	Layer Thickness (in.)			Nature of Material			Remarks
		AC	Base	Subbase	Base	Subbase	Subgrade	
Beaumont	SH 73	3.1	10	24	Granular (0)	Clayey (60)	Clay (50)	Forensic Site, premature cracking, distressed area was avoided
Dallas	US 67	6.0	13	9	Granular(10)	Select Fill(50)	Clay (50)	Brand New Construction
Fort Worth	FM 2738	2.0	6	--	Granular (0)	--	Clay (60)	Old construction, concerns with the quality of base, some distress observed
	FM 2415	2.2	7	--	Granular (0)	--	Clay (60)	
	FM 51	1.9	7	--	Granular (0)	--	Clay (60)	
El Paso	Loop 375	3.0	10	--	Granular (6)	--	Sand (0)	Forensic Site, distressed, original test with FWD indicated poor base, investigation indicated debonding of adjacent AC layers
	MLK	2.0	15	--	Granular (6)	--	Sand (0)	Forensic Site, distressed, distressed area could not be avoided
Odessa	IH 20	7.0	17	--	Granular (0)	--	Clay (60)	Forensic Site, distressed, distressed area was avoided
Waco	FM 933	2.0	17	--	Granular(10)	--	Clay (50)	Brand New Construction
ERDC	Item 5	2.2	6	--	Granular (0)	--	Clay (60)	About 15 year old construction, distressed due to loading and environment, some indications of stripping in the AC layer
	Item 6	2.4	8	--	Granular (0)	--	Clay (60)	
	Item 7	3.9	--	--	--	--	Clay (60)	
	Item 8	3.9	8	--	Granular (0)	--	Clay (60)	
	Item 9	4.1	6	--	Granular (0)	--	Clay (60)	
	Item 10	3.9	4	--	Granular (0)	--	Clay (60)	
	Item 11	5.0	--	--	--	--	Clay (60)	
	Item 12	4.3	--	--	--	--	Clay (60)	
	Hangar 4	2.1	4	--	Granular (0)	--	Clay (60)	Brand New Construction

Note: Values in parenthesis are the PI of the layer

in Chapter 4. For the FSR sites, test points were placed at 25 ft intervals. Since the lengths of the sections varied between 75 ft and 150 ft, between 4 to 6 points are available for each section. For the two El Paso sites, the FWD tests program derived the data collection with the SPA. It should also be mentioned that the SPA and FWD tests were carried out a few days apart at these two sites because of scheduling conflict.

NONLINEAR PARAMETERS

The results from the resilient modulus tests on the materials retrieved from the field are summarized in Table 5.2. The table contains the nonlinear parameters k_2 and k_3 used in the validation process for each material as well as the associated coefficient of determination (R^2) calculated from the curve-fitting process. In general, the coefficients of determination are above 0.9 indicating that the nonlinear model presented in Chapter 4 is representative of the collected data.

Table 5.2 - Nonlinear Parameters Used in the Validation Process

District	Site	Nonlinear Parameters.					
		Base/ Subbase			Subgrade		
		k_2	k_3	R^2	k_2	k_3	R^2
Beaumont	SH 73	0.43/0.6	-0.02/-0.3	0.97/0.99	0.33	-0.55	0.99
Dallas	US 67	0.67/0.25	0/-0.22	0.99/0.96	0.66	-0.06	0.99
Fort Worth	FM 2738	0.26	-0.12	0.91	0.12	-0.49	0.96
	FM 2415	0.49	-0.35	0.98	0.15	-0.36	0.92
	FM 51	0.24	-0.09	0.92	0.17	-0.35	0.94
El Paso	Loop 375	0.2	-0.25	0.95	0.32	-0.36	0.99
	MLK	0.1	-0.4	-	0.4	-0.2	-
Odessa	IH 20	0.52	-0.09	0.99	0.1	-0.5	-
Waco	FM 933	0.50	-0.30	0.98	0.04	-0.40	0.97
ERDC	All Items	0.70	-0.08	0.92	0.00	-0.11	0.96
	Hangar 4	0.34	-0.22	0.97	0.00	-0.11	0.96

Note - Shaded areas correspond to cases that the nonlinear parameters have to be assumed

For the FSR sites, the resilient modulus tests were carried out on samples retrieved from an unpaved area of the track about 1000 ft away from the sections tested since trenching of the facility was not prudent. Even though the ERDC staff ensured us that only one base was used through out the project, this could not be validated. The nonlinear parameters of the subgrade for the ERDC site were obtained from specimen prepared from materials stockpiled by ERDC staff, and not from the site.

For the MLK site, nonlinear parameters from literature was used since no trenching activity was carried out. Also for the Odessa site, since the subgrade was too thin, no specimen was retrieved and typical values from literature was used.

FALLING WEIGHT DEFLECTOMETER RESULTS

The deflections measured at each site are included in Appendix A. The average deflections at each site with corresponding coefficients of variation (COVs) are included in Table 5.3. The deflections vary significantly between the sites. The coefficients of variation associated with each deflection also vary significantly. For some sites such as US 73 the COV of deflections are less than 5% indicating a reasonably uniform site; whereas for some of the FSR sites the COVs are greater than 25% indicating significant variability in properties within the site.

The backcalculated moduli with MODULUS and EVERCALC are included in Appendix B. The average moduli at each site are included in Table 5.4. The moduli of the AC layers varied from 300 ksi to 1600 ksi. For the AC layers thinner than 3 in., the moduli were set to a constant value of 500 ksi.

The moduli of the base layers varied from a low of 9 ksi to a high of about 1750 ksi. Typical COV of the base moduli at a given site is about 30% to 40%. The moduli of the subgrade layer seem to agree better between the two backcalculation algorithms except in a few occasions.

The average RMS errors after the completion of backcalculation process for each site from each backcalculation program are also included in Table 5.4. The RMS errors varied from 1% to 35% for MODULUS and 1% to 54 % for EVERCALC. Two sites, FM 2378 and FSR Item 6, were difficult to backcalculate with EVERCALC; while the Hangar 4 site deflection basin could not be reduced because of the nature of the deflection basin measured. The deflections measured with sensors 4 and 5 were smaller than those measured with sensors 6 and 7.

SEISMIC MODULI FROM SEISMIC PAVEMENT ANALYZER

The average modulus and thickness of each pavement layer along with their coefficients of variation for all sites are included in Table 5.5. The detailed results for each point test for all sites are included in Appendix C.

In general, the moduli of the AC layers are measured with small variability. The coefficients of variation range from 1% to 8%. The moduli vary from 1000 ksi to 2500 ksi, which are typical of seismic moduli measured for AC layers. These values are larger than reported by other devices, since they are representative of the linear-elastic, high frequency moduli of the layers.

Table 5.3 - Summary of Deflections Measured at Different Sites

District	Site	Average Deflection (mils) (COV)						
		0 in.	**12 in.**	**24 in.**	**36 in.**	**48 in.**	**60 in.**	**72 in.**
Beaumont	SH 73	17.8 (3%)	11.5 (5%)	6.9 (7%)	3.9 (6%)	2.7 (7%)	2.1 (8%)	1.8 (11%)
Dallas	US 67	10.9 (11%)	5.9 (11%)	3.7 (14%)	2.7 (17%)	2.2 (18%)	1.8 (19%)	1.5 (19%)
Fort Worth	FM 2738	22.0 (11%)	11.9 (11%)	6.2 (13%)	2.8 (15%)	1.9 (11%)	1.5 (10%)	1.2 (8%)
	FM 2415	28.8 (9%)	17.1 (9%)	8.4 (15%)	4.4 (12%)	2.8 (14%)	2.1 (16%)	1.6 (17%)
	FM 51	23.7 (12%)	12.6 (11%)	5.4 (12%)	3.1 (10%)	2.0 (9%)	1.7 (47%)	1.1 (13%)
El Paso	Loop 375	19.6 (25%)	9.5 (26%)	3.3 (24%)	1.9 (22%)	1.4 (17%)	1.1 (14%)	0.9 (15%)
	MLK	20.7 (12%)	9.0 (25%)	3.9 (22%)	2.5 (21%)	1.8 (21%)	1.4 (20%)	1.1 (22%)
Odessa	IH 20	5.7 (28%)	4.0 (26%)	2.1 (25%)	1.2 (26%)	0.7 (31%)	0.5 (35%)	0.3 (37%)
Waco	FM 933	6.9 (17%)	3.8 (13%)	2.9 (12%)	2.3 (13%)	1.8 (16%)	1.5 (16%)	1.2 (17%)
ERDC	Item 5	28.2 (10%)	16.7 (10%)	4.3 (19%)	2.9 (21%)	2.2 (24%)	1.8 (23%)	1.5 (24%)
	Item 6	26.1 (2%)	15.6 (1%)	4.3 (12%)	2.8 (9%)	2.4 (6%)	1.9 (8%)	1.6 (9%)
	Item 7	18.7 (7%)	12.2 (9%)	4.2 (9%)	2.1 (5%)	1.6 (3%)	1.4 (5%)	1.2 (5%)
	Item 8	22.9 (13%)	14.9 (14%)	5.8 (13%)	3.5 (18%)	2.7 (21%)	2.1 (20%)	1.8 (19%)
	Item 9	12.0 (6%)	5.6 (9%)	4.4 (7%)	2.6 (8%)	1.8 (7%)	1.4 (7%)	1.1 (6%)
	Item 10	27.3 (22%)	18.4 (25%)	9.5 (33%)	5.1 (31%)	3.7 (25%)	2.9 (23%)	2.5 (22%)
	Item 11	17.6 (10%)	11.9 (10%)	5.4 (14%)	3.2 (14%)	2.3 (13%)	1.8 (12%)	1.5 (13%)
	Item 12	15.5 (8.5%)	9.9 (8%)	4.4 (9%)	2.6 (8%)	1.9 (10%)	1.5 (11%)	1.3 (12%)
	Hangar 4	78.7 (4%)	26.2 (6%)	2.6 (58%)	2.4 (50%)	2.9 (13%)	2.2 (10%)	1.7 (18%)

Table 5.4 - Modulus Profile from FWD Backcalculation

District	Site	Modulus from MODULUS (ksi)				Modulus from EVERCALC (ksi)			
		AC	Base/Subbase	Subgrade	RMS Error	AC	Base/Subbase	Subgrade	RMS Error
Beaumont	SH 73	1446*(14%)*	9/88*(7%/24%)*	10*(6%)*	4%	1838*(13%)*	21/10*(29%/34%)*	18*(7%)*	4%
Dallas	US 67	334*(55%)*	46/329*(37%/102%)*	24*(17%)*	1%	325*(51%)*	43/636*(33%/74%)*	18*(17%)*	1%
Fort Worth	FM 2738	500*(0%)*	114*(19%)*	9*(14%)*	21%	500*(0%)*	37*(15%)*	9*(0%)*	>100%
	FM 2415	424*(51%)*	80*(83%)*	8*(17%)*	11%	1810*(11%)*	14*(22%)*	8*(0%)*	88%
	FM 51	500*(0%)*	54*(18%)*	12*(9%)*	12%	500*(0%)*	34*(21%)*	15 *(0%)*	56%
El Paso	Loop 375	500*(0%)*	57*(80%)*	15*(23%)*	29%	500*(0%)*	25*(79%)*	39*(17%)*	7%
	MLK	500*(0%)*	31*(15%)*	23(25%)	11%	500(*0%)*	28*(31%)*	28*(8%)*	17%
Odessa	IH 20	1050*(46%)*	83*(27%)*	4*(30%)*	8%	1602*(45%)*	25*(33%)*	106*(30%)*	5%
Waco	FM 933	500*(0%)*	285*(27%)*	27*(12%)*	5%	500*(0%)*	265(27%)	34*(13%)*	4%
ERDC	Item 5	1030*(26%)*	31*(28%)*	8*(18%)*	35%	1385*(11%)*	15*(13%)*	12*(0%)*	54%
	Item 6	819*(19%)*	31*(32%)*	8*(13%)*	33%	1000*(0%)*	20*(5%)*	9*(0%)*	>100%
	Item 7	596*(20%)*	-	9*(5%)*	24%	13*(27%)*	-	21*(4%)*	21%
	Item 8	408*(9%)*	28*(14%)*	10*(18%)*	17%	572*(26%)*	17*(29%)*	14*(0%)*	33%
	Item 9	56*(5%)*	1759*(34%)*	22*(7%)*	4%	187*(153%)*	825*(71%)*	29*(3%)*	8%
	Item 10	727*(15%)*	71*(52%)*	13*(22%)*	10%	1031*(21%)*	10*(63%)*	20*(17%)*	7%
	Item 11	790*(13%)*	-	12*(15%)*	17%	298*(16%)*	-	22*(12%)*	9%
	Item 12	1449*(22%)*	-	14*(8%)*	21%	431*(24%)*	-	26*(9%)*	8%
	Hangar 4*	146*(22%)*	4*(0%)*	12*(16%)*	62%	-	-	-	-

Note – the COV values are in parenthesis

*** - Evercalc values are not available due to erratic FWD deflection bowl**

Table 5.5 - Modulus Profile from SASW Tests

District	Site	Seismic Modulus (ksi) (COV)			Thickness (in.) (COV)	
		AC	Base/ Subbase	Subgrade	AC	Base/ Subbase
Beaumont*	SH 73	1435 *(4%)*	79/43/29 *(19%/17%/22%)*	13 *(11%)*	3.1 *(3%)*	5/5/9 *(0%/0%/0%)*
Dallas	US 67	1433 *(7%)*	50/39 *(17%/24%)*	24 *(23%)*	5.7 *(3%)*	13/9 *(0%/0%)*
Fort Worth	FM 2738	1099 *(4%)*	118 *(8%)*	22 *(12%)*	2.0 *(10%)*	6 *(4%)*
	FM 2415	1041 *(8%)*	85 *(16%)*	19 *(15%)*	2.2 *(9%)*	7 *(5%)*
	FM 51	970 *(4%)*	128 *(23%)*	27 *(18%)*	1.9 *(10%)*	7.3 *(3%)*
El Paso	Loop 375	1002 *(8%)*	120 *(24%)*	37 *(12%)*	3.1 *(7%)*	10 *(4%)*
	MLK	1075 *(8%)*	147 *(31%)*	33 *(11%)*	2.1 *(16%**)*	14 *(6%)*
Odessa	IH 20	2073 *(6%)*	88 *(22%)*	27 *(20%)*	6.7 *(6%)*	17 *(3%)*
Waco	FM 933	2504 *(6%)*	327 *(24%)*	27 *(12%)*	2.4 *(12%)*	17 *(5%)*
ERDC	Item 5	1368 *(3%)*	75 *(49%)*	22 *(23%)*	2.2 *(4%)*	6 *(3%)*
	Item 6	1316 *(1%)*	75 *(38%)*	22 *(10%)*	2.4 *(9%)*	8 *(1%)*
	Item 7	1291 *(3%)*	-	26 *(26%)*	3.9 *(4%)*	-
	Item 8	1340 *(10%)*	56 *(10%)*	19 *(21%)*	3.8 *(4%)*	8 *(3%)*
	Item 9	1446 *(3%)*	50 *(14%)*	30 *(23%)*	4.1 *(7%)*	6 *(3%)*
	Item 10	1451 *(5%)*	31 *(19%)*	25 *(22%)*	3.9 *(5%)*	4 *(5%)*
	Item 11	1369 *(2%)*	-	26 *(12%)*	5.0 *(5%)*	-
	Item 12	1417 *(4%)*	-	30 *(15%)*	4.3 *(6%)*	-
	Hangar 4	1293 *(1%)*	39 *(23%)*	24 *(8%)*	2.1 *(7%)*	4 *(4%)*

*** - Beaumont was analyzed with two bases, one subbase over subgrade**

**** - This value misleading (Appendix C shows that 22 out of 25 test points measured thickness of AC at 2 in.)**

The base moduli vary significantly between the sites from a low of about 30 ksi to a high of about 300 ksi. The coefficients of variation vary from about 8% to about 50% with a typical variation of about 20%. This is typical trends that are measured for base moduli with the seismic method.

Subgrade moduli are also quite variable from a low of about 10 ksi to a high of about 40 ksi. The COV of the subgrade moduli ranges from 5% to 30% with a typical value of about 20%. The softest subgrade is from SH 73 from Beaumont with a modulus of 13 ksi.

The thickness of the AC and base reported from the SASW tests are consistent with those measured at the test pits. The largest COV reported was for the thickness of the AC at MLK with a value of 16 %. This value is misleading since the thickness of AC for 22 out of 25 points tested was determined at 2.0 in. for MLK test site (see Appendix C). For US 73 and US 67, the thickness of the base and subbase were too thin to be distinguishable. As such they were considered as constants.

RESULTS OF SEISMIC ANALYSIS USING SMART

The next step in the validation process consisted of determining the deflection basins from the SASW moduli and the nonlinear parameter of each layer using the program SMART. Based on the nonlinear parameters included in Table 5.2 and seismic moduli included in Table 5.5, the deflections that would have been measured with an FWD under a load of 9000 lb were calculated and compared to the measured deflections. The RMS error was used as a measure of the closeness of the calculated and measured deflections.

Deflections obtained using SMART at all sites are included in Table 5.6. The RMS error shows an average value of 11% ranging from a minimum of 5% at FM 2378 and a maximum of 30% at Hangar 4 site. The reasons for differences between the measured and calculated deflections, aside from uncertainty in the analysis and errors in the backcalculation process can be attributed to other parameters such as approximations in the models, lack of consideration of the dynamic nature of loads.

A detailed comparison of the measured and calculated deflections at each test point is included in Appendices D and E. A close look at the results indicates that most of the points with large RMS errors are those that are tested near distressed pavements. In those cases, the deflections measured with the FWD contain both the response of the pavement as described by the layered theory as well as the manifestation of the damage. Seismic devices would not provide useful and interpretable results when directly tested on a badly cracked pavement. These areas are avoided during the field testing. As such, the calculated deflections cannot consider the constructive (providing higher deflection) or destructive (providing lower deflections) impacts of the FWD tests. It can only provide the deflections that are related to the movement of the pavement due to load. In many cases when a major crack is in the vicinity of the FWD, the near sensors may not match favorably because those are the deflections that are most affected by the existence of the crack.

Table 5.6 - Deflection Results of Equivalent-linear Analysis with SMART

District	Site	Average Deflection (mils) (COV)							
		0 in.	12 in.	24 in.	36 in.	48 in.	60 in.	72 in.	RMS Error
Beaumont	SH 73	19.19 *(6%)*	11.53 *(6%)*	6.80 *(8%)*	4.50 *(10%)*	3.15 *(11%)*	2.32 *(11%)*	1.76 *(12%)*	7.4% *(49%)*
Dallas	US 67	10.05 *(13%)*	6.17 *(16%)*	3.64 *(18%)*	2.44 *(18%)*	1.78 *(18%)*	1.35 *(19%)*	1.05 *(20%)*	9.2% *(43%)*
Fort Worth	FM 2738	22.10 *(9%)*	11.41 *(11%)*	5.25 *(13%)*	2.74 *(15%)*	1.82 *(14%)*	1.32 *(13%)*	1.00 *(13%)*	5.2% *(39%)*
	FM 2415	25.50 *(11%)*	11.90 *(12%)*	5.70 *(14%)*	3.20 *(16%)*	2.20 *(15%)*	1.60 *(15%)*	1.20 *(15%)*	10% *(22%)*
	FM 51	16.20 *(17%)*	8.30 *(20%)*	4.10 *(23%)*	2.30 *(23%)*	1.50 *(23%)*	1.10 *(22%)*	0.90 *(22%)*	11% *(29%)*
El Paso	Loop 375	12.83 *(16%)*	4.76 *(12%)*	2.57 *(12%)*	1.65 *(13%)*	1.13 *(14%)*	0.82 *(13%)*	0.62 *(13%)*	11.8% *(21%)*
	MLK	12.98 *(25%)*	4.56 *(14%)*	2.69 *(11%)*	1.83 *(11%)*	1.29 *(11%)*	0.95 *(11%)*	0.72 *(11%)*	13.4% *(22%)*
Odessa	IH 20	6.37 *(13%)*	3.82 *(15%)*	2.10 *(16%)*	1.18 *(17%)*	0.66 *(18%)*	0.36 *(24%)*	0.18 *(32%)*	13.9% *(32%)*
Waco	FM 933	6.45 *(13%)*	4.03 *(11%)*	2.89 *(10%)*	2.20 *(12%)*	1.68 *(13%)*	1.30 *(14%)*	1.02 *(15%)*	6.3% *(57%)*
ERDC	Item 5	17.62 *(14%)*	8.93 *(18%)*	4.51 *(21%)*	2.77 *(21%)*	1.90 *(20%)*	1.40 *(21%)*	1.08 *(21%)*	12.9% *(26%)*
	Item 6	15.73 *(8%)*	7.98 *(3%)*	4.21 *(8%)*	2.64 *(10%)*	1.82 *(10 %)*	1.34 *(7%)*	1.03 *(90%)*	11.8% *(0%)*
	Item 7	10.98 *(19%)*	5.85 *(22%)*	2.64 *(23%)*	1.55 *(22%)*	1.07 *(23%)*	0.80 *(21%)*	0.62 *(24%)*	15.6% *(26%)*
	Item 8	14.05 *(20%)*	8.26 *(25%)*	4.47 *(28%)*	2.80 *(29%)*	1.93 *(29%)*	1.42 *(27%)*	1.09 *(28%)*	12.9% *(42%)*
	Item 9	12.23 *(8%)*	6.78 *(14%)*	3.35 *(19%)*	2.03 *(21%)*	1.39 *(20%)*	1.03 *(20%)*	0.80 *(18%)*	10.0% *(24%)*
	Item 10	23.83 *(17%)*	13.14 (20%)	6.13 *(20%)*	3.61 *(20%)*	2.48 *(20%)*	1.84 *(19%)*	1.43 *(21%)*	12.0% *(20%)*
	Item 11	13.41 *(10%)*	7.87 *(11%)*	3.89 *(11%)*	2.27 *(10%)*	1.54 *(12%)*	1.14 *(10%)*	0.88 *(10%)*	12.1% *(25%)*
	Item 12	13.88 *(10%)*	7.30 (14%)	3.33 *(17%)*	1.96 *(15%)*	1.35 *(14%)*	1.01 *(14%)*	0.78 *(14%)*	10.8% *(27%)*
	Hangar 4	21.30 *(15%)*	8.70 *(10%)*	3.70 *(9%)*	2.30 *(9%)*	1.60 *(9%)*	1.20 *(9%)*	0.90 *(9%)*	30% *(22%)*

The deflection basins using the results from the PI model are included in Table 5.7. The results seem to be reasonably close to the equivalent-linear calculation. In many cases, the PI model provides higher deflections as compared to the equivalent-linear model. The deflections from the last four or five sensors are quite close from both models, since they are not impacted by the load-induced nonlinear behavior. As such, the RMS errors from the two models are reasonably close as well. Based on this study, the PI models may be a second best alternative in the absence of the resilient modulus tests.

To use SMART outputs for designing pavement with the existing design programs, such as FPS-19, each layer should be represented by one modulus. As indicated before, SMART provides two such values, the conservative modulus which is the minimum value calculated for each layer and the average modulus. The representative average and conservative moduli for each project as determined by SMART are included in Table 5.8. In some occasions, the same value is reported for the conservative and average moduli. For the base layer, this condition occurs when the base is too thin as such the state of stress is fairly uniform under the load. When the layers above the subgrade are too thick, the load-induced nonlinearity in the subgrade is minimal, as such the difference between the conservative and average moduli are rather small.

In general the moduli from the seismic analysis for the AC seem to be more reasonable and more representative of the materials encountered in the field. The base and subgrade moduli also seem to be more consistent than the FWD moduli especially when the backcalculation RMS errors are large.

The deflection RMS errors from the backcalculation procedure with MODULUS and the seismically derived procedure are compared in Figure 5.1. For the case where the RMS errors are less than 10%, the FWD backcalculation process yields smaller errors than those calculated from the seismic moduli. On the other hand, for those cases were the FWD backcalculation errors are quite large, the errors from the seismic methods are much smaller and under control.

RESULTS FROM NONLINEAR ESTIMATION OF PARAMETER K_3

The nonlinear parameters of the base and subgrade were estimated for all sites using the FWD deflections and the seismic modulus values. The analysis was performed as explained in Chapter 4 with a rigid layer obtained from an algorithm very similar to that used in the MODULUS program. Values measured in the lab were assigned to those layer parameters that were not being determined.

The backcalculated nonlinear parameters along with their corresponding RMS errors, after the completion of the backcalculation process, are presented in Table 5.9. The laboratory values for the parameters are also provided in the table. As discussed in Chapter 4, the following three backcalculation activities were carried out:

A) the k_3 of the subgrade was assumed as constant and the k_3 of the base was extracted,
B) the k_3 of the subgrade was extracted and the k_3 of the base was assumed as constant, and
C) both k_3 of the base and subgrade were extracted.

Table 5.7 - Deflection Results of Plasticity Index Analysis

District	Site	Average Deflection, mils (Coefficient of Variation)							
		0 in.	12 in.	24 in.	36 in.	48 in.	60 in.	72 in.	RMS Error
Beaumont	SH 73	23.07 *(9%)*	10.09 *(6%)*	6.10 *(8%)*	4.26 *(10%)*	3.07 *(11%)*	2.29 *(12%)*	1.75 *(12%)*	7.69% *(24%)*
Dallas	US 67	11.23 (15%)	6.32 (18%)	3.6 (19%)	2.44 (20%)	1.78 (20%)	1.35 (20%)	1.05 (20%)	9.44% *(41%)*
Fort Worth	FM 2738	20.21 *(12%)*	8.3 *(12%)*	4.41 *(14%)*	2.67 *(14%)*	1.8 *(14%)*	1.31 *(13%)*	1 *(13%)*	7.56% *(30%)*
	FM 2415	23.99 *(12%)*	9.69 *(15%)*	5.17 *(16%)*	3.15 *(16%)*	2.13 *(16%)*	1.55 *(15%)*	1.18 *(15%)*	11.48% *(19%)*
	FM 51	17.07 *(21%)*	6.91 *(21%)*	3.73 *(23%)*	2.27 *(23%)*	1.53 *(23%)*	1.11 *(22%)*	0.85 *(22%)*	12.18% *(27%)*
El Paso	Loop 375	12.9 *(16%)*	5.23 *(14%)*	2.64 *(13%)*	1.64 *(13%)*	1.13 *(14%)*	0.82 *(13%)*	0.62 *(13%)*	11.22% *(26%)*
	MLK	11.64 *(20%)*	4.95 *(14%)*	2.78 *(12%)*	1.83 *(10%)*	1.29 *(10%)*	0.95 *(10%)*	0.72 *(10%)*	13.36% *(22%)*
Odessa	IH 20	6.71 (14%)	3.58 (16%)	1.88 *(16%)*	1.1 *(17%)*	0.64 *(19%)*	0.36 *(22%)*	0.18 *(26%)*	13.81% *(31%)*
Waco	FM 933	7.19 *(11%)*	4.00 *(12%)*	2.76 *(11%)*	2.12 *(12%)*	1.65 *(13%)*	1.29 *(15%)*	1.01 *(15%)*	6.44% *(59%)*
ERDC	Item 5	21.24 *(16%)*	8.56 *(20%)*	4.40 *(25%)*	2.72 *(25%)*	1.88 *(24%)*	1.38 *(24%)*	1.07 *(23%)*	12.64% *(33%)*
	Item 6	19.5 *(13%)*	7.80 *(3%)*	4.15 *(10%)*	2.62 *(12%)*	1.82 *(12%)*	1.34 *(11%)*	1.03 *(10%)*	11.18% *(3%)*
	Item 7	10.46 *(21%)*	5.66 *(25%)*	2.63 *(26%)*	1.54 *(25%)*	1.07 *(25%)*	0.8 *(25%)*	0.62 *(25%)*	15.85% *(30%)*
	Item 8	16.26 *(24%)*	8.22 *(29%)*	4.4 *(33%)*	2.78 *(34%)*	1.92 *(34%)*	1.41 *(34%)*	1.09 *(33%)*	12.38% *(50%)*
	Item 9	13.69 *(8%)*	6.68 *(17%)*	3.32 *(22%)*	2.01 *(22%)*	1.39 *(21%)*	1.03 *(21%)*	0.79 *(21%)*	10.23% *(22%)*
	Item 10	26.83 *(21%)*	13.16 *(23%)*	6.09 *(23%)*	3.58 *(23%)*	2.47 *(22%)*	1.84 *(22%)*	1.43 *(22%)*	11.97% *(22%)*
	Item 11	12.85 *(11%)*	7.63 *(12%)*	3.87 *(12%)*	2.26 *(12%)*	1.53 *(12%)*	1.13 *(12%)*	0.88 *(11%)*	12.4% *(27%)*
	Item 12	13.25 *(11%)*	7.07 *(15%)*	3.31 *(18%)*	1.95 *(18%)*	1.35 *(17%)*	1.01 (16%)	0.78 (16%)	10.97% (31%)
	Hangar 4	25.46 *(22%)*	8.32 *(10%)*	3.67 *(8%)*	2.27 *(9%)*	1.60 *(9%)*	1.19 *(9%)*	0.92 *(9%)*	29.42% *(22%)*

Table 5.8 - Comparison of Design Modulus Values from SMART and Backcalculation Programs

Site	Design Modulus Values (ksi)								
	AC			Base			Subgrade		
	SMART	Modulus 5.1	EverCalc 5.0	SMART Cons. – Avg.	Modulus 5.1	EverCalc 5.0	SMART Cons. – Avg.	Modulus 5.1	EverCalc 5.0
SH 73**[a]	448	1446	1838	79	9	21	39-40/8-11/15-17	10	18
SH 73**[b]	448	1446	1838	72-77/39-41/18-21	9	21	13	10	18
US 67***	447	325	334	49/30-31*	43	46	23*	18	24
FM 2738	343	500	500	76-94	114	37	8-16	9	9
FM 2415	306	424	1810	27-47	80	14	27-47	8	8
FM 51	305	500	500	94-112	54	34	15-22	12	15
Loop 375	313	500	500	53-54	57	25	35-36	15	39
MLK	335	500	500	65-70	31	28	32-33	23	28
IH 20	647	1059	1601	74-81	83	25	17-23	4	106
FM 933	782	500	500	222-280	285	265	18-23	27	34
Item 12	442	1449	431				28-29	14	26
Item 11	427	790	298				24-25	12	22
Item 10	453	727	1031	30*	71	10	23-24	13	20
Item 9	451	56	187	49*	1759	825	28-29	22	29
Item 8	418	408	572	41-52	28	17	21-22	10	14
Item 7	403	596	13				24-25	9	21
Item 6	411	820	1000	56-69	31	20	20-21	8	9
Item 5	427	1029	1385	55-69	31	15	20-21	8	12
Hangar 4	665	146	-	31-37	4	-	16-21	12	-

* - Both conservative and average values were the same

** - Section was analyzed as five layer system with two bases, one subbase and subgrade. Modulus results for the bases and subbase are included with the base values (base1/base2/subbase)

*** - Section was analyzed as four layer system with one bases, one subbase and subgrade. Modulus results for the base and subbase are included with the base values (base/subbase)

[a] - base2, subbase and subgrade were analyzed set to nonlinear layers base 1 was analyzed as linear

[b] - base1, base2 and subbase were analyzed set to nonlinear subgrade was analyzed as a linear layer

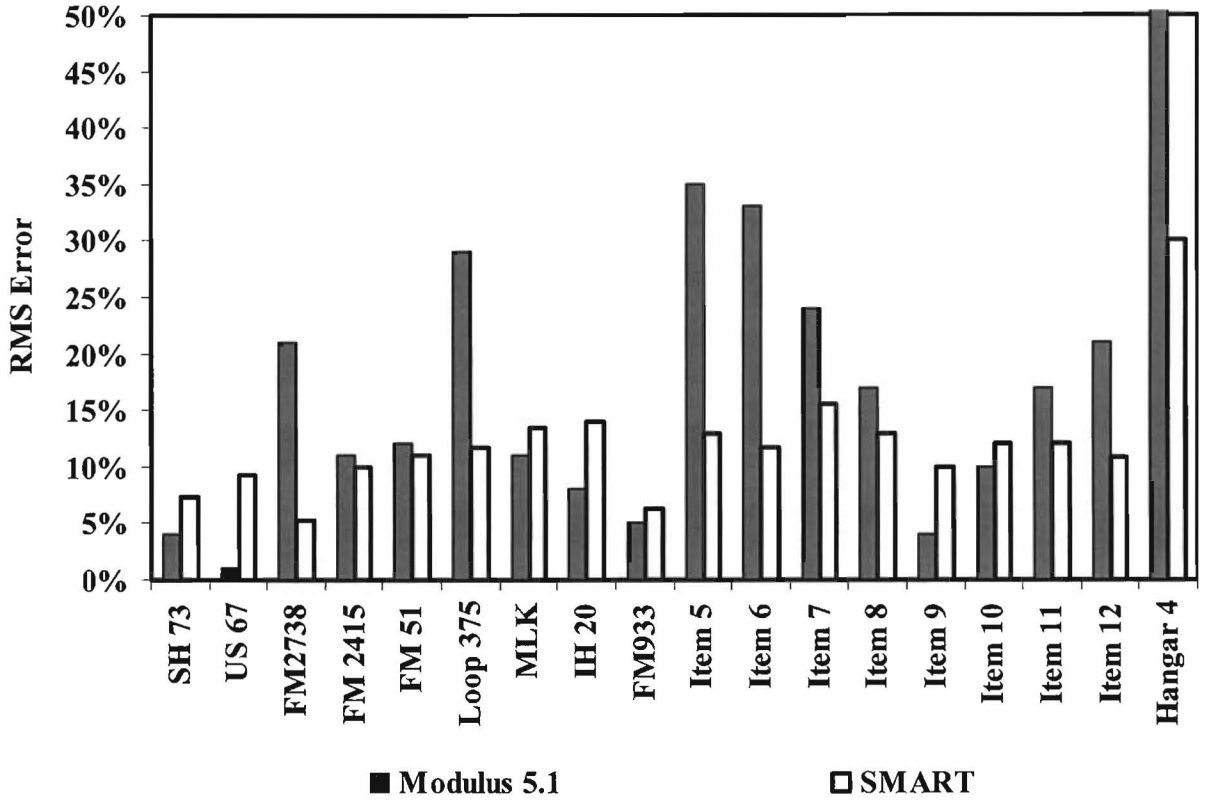

Figure 5.1 - Comparison of RMS Errors for of all Sites

The RMS errors between the calculated and measured deflections were typically less than 10%. This is better than the RMS errors obtained from the backcalculation of the FWD data alone. When the k_3 of the base was the only unknown, values close to the measured ones were obtained in a few occasions. When the focus was on backcalculating the k_3 of the subgrade by itself, the results were mostly close when the pavement structure was not very thick or very thin (no base layer). Extracting reliable k_3 for subgrade is not feasible under thick pavements because that layer does not experience appreciable load-induced nonlinearity. For very weak pavements, the distribution of the loads under the load is not uniform (Touma et al., 1991). In this condition, fitting the deflection from the first senor is practically impossible using the current algorithm that assumes a uniform stress distribution under the FWD plate. When both parameters are estimated simultaneously, the results are again reasonably close for the cases when the pavement is not too thick. Overall, it seems that determining the nonlinear parameters from the laboratory tests is still the most desirable method.

Table 5.9 - Estimated Nonlinear Parameters of Base and Subgrade from Seismic Modulus and FWD Deflections

District	Site	k_3 of Base only (Case A)	k_3 of Subgrade only (Case B)	k_3 of Base and Subgrade simultaneously (Case C)	
				k_3 of Base	k_3 of Subgrade
Beaumont	SH 73	-0.2 (6.0%)	-0.2 (6.4%)	-0.2 (6.6%)	-0.2 (6.6)
Dallas	US 67	-0.2 (9.9%)	-0.2 (9.8%)	-0.5 (9.7%)	-0.2 (9.7%)
Fort Worth	FM 2738	-0.08 (1.9%)	-0.41 (1.9%)	-0.06 (1.9%)	-0.5 (1.9%)
	FM 2415	-0.5 (6.1%)	-0.5 (6%)	0 (6.3%)	-0.5 (6.3%)
	FM 51	-0.5 (6.8%)	-0.5 (7.1%)	-0.5 (6.7%)	-0.5 (6.7%)
El Paso	Loop 375	-0.5 (5.3%)	-0.5 (5.2%)	-0.5 (5%)	-0.5 (5%)
	MLK	-0.5 (7.6%)	-0.5 (7.3%)	-0.5 (7%)	-0.5 (7%)
Odessa	IH 20	0 (3.6%)	-0.27 (3.6%)	-0.5 (4%)	-0.32 (4%)
Waco	FM 933	-0.5 (1.2%)	-0.5 (1.2%)	-0.5 (1.2)	-0.3 (1.2%)
ERDC	Item 5	-0.5 (6.1%)	0 (6.2%)	-0.5 (6%)	0 (6.2%)
	Item 6	-0.5 (6.2%)	0 (6.33%)	-0.5 (6.2%)	0 (6.2%)
	Item 7		-0.5 (5.4%)	-	-
	Item 8	-0.5 (5.2%)	-0.5 (5.3%)	-0.5 (4.9%)	-0.5 (4.9%)
	Item 9	-0.5 (4.7%)	0 (4.5%)	0 (4.5%)	0 (4.5%)
	Item 10	0 (3.8%)	-0.5 (3.7%)	0 (3.7%)	-0.5 (3.7%)
	Item 11	-	-0.36 (3.6%)	-	-
	Item 12	-	0 (4.7%)	-	-
	Hangar 4	0 (9.78%)	-0.5 (9.7%)	0 (9.7%)	-0.5 (9.7%)

Note: 1) Values in Parenthesis correspond to RMS Values and 2) Shaded Values correspond to actual values measured in the Lab.

Chapter 6

Summary and Conclusions

Nondestructive testing (NDT) methods are typically used to measure the variations in the modulus of different pavement layers. The critical strains necessary to estimate the remaining lives of a pavement system are then determined from the estimated moduli. The Falling Weight Deflectometer (FWD) and the Seismic Pavement Analyzer (SPA) are two of the NDT devices used for this purpose.

The Falling Weight Deflectometer applies an impulse load to the pavement and measures the surface deflection with seven sensors. Moduli of different pavement layers can then be backcalculated from these deflections. The shortcomings of this method are the uncertainties associated with the backcalculation procedure.

The Seismic Pavement Analyzer is based on generating and detecting stress waves in a layered system. The elastic moduli of different layers are obtained from an inversion process. The SPA imparts small external loads to the pavement; therefore, seismic moduli are linear elastic moduli. To incorporate in pavement design and analysis, seismic moduli of different layers have to be adjusted to represent moduli at strain and stress levels that are close to those applied by truck traffic. To do so, the nonlinear and viscoelastic behaviors of different layers should be accurately determined. These nonlinear parameters vary widely for different types of granular base and subgrade materials. The nonlinear parameters of each pavement layer can be preferably obtained from laboratory testing. However, adequate published information is available to be used as a first approximation.

The major objective of this study is to develop an algorithm for predicting the design modulus of each layer given the seismic modulus and the nonlinear and/or viscoelastic parameters of each pavement layer. Our efforts have yielded a software package called SMART (Seismic Modulus Analysis and Reduction Tool). More than a dozen sites were visited to validate SMART.

The results from this validation indicate that the program is capable of providing reasonable values to design engineers. The procedure is particularly attractive in the situations where the depth to bedrock is shallow or when the water table is close to the pavement surface.

In general the moduli from the seismic analysis for the AC seem to be more reasonable and more representative of the materials encountered in the field. The base and subgrade moduli also seem to be more consistent than the FWD moduli especially when the backcalculation RMS errors from FWD analysis are large.

For the case where the RMS errors from the backcalculation process are less than 10%, the FWD backcalculation process yields smaller errors than those calculated from the seismic moduli. The reported moduli under this condition are still more consistent from the seismic analysis. For those cases were the FWD backcalculation errors are quite large, the errors from the seismic methods are much smaller and the moduli are better under control.

A study was carried out to determine whether these nonlinear parameters of the base and subgrade can be estimated by integrating the seismic and FWD data together. Combining the seismic and deflection data together would allow the estimation of some of the nonlinear parameters for weaker pavement structures. In our experience, the most reliable way to estimate the nonlinear parameters of bases and subgrade is still laboratory testing

References

- Abdallah, I., and Nazarian, S. (2004), "Determination of Nonlinear Parameters of Flexible Pavement Layers from Nondestructive Testing," Research Report 1780-4, Center for Transportation Infrastructure Systems, the University of Texas at El Paso, TX

- Aouad, M. F., Stokoe, K. H., and Briggs, R. C. (1993), "Stiffness of Asphalt Concrete Surface Layer from Stress Wave Measurements," Transportation Research Record 1384, Washington, D.C., pp. 29-35.

- Barksdale, R. D., Alba, J., Khosla, P. N., Kim, R., Lambe, P. C. and Rahman, M. S., (1997), "Laboratory Determination of Resilient Modulus for Flexible Pavement Design," NCHRP Web Document 14, Federal Highway Administration, Washington, D.C., 486p.

- Brown, S. F. (1996), "Soil Mechanics in Pavement Engineering," Geotechnique, Vol 46, No. 3, pp. 383-426.

- De Jong, D. L., Peatz, M. G. F., and Korswagen, A. R. (1973), "Computer Program BISAR Layered Systems under Normal and Tangential Loads," Konin Klijke Shell-Labaratorium, External Report AMSR.0006.73, Amsterdam.

- Ferry, J.D, (1970), "Viscoelastic Properties of Polymers," 2nd edition, John Willy, New York.

- Huang, Y. H. (1994), Pavement Analysis and Design, Prentice Hall, Inc., Englewood Cliffs, NJ, 805p.

- Ishibashi, I. and Zhang, X. (1993), "Unified Dynamic Shear Moduli and Damping Ratios of Sand and Clay," Soils and Foundations, Vol. 33, No. 1, pp. 182-191.

- Ke, L., Nazarian, S., Abdallah, I., and Yuan, D., (2002), "A Sensitivity Study of Parameters Involved in Design with Seismic Moduli," Research Report 1780-2, Center for Highway Materials Research, the University of Texas at El Paso.

- Kramer, S. L. (1996), Geotechnical Earthquake Engineering, Prentice Hall, Inc., Englewood Cliffs, NJ, 653 p.

- Li, Y. and Nazarian, S. (1994), "Evaluation of Aging of Hot-Mix Asphalt Using Wave Propagation Techniques," Proceedings, Engineering Properties of Asphalt Mixtures And the Relationship to Their Performance, ASTM STP 1265, Philadelphia, PA, pp.166-179.

- Lukanen, E. O., Stubstad, R., Briggs, R. (2000), "Temperature Predictions and Adjustment Factors for Asphalt Pavement," Research Report FHWA-RD-98-085, Braun Intertec Corporation, 6875 Washington Avenue South, P.O. Box 39108, Minneapolis, Minnesota, 55439-0108, pp. 46-56.

- Meshkani, A., Abdallah, I., and Nazarian, S. (2004), "Determination of Nonlinear Parameters of Flexible Pavement Layers from Nondestructive Testing," Research Report 1780-3, Center for Transportation Infrastructure Systems, the University of Texas at El Paso, TX, 97 p.

- Michalak, C.H. and Scullion, T. (1995), "MODULUS 5.0: User's Manual," Texas Transportation Institute, Research Report 1987-1, College Station, TX.

- Mirza, M. W., and Witczak, M.W. (1995), "Development of a Global Aging System for Short and Long Term Aging of Asphalt Cements," Journal of Association of Asphalt Paving Technologies, Volume 64, Association of Asphalt Paving Technologies, St Paul, Minnesota, pp. 393-430.

- Nazarian, S. and Desai, M. R. (1993), "Automated Surface Wave Method: Field Testing," Journal of Geotechnical Engineering Division, ASCE, Vol. 119, No. GT7, New York, NY, pp. 1094-1111.

- Nazarian, S., Abdallah, I., Yuan, D., and Ke, L. (1999), "Design Modulus Values Using Seismic Data Collection," Research Report 1780-1, Center for Highway Materials Research, the University of Texas at El Paso.

- Nazarian, S., Peso, R., and Picornell, M. (1996), "An Approach to Relate Laboratory and Field Moduli of Base Materials," Research Report 1336-2F, Center for Geotechnical and Highway Materials Research, the University of Texas at El Paso.

- Nazarian, S., Yuan D. and Baker M. R. (1995), "Rapid Determination of Pavement Moduli with Spectral-Analysis-of-Surface-Waves Method," Research Report 1243-1F, Center for Geotechnical and Highway Materials Research, The University of Texas at El Paso, El Paso, TX, 76 p.

- Rohde, G.T., Scullion, T. (1990), "MODULUS 4.0: Expansion and Validation of the Modulus Backcalculation System," Research Report 1123-3, Texas Transportation Institute, The Texas A&M University System, College Station, Texas, 77843.

- Saeed, A., Hall, J. W Jr. (2001), "Determination of In Situ Material Properties of Asphalt Concrete Pavement Layers," Final Report for NCHRP, TRB and NRC, ERES Consultant Division of Applied Research Associates, Inc., 112 Monument Place, Vicksburg, Mississippi, 39180, pp. 35- 84.

- Santha, B.L. (1994), "Resilient Modulus of Subgrade Soils: Comparison of Two Constitutive Equations," Transportation Research Record 1462, Washington D.C., pp. 79-90.

- Scullion, T. (1987), "Incorporating a Structural Strength Index into the Texas Pavement Evaluation System," Research Report 409-3F, Texas Transportation Institute, The Texas A&M University System, College Station, Texas, 77843, pp. 22 - 48.

- Touma, B.E., Crovetti, J.A., and Shahin, M.Y. (1991), "Effects of Various Load Distributions of Backcalculated Moduli Values in Flexible Pavements," TRR No. 1293, Transportation Research Board, National Research Council, Washington, D.C

- Van Cauwelaert, F. J., Alexander, D. R., White, T. D., and Baker, W. R. (1989). "Multilayer Elastic Program for Backcalculating Layer Moduli in Pavement Evaluation," ASTM, STP 1026, Philadelphia, PA, pp.171-188.

- Witczak, M.W., Bonaquist, R., Von Quintus, H., and Kaloush, K.,(1999) "Specimen Geometry and Aggregate Size Effects in Uniaxial Compression and Constant Height Shear Tests," Journal of Association of Asphalt Paving Technologist, Volume 69, pp 733-793.

APPENDIX A

DEFLECTIONS FROM FWD TESTS

Table A1 - Deflections from FWD Tests for SH 73 Normalized to 9000 lbs. Load

Point	Deflection (mils)						
	0 in.	12 in.	24 in.	36 in.	48 in.	60 in.	72 in.
1	17.9	11.8	7.3	4.1	2.9	2.3	1.9
2	18.1	11.8	7.2	3.9	2.6	2.1	1.9
3	18.5	12.2	7.6	4.2	2.8	2.3	2.1
4	17.9	11.7	7.2	3.9	2.7	2.2	2.2
5	17.9	11.7	7.2	4.0	2.8	2.0	1.9
6	18.6	11.9	7.1	4.1	2.8	2.0	1.7
7	17.4	11.1	6.6	3.8	2.8	2.2	1.8
8	17.8	11.2	6.6	3.8	2.5	1.9	1.6
9	16.7	10.5	6.1	3.5	2.4	2.0	1.6
10	16.9	10.7	6.3	3.6	2.5	1.9	1.7
11	18.4	11.8	7.2	3.6	2.4	1.9	1.7
Mean	17.8	11.5	6.9	3.9	2.7	2.1	1.8
Std. Dev.	0.6	0.5	0.5	0.2	0.2	0.2	0.2
C.V.	3.4%	4.7%	6.8%	5.9%	6.8%	7.5%	10.7%

Table A2 - Deflections from FWD Tests for US 67 Normalized to 9000 lbs. Load

Point	Deflection (mils)						
	0 in.	12 in.	24 in.	36 in.	48 in.	60 in.	72 in.
-5	9.7	5.7	3.4	2.4	1.8	1.5	1.3
-4	9.9	6.1	3.4	2.3	1.8	1.5	1.3
-3	11.1	6.4	4.1	3.1	2.5	2.1	1.7
-2	10.0	6.9	4.5	3.5	3.0	2.6	2.2
-1	12.0	5.9	3.7	2.7	2.2	1.9	1.6
0	11.0	4.6	3.0	2.4	2.0	1.7	1.4
1	12.2	6.7	4.3	3.1	2.3	1.9	1.6
2	9.4	5.8	3.7	2.7	2.0	1.7	1.4
3	9.8	6.1	4.2	3.2	2.6	2.1	1.8
4	11.9	5.8	3.1	2.2	1.7	1.4	1.2
5	12.5	5.0	3.1	2.3	1.8	1.6	1.3
Mean	10.9	5.9	3.7	2.7	2.2	1.8	1.5
Std. Dev.	1.2	0.7	0.5	0.5	0.4	0.3	0.3
C.V.	10.6%	11.1%	14.4%	16.7%	18.3%	19.1%	19.0%

Table A3 - Deflections from FWD Tests for FM 2738 Normalized to 9000 lbs. Load

Point	Deflection (mils)						
	0 in.	12 in.	24 in.	36 in.	48 in.	60 in.	72 in.
1	20.5	11.6	6.4	2.7	1.8	1.4	1.2
2	22.4	12.2	6.5	2.8	1.7	1.3	1.1
3	20.2	10.8	5.8	2.3	1.6	1.3	1.1
4	23.4	12.2	6.1	2.8	1.9	1.5	1.3
5	21.5	11.3	5.6	2.8	1.9	1.5	1.2
6	17.9	9.1	4.5	2.2	1.7	1.4	1.2
7	20.9	11.9	6.5	2.9	2.0	1.6	1.4
8	22.5	13.3	7.4	3.5	2.1	1.6	1.3
9	25.2	13.4	6.6	3.3	2.2	1.7	1.3
10	25.5	13.2	6.6	2.9	2.1	1.7	1.4
Mean	22.0	11.9	6.2	2.8	1.9	1.5	1.2
Std. Dev.	2.3	1.3	0.8	0.4	0.2	0.1	0.1
C.V.	10.6%	11.1%	12.5%	14.6%	10.5%	9.8%	8.3%

Table A4 - Deflections from FWD Tests for FM 2415 Normalized to 9000 lbs. Load

Point	Deflection (mils)						
	0 in.	12 in.	24 in.	36 in.	48 in.	60 in.	72 in.
1	31.6	18.2	8.6	4.8	3.3	2.6	2.1
2	31.3	18.2	8.7	4.9	3.3	2.7	2.0
3	32.2	18.6	8.9	5.0	3.2	2.4	1.9
4	31.0	17.7	8.2	4.8	3.2	2.3	1.8
5	28.9	17.0	8.3	4.4	2.6	1.9	1.5
6	30.1	18.1	9.4	4.4	2.6	1.9	1.5
7	28.8	17.6	9.2	4.4	2.7	1.9	1.6
8	27.9	17.8	9.8	4.5	2.5	2.0	1.4
9	26.6	16.0	8.0	4.1	2.6	1.8	1.5
10	28.0	17.7	9.6	4.6	2.6	2.6	1.5
11	24.1	13.4	5.7	3.5	2.2	1.8	1.1
12	24.7	14.8	6.4	3.3	2.4	1.9	1.5
Mean	28.8	17.1	8.4	4.4	2.8	2.1	1.6
Std. Dev.	2.6	1.6	1.3	0.5	0.4	0.3	0.3
C.V.	9.2%	9.2%	14.9%	12.3%	13.9%	16.0%	17.4%

Table A5 - Deflections from FWD Tests for FM 51 Normalized to 9000 lbs. Load

Point	Deflection (mils)						
	0 in.	12 in.	24 in.	36 in.	48 in.	60 in.	72 in.
1	25.7	13.2	5.2	3.5	2.5	1.9	1.5
2	23.7	12.2	5.0	2.9	2.0	1.5	1.2
3	24.8	13.0	5.5	3.0	2.1	4.5	1.2
4	30.4	16.1	7.1	3.8	2.2	1.5	1.0
5	22.7	12.4	5.4	3.4	2.1	1.4	1.0
6	22.8	12.2	5.3	3.0	2.0	1.5	1.2
7	23.2	12.5	5.4	3.1	2.1	1.5	1.1
8	20.7	11.3	5.0	2.9	2.0	1.5	1.1
9	22.1	11.8	5.0	2.9	2.0	1.5	1.1
10	19.6	10.8	4.8	2.8	1.9	1.4	0.9
11	23.0	11.9	4.9	2.8	1.8	1.4	0.9
12	23.4	12.7	5.7	3.1	2.0	1.6	1.1
13	23.4	12.2	5.2	2.7	1.8	1.3	1.0
14	22.4	11.6	4.7	2.7	1.7	1.3	1.0
15	28.4	15.0	6.6	3.3	2.1	1.5	1.1
Mean	23.7	12.6	5.4	3.1	2.0	1.7	1.1
Std. Dev.	2.7	1.4	0.7	0.3	0.2	0.8	0.1
C.O.V.	11.5%	10.7%	12.2%	9.8%	8.8%	46.7%	12.9%

Table A6 - Deflections from FWD Tests for Loop 375 Normalized to 9000 lbs. Load

Point	Deflection (mils)						
	0 in.	12 in.	24 in.	36 in.	48 in.	60 in.	72 in.
1	20.9	10.7	4.3	2.5	1.7	1.3	1.1
2	20.6	10.2	3.6	2.1	1.6	1.3	1.1
3	11.9	5.7	2.6	1.7	1.3	1.0	0.8
4	19.1	8.5	2.4	1.4	1.1	1.0	0.8
5	25.5	12.3	3.6	1.8	1.3	1.1	0.9
Mean	19.6	9.5	3.3	1.9	1.4	1.1	0.9
Std. Dev.	4.9	2.5	0.8	0.4	0.2	0.2	0.1
C.V.	25.2%	26.4%	24.2%	21.5%	17.1%	13.8%	14.9%

Table A7 - Deflections from FWD Tests for MLK Normalized to 9000 lbs. Load

Point	Deflection (mils)						
	0 in.	12 in.	24 in.	36 in.	48 in.	60 in.	72 in.
0	17.1	5.7	2.7	1.8	1.3	1.0	0.7
1.5	17.7	5.7	2.8	1.9	1.4	1.1	0.8
3	16.3	5.9	2.5	1.6	1.2	0.9	0.7
4.5	16.9	8.9	2.9	1.7	1.2	0.9	0.7
6	16.4	8.6	2.7	1.6	1.2	1.0	0.8
7.5	21.0	8.4	4.0	2.6	1.9	1.4	1.1
9	22.2	9.8	4.3	2.9	2.1	1.6	1.2
10.5	22.3	9.4	4.3	2.9	2.1	1.6	1.4
12	21.9	8.7	4.0	2.9	2.2	1.8	1.4
13.5	22.0	7.8	4.1	2.9	2.2	1.7	1.4
15	21.5	7.4	3.8	2.8	2.2	1.7	1.4
16.5	23.2	10.9	4.8	3.1	2.2	1.6	1.3
18	25.4	14.3	6.1	3.4	2.3	1.7	1.3
19.5	24.1	12.1	5.2	3.3	2.3	1.8	1.4
21	20.7	9.2	3.8	2.5	1.8	1.4	1.1
22.5	22.3	10.6	4.6	2.8	2.1	1.6	1.3
24	20.3	8.6	4.1	2.3	1.6	1.2	1.0
25.5	20.5	7.5	3.8	2.5	1.7	1.3	1.0
27	20.1	7.8	3.6	2.4	1.6	1.3	1.0
28.5	22.0	13.0	4.7	2.7	1.9	1.5	1.2
30	22.8	10.8	4.6	3.0	2.1	1.6	1.2
31.5	20.8	9.0	4.0	2.5	1.8	1.3	1.0
33	19.1	6.9	3.3	2.2	1.6	1.3	1.0
Mean	20.7	9.0	3.9	2.5	1.8	1.4	1.1
Std. Dev.	2.5	2.2	0.9	0.5	0.4	0.3	0.2
C.V.	11.9%	24.6%	22.2%	20.9%	20.6%	20.3%	22.1%

Table A8 - Deflections from FWD Tests for IH 20 Normalized to 9000 lbs. Load

Point	Deflection (mils)						
	0 in.	12 in.	24 in.	36 in.	48 in.	60 in.	72 in.
1	8.3	5.5	3.0	1.6	0.9	0.6	0.4
2	7.2	6.1	1.3	0.8	0.5	0.4	0.3
3	6.2	4.4	2.5	1.4	0.9	0.6	0.4
4	5.5	3.9	2.1	1.2	0.7	0.6	0.5
5	6.9	5.2	3.0	1.7	0.9	0.5	0.3
6	5.2	3.6	1.9	1.0	0.5	0.4	0.3
7	6.9	5.2	2.6	1.4	0.9	0.6	0.5
8	4.8	3.6	2.2	1.4	1.0	0.7	0.4
9	5.9	4.3	2.7	1.6	1.1	0.7	0.5
10	10.1	6.1	3.0	1.4	0.9	0.8	0.6
11	5.3	3.5	1.7	0.9	0.6	0.5	0.4
12	5.2	3.6	1.9	0.9	0.4	0.3	0.2
13	6.0	4.3	2.5	1.4	0.9	0.7	0.5
14	4.2	3.1	1.8	1.0	0.6	0.4	0.3
15	3.8	2.8	1.6	0.9	0.5	0.3	0.2
16	3.5	2.5	1.4	0.7	0.4	0.2	0.2
17	4.0	2.9	1.6	0.9	0.5	0.3	0.2
18	4.4	3.4	2.1	1.2	0.7	0.4	0.3
19	4.0	2.9	1.7	1.0	0.5	0.3	0.2
20	5.8	3.7	1.9	0.9	0.5	0.3	0.2
21	6.4	4.3	2.4	1.1	0.6	0.4	0.3
Mean	5.7	4.0	2.1	1.2	0.7	0.5	0.3
Std. Dev.	1.6	1.1	0.5	0.3	0.2	0.2	0.1
C.V.	28.2%	26.3%	24.6%	25.6%	31.1%	34.9%	37.2%

Table A9 - Deflections from FWD Tests for FM 933 Normalized to 9000 lbs. Load

Point	Deflection (mils)						
	0 in.	12 in.	24 in.	36 in.	48 in.	60 in.	72 in.
-5	8.3	4.3	3.2	2.6	2.1	1.7	1.3
-4	7.4	4.2	3.4	2.7	2.3	1.9	1.5
-3	7.9	4.6	3.4	2.6	2.1	1.6	1.3
-2	8.0	4.2	3.0	2.4	1.8	1.5	1.2
-1	6.9	3.7	2.8	2.3	1.8	1.5	1.2
0	6.6	3.6	2.6	2.0	1.5	1.2	1.0
1	5.6	3.3	2.5	2.0	1.6	1.3	1.0
2	5.3	3.2	2.5	1.9	1.6	1.3	0.9
3	6.2	3.7	2.9	1.9	1.4	1.2	0.9
4	5.5	3.1	2.5	2.1	1.6	1.4	1.1
5	8.5	4.2	3.2	2.5	2.1	1.8	1.3
Mean	6.9	3.8	2.9	2.3	1.8	1.5	1.2
Std. Dev.	1.2	0.5	0.3	0.3	0.3	0.2	0.2
C.V.	16.9%	13.3%	11.5%	13.4%	15.5%	16.4%	16.5%

Table A10 - Deflections from FWD Tests for FSR Item 5 Normalized to 9000 lbs. Load

Point	Deflection (mils)						
	0 in.	12 in.	24 in.	36 in.	48 in.	60 in.	72 in.
1	25.2	14.9	3.5	2.2	1.9	1.6	1.4
2	25.2	14.7	3.3	2.4	1.7	1.4	1.1
3	25.7	15.3	4.0	2.3	1.6	1.3	1.0
4	29.4	17.8	4.9	3.0	2.2	1.7	1.4
5	31.4	18.6	5.6	3.8	3.0	2.4	2.0
6	30.1	17.4	4.3	3.2	2.6	2.1	1.8
7	30.3	17.9	4.8	3.3	2.6	2.1	1.9
Mean	28.2	16.7	4.3	2.9	2.2	1.8	1.5
Std. Dev.	2.7	1.6	0.8	0.6	0.5	0.4	0.4
C.V.	9.6%	9.7%	18.6%	21.2%	23.6%	22.9%	24.3%

Table A11 - Deflections from FWD Tests for FSR Item 6 Normalized to 9000 lbs. Load

Point	Deflection (mils)						
	0 in.	12 in.	24 in.	36 in.	48 in.	60 in.	72 in.
1	25.9	15.6	4.9	3.1	2.5	2.1	1.8
2	25.9	15.3	3.9	2.6	2.3	1.9	1.6
3	26.6	15.7	4.2	2.8	2.3	1.8	1.5
Mean	26.1	15.6	4.3	2.8	2.4	1.9	1.6
Std. Dev.	0.5	0.2	0.5	0.3	0.1	0.2	0.1
C.V.	1.7%	1.3%	12.1%	9.4%	5.7%	7.8%	8.8%

Table A12 - Deflections from FWD Tests for FSR Item 7 Normalized to 9000 lbs. Load

Point	Deflection (mils)						
	0 in.	12 in.	24 in.	36 in.	48 in.	60 in.	72 in.
1	18.4	11.8	4.8	2.3	1.7	1.5	1.2
2	20.1	13.4	4.1	2.2	1.6	1.3	1.1
3	19.9	13.4	4.1	2.1	1.6	1.4	1.2
4	17.3	11.1	4.3	2.0	1.6	1.3	1.1
5	17.6	11.3	3.8	2.1	1.6	1.4	1.2
Mean	18.7	12.2	4.2	2.1	1.6	1.4	1.2
Std. Dev.	1.3	1.1	0.4	0.1	0.0	0.1	0.1
C.V.	7.0%	9.2%	9.3%	4.7%	2.5%	4.6%	5.4%

Table A13 - Deflections from FWD Tests for FSR Item 8 Normalized to 9000 lbs. Load

Point	Deflection (mils)						
	0 in.	12 in.	24 in.	36 in.	48 in.	60 in.	72 in.
1	19.3	12.4	4.7	2.8	2.1	1.6	1.4
2	25.5	16.7	6.5	4.3	3.3	2.6	2.2
3	25.2	16.7	6.2	3.7	3.0	2.1	1.9
4	21.8	14.0	5.8	3.2	2.4	2.0	1.7
Mean	22.9	14.9	5.8	3.5	2.7	2.1	1.8
Std. Dev.	3.0	2.1	0.8	0.6	0.6	0.4	0.4
C.V.	13.0%	14.1%	13.4%	18.2%	20.9%	20.0%	19.4%

Table A14 - Deflections from FWD Tests for FSR Item 9 Normalized to 9000 lbs. Load

Point	Deflection (mils)						
	0 in.	12 in.	24 in.	36 in.	48 in.	60 in.	72 in.
1	12.2	5.8	4.1	2.3	1.6	1.2	1.0
2	12.7	6.2	4.5	2.5	1.7	1.3	1.1
3	11.9	5.6	4.5	2.7	1.9	1.4	1.1
4	10.7	4.8	4.2	2.5	1.7	1.4	1.1
5	12.3	5.6	4.9	2.8	2.0	1.5	1.2
Mean	12.0	5.6	4.4	2.6	1.8	1.4	1.1
Std. Dev.	0.7	0.5	0.3	0.2	0.1	0.1	0.1
C.V.	6.1%	9.2%	7.3%	7.8%	7.1%	7.1%	5.5%

Table A15 - Deflections from FWD Tests for FSR Item 10 Normalized to 9000 lbs. Load

Point	Deflection (mils)						
	0 in.	12 in.	24 in.	36 in.	48 in.	60 in.	72 in.
1	26.2	17.6	8.0	4.4	3.5	3.0	2.6
2	37.5	26.2	14.9	7.9	5.2	4.0	3.3
3	25.1	16.4	9.3	4.9	3.5	2.8	2.4
4	21.5	14.0	7.3	3.9	3.0	2.4	2.1
5	26.0	17.5	8.2	4.4	3.1	2.4	2.0
Mean	27.3	18.4	9.5	5.1	3.7	2.9	2.5
Std. Dev.	6.1	4.6	3.1	1.6	0.9	0.7	0.5
C.V.	22.2%	25.1%	32.6%	31.4%	24.7%	22.5%	21.7%

Table A16 - Deflections from FWD Tests for FSR Item 11 Normalized to 9000 lbs. Load

Point	Deflection (mils)						
	0 in.	12 in.	24 in.	36 in.	48 in.	60 in.	72 in.
1	16.9	11.4	5.2	3.1	2.1	1.6	1.3
2	19.0	13.0	6.5	3.9	2.7	2.0	1.6
3	14.9	10.1	4.5	2.6	1.9	1.6	1.2
4	18.6	12.6	5.5	3.3	2.4	1.9	1.6
5	18.4	12.3	5.1	3.1	2.4	1.9	1.6
Mean	17.6	11.9	5.4	3.2	2.3	1.8	1.5
Std. Dev.	1.7	1.1	0.7	0.5	0.3	0.2	0.2
C.V.	9.5%	9.6%	13.5%	14.3%	13.1%	11.6%	13.3%

Table A17 - Deflections from FWD Tests for FSR Item 12 Normalized to 9000 lbs. Load

Point	Deflection (mils)						
	0 in.	12 in.	24 in.	36 in.	48 in.	60 in.	72 in.
1	14.2	9.2	4.3	2.5	1.9	1.6	1.3
2	16.2	10.3	5.0	2.9	2.2	1.7	1.4
3	14.1	9.1	4.2	2.4	1.7	1.4	1.1
4	17.1	11.0	4.5	2.8	2.1	1.6	1.4
5	15.8	10.1	4.1	2.4	1.7	1.3	1.1
Mean	15.5	9.9	4.4	2.6	1.9	1.5	1.3
Std. Dev.	1.3	0.8	0.4	0.2	0.2	0.2	0.2
C.V.	8.5%	7.8%	8.5%	8.2%	10.4%	11.0%	11.7%

Table A18 - Deflections from FWD Tests for FSR Hangar 4 Normalized to 9000 lbs. Load

Point	Deflection (mils)						
	0 in.	12 in.	24 in.	36 in.	48 in.	60 in.	72 in.
1	80.5	25.1	4.3	3.1	3.4	2.3	1.7
2	75.0	28.0	3.7	0.7	2.5	1.9	1.4
3	76.8	24.8	1.2	2.5	2.6	2.1	1.8
4	82.5	26.8	1.5	3.5	3.0	2.4	2.1
Mean	78.7	26.2	2.6	2.4	2.9	2.2	1.7
Std. Dev.	3.4	1.5	1.5	1.2	0.4	0.2	0.3
C.V.	4.3%	5.8%	58.1%	49.9%	13.3%	9.5%	17.6%

APPENDIX B

MODULUS PROFILES FROM FWD TESTS

Table B1 – Modulus Profiles from FWD Tests for SH 73

Point	Modulus from EverCalc 5.0 (ksi)					Modulus from Modulus 5.1 (ksi)				
	AC	Base	Subbase	Subgrade	RMS Error	AC	Base	Subbase	Subgrade	RMS Error
1	2000	21.3	9.9	16.7	3%	1599	9	93	9	4%
2	2000	17.2	10.2	17.4	4%	1521	9	89	10	4%
3	2000	16.9	10.3	16.1	5%	1524	9	92	9	3%
4	2000	13.4	18.7	16.4	7%	1426	9	90	9	4%
5	2000	21.7	7.9	17.6	4%	1353	9	89	9	3%
6	1332.8	32.2	5.5	17.9	2%	1384	8	82	9	4%
7	1626.2	24.8	9.6	16.6	2%	948	9	90	9	5%
8	1568.9	26.6	6.9	18.9	2%	1675	9	101	10	3%
9	1688.9	27.1	9.9	19.8	3%	1714	10	108	11	3%
10	2000	21	9.2	18.8	3%	1451	8	107	10	3%
11	2000	12.2	9.9	18	5%	1311	9	30	10	4%
Average	1837.9	21.3	9.8	17.7	3.7%	1446.0	8.8	88.4	9.7	3.6%
Std. Dev.	240.5	6.1	3.3	1.2	1.4%	209.0	0.6	21.0	0.6	0.7%
C.O.V.	13.1%	28.7%	33.9%	6.6%	38.2%	14.0%	7.2%	23.7%	6.0%	19.9%

Table B2 – Modulus Profiles from FWD Tests for US 67

Point	Modulus from EverCalc 5.0 (ksi)					Modulus from Modulus 5.1 (ksi)				
	AC	Base	Subbase	Subgrade	RMS Error	AC	Base	Subbase	Subgrade	RMS Error
-5	456	35	338	20	1.7%	503	34	174	27	1.5%
-4	583	22	1488	21	0.9%	632	21	1147	27	0.9%
-3	307	28	1039	22	1.1%	312	30	300	29	1.2%
-2	248	45	763	20	1.6%	253	48	323	27	1.6%
-1	214	47	240	15	0.9%	211	51	98	21	0.7%
0	406	34	1108	11	1.2%	426	33	721	16	0.8%
1	198	37	837	17	1.8%	198	40	316	22	1.5%
2	270	54	854	19	1.6%	228	64	363	26	1.0%
3	605	41	94	16	1.1%	633	45	43	21	0.9%
4	155	63	81	20	1.1%	156	66	50	25	1.0%
5	134	68	157	15	1.1%	125	78	79	20	0.8%
Average	325.1	43.1	636.3	17.8	1.3%	334.3	46.4	328.5	23.7	1.1%
Std. Dev.	164.9	14.2	478.7	3.3	0.3%	185.1	17.3	335.3	4.0	0.3%
C.O.V.	50.7%	33.0%	75.2%	18.6%	25.6%	55.4%	37.4%	102.1%	16.8%	29.5%

Table B3 – Modulus Profiles from FWD Tests for FM 2738

Point	Modulus from EverCalc 5.0 (ksi)				Modulus from Modulus 5.1 (ksi)			
	AC*	Base	Subgrade	RMS Error	AC	Base	Subgrade	RMS Error
1	500	41	9	>100%	500	142	10	20%
2	500	32	9	>100%	500	107	9	19%
3	500	33	9	>100%	500	113	11	22%
4	500	33	9	>100%	500	93	9	22%
5	500	39	9	>100%	500	111	10	23%
6	500	44	9	>100%	500	126	12	25%
7	500	44	9	>100%	500	140	9	21%
8	500	43	9	>100%	500	140	8	17%
9	500	34	9	>100%	500	91	8	22%
10	500	29	9	>100%	500	81	8	23%
Average	500	37.3	9	>100%	500.0	114.3	9.3	21.4%
Std. Dev.	0	5.6	0	-	0.0	22.2	1.3	2.3%
C.O.V	0.00%	14.90%	0.00%	-	0.0%	19.4%	14.3%	10.5%

*** - constant AC Modulus**

Table B4 – Modulus Profiles from FWD Tests for FM 2415

Point	Modulus from EverCalc 5.0 (ksi)				Modulus from Modulus 5.1 (ksi)			
	AC	Base	Subgrade	RMS Error	AC	Base	Subgrade	RMS Error
1	1572	17	8	66%	392	53	7	14%
2	1602	16	8	61%	381	53	7	13%
3	1469	15	8	69%	377	49	7	12%
4	1643	15	8	75%	386	49	7	13%
5	1924	12	8	99%	469	51	8	9%
6	1975	9	8	>100%	651	44	7	8%
7	2000	12	8	97%	544	54	7	8%
8	2000	10	8	>100%	32	190	7	9%
9	2000	14	8	>100%	501	59	8	9%
10	2000	12	8	87%	21	246	7	11%
11	1876	19	8	>100%	621	58	12	14%
12	1662	17	8	>100%	711	50	10	16%
Average	1810	14	8	88%	424	80	8	11%
Std. Dev.	203	3	0	15%	217	66	1	3%
C.O.V	11.2%	21.8%	0.0%	0.2%	51.0%	82.7%	17.1%	24.4%

Table B5 – Modulus Profiles from FWD Tests for FM 51

Point	Modulus from EverCalc 5.0 (ksi)				Modulus from Modulus 5.1 (ksi)			
	AC*	Base	Subgrade	RMS Error	AC	Base	Subgrade	RMS Error
1	500	31	15	27.8%	500	47	11	16%
2	500	32	15	47.3%	500	49	12	14%
3	500	30	15	50.3%	500	51	11	19%
4	500	20	15	58.7%	500	38	10	6%
5	500	37	15	52.8%	500	60	11	10%
6	500	35	15	48.3%	500	56	12	11%
7	500	35	15	47.6%	500	56	12	11%
8	500	43	15	51.2%	500	66	12	12%
9	500	37	15	50.0%	500	57	12	13%
10	500	50	15	72.4%	500	78	13	12%
11	500	34	15	76.3%	500	54	14	12%
12	500	35	15	54.5%	500	58	12	11%
13	500	31	15	67.2%	500	49	13	11%
14	500	35	15	76.7%	500	55	14	11%
15	500	24	15	51.5%	500	42	11	9%
Average	500	34	15	55.5%	500	54	12	12%
Std. Dev.	0	7	0	13.0%	0	10	1	3%
C.O.V	0.0%	20.7%	0.0%	0.2%	0.0%	17.8%	9.2%	0.3%

*** - constant AC Modulus**

Table B6 – Modulus Profiles from FWD Tests for Loop 375

Point	Modulus from EverCalc 5.0 (ksi)				Modulus from Modulus 5.1 (ksi)			
	AC*	Base	Subgrade	RMS Error	AC	Base	Subgrade	RMS Error
1	500	20	31	9%	500	51	11	24%
2	500	19	34	6%	500	41	13	28%
3	500	60	45	4%	500	136	17	27%
4	500	17	47	6%	500	34	19	34%
5	500	10	37	8%	500	23	13	30%
Average	500	25.2	38.8	6.6%	500.0	57.0	14.6	28.6%
Std. Dev.	0	19.8	6.9	1.9%	0.0	45.3	3.3	3.7%
C.O.V.	0.0%	78.7%	17.9%	29.5%	0.0%	79.5%	22.5%	13.0%

*** - constant AC Modulus**

Table B7 – Modulus Profiles from FWD Tests for MLK

Point	Modulus from EverCalc 5.0 (ksi)				Modulus from Modulus 5.1 (ksi)			
	AC*	Base	Subgrade	RMS Error	AC	Base	Subgrade	RMS Error
0	500	46	30	48.30%	500	39	34	14.70%
1.5	500	47	30	36.10%	500	38	32	16.40%
3	500	41	30	61.60%	500	39	35	10.50%
4.5	500	27	30	49.70%	500	33	29	8.20%
6	500	28	30	44.80%	500	33	30	11.00%
7.5	500	28	30	5.50%	500	32	22	11.00%
9	500	23	28	5.70%	500	29	19	9.40%
10.5	500	25	26	3.20%	500	29	19	11.90%
12	500	29	26	5.80%	500	31	20	15.60%
13.5	500	34	27	7.60%	500	33	21	17.10%
15	500	36	28	9.20%	500	34	22	19.50%
16.5	500	21	26	5.80%	500	26	17	7.00%
18	500	15	24	12.30%	500	22	15	4.80%
19.5	500	19	24	5.10%	500	25	16	6.70%
21	500	24	30	3.70%	500	29	21	9.20%
22.5	500	21	26	4.00%	500	27	18	8.10%
24	500	25	30	13.30%	500	30	22	5.90%
25.5	500	32	30	12.00%	500	33	23	11.80%
27	500	29	30	13.60%	500	32	24	10.60%
28.5	500	17	27	9.20%	500	24	18	9.10%
30	500	21	26	6.40%	500	27	18	6.90%
31.5	500	25	30	10.50%	500	30	22	7.30%
33	-	-	-	-	500	34	26	13.90%
Average	500	27.9	28.1	17.0%	500	30.8	22.7	10.7%
Std. Dev.	0.0	8.6	2.2	18.0%	0	4.5	5.7	3.9%
C.O.V.	0.0%	30.9%	7.7%	106.0%	0.0%	14.7%	25.1%	36.5%

*** - constant AC Modulus**

Table B8 – Modulus Profiles from FWD Tests for IH 20

Point	Modulus from EverCalc 5.0 (ksi)				Modulus from Modulus 5.1 (ksi)			
	AC	Base	Subgrade	RMS Error	AC	Base	Subgrade	RMS Error
1	954	16	75	2%	524	61	3	7%
2	418	35	108	17%	468	56	5	32%
3	1537	19	81	5%	831	80	3	6%
4	1172	33	78	2%	816	101	3	9%
5	1765	10	116	4%	1075	45	3	4%
6	1377	26	110	3%	941	84	4	9%
7	960	22	68	4%	717	66	3	10%
8	3000	16	92	10%	1140	135	3	4%
9	1953	18	67	3%	1063	88	2	4%
10	429	22	56	3%	282	61	3	12%
11	907	43	91	3%	591	122	4	11%
12	1347	23	145	3%	1064	66	5	10%
13	1345	26	68	2%	856	91	3	7%
14	2339	25	127	1%	1633	91	4	5%
15	2268	30	137	2%	1582	107	5	6%
16	1708	38	150	18%	1565	106	7	8%
17	2402	25	148	1%	1655	92	5	4%
18	2483	20	111	3%	2000	72	4	2%
19	2415	23	150	3%	1788	83	5	5%
20	1261	22	135	3%	713	77	5	8%
21	-	-	-	-	747	66	4	9%
Average	1602.0	24.6	105.7	4.6%	1050.0	83.3	4.0	8.2%
Std. Dev.	716.7	8.0	31.8	4.8%	479.3	22.4	1.2	6.1%
C.O.V.	44.7%	32.5%	30.1%	104.2%	45.6%	26.9%	29.4%	74.2%

Table B9 – Modulus Profiles from FWD Tests for FM 933

Point	Modulus from EverCalc 5.0 (ksi)				Modulus from Modulus 5.1 (ksi)			
	AC*	Base	Subgrade	RMS Error	AC	Base	Subgrade	RMS Error
-5	500	211	30	4%	500	215	26	6%
-4	500	308	28	4%	500	311	22	5%
-3	500	204	30	1%	500	230	24	2%
-2	500	191	33	2%	500	206	28	4%
-1	500	276	34	4%	500	284	28	5%
0	500	223	38	2%	500	250	32	2%
1	500	330	38	2%	500	361	30	3%
2	500	355	38	5%	500	407	29	4%
3	500	229	39	5%	500	270	31	6%
4	500	396	36	4%	500	405	28	5%
5	500	196	28	6%	500	195	24	7%
Average	500.0	265.3	33.6	3.5%	500.0	285.0	27.4	4.5%
Std. Dev.	0.0	71.7	4.2	1.5%	0.0	77.2	3.2	1.6%
C.O.V	0.0%	27.0%	12.5%	43.7%	0.0%	27.1%	11.6%	35.4%

*** - constant AC Modulus**

Table B10 – Modulus Profiles from FWD Tests for FSR Item 5

Point	Modulus from EverCalc 5.0 (ksi)				Modulus from Modulus 5.1 (ksi)			
	AC	Base	Subgrade	RMS Error	AC	Base	Subgrade	RMS Error
1	1500	18	12	> 100%	1122	29	10	37%
2	1500	18	12	> 100%	988	29	10	38%
3	1500	15	12	> 100%	1422	27	9	31%
4	1500	14	12	75%	813	40	7	31%
5	1236	13	12	33%	624	46	6	34%
6	1150	14	12	56%	974	24	8	39%
7	1310	14	12	50%	1264	23	8	36%
Average	1385	15.1	12.0	53.5%	1029.6	31.1	8.3	35.1%
Std. Dev.	151	2.0	0.0	17.3%	268.9	8.6	1.5	3.2%
C.O.V.	10.9%	13.4%	0.0%	32.4%	26.1%	27.6%	18.1%	9.2%

Table B11 – Modulus Profiles from FWD Tests for FSR Item 6

Point	Modulus from EverCalc 5.0 (ksi)				Modulus from Modulus 5.1 (ksi)			
	AC	Base	Subgrade	RMS Error	AC	Base	Subgrade	RMS Error
1	1000	21	9	> 100%	646	42	7	29%
2	1000	20	9	> 100%	868	26	9	35%
3	1000	19	9	> 100%	944	24	8	34%
Average	1000	20	9	> 100%	819	31	8.0	33%
Std. Dev.	0	1	0	-	155	10	1	3%
C.O.V.	0%	5%	0%	-	19%	32%	12.5%	10%

Table B12 – Modulus Profiles from FWD Tests for FSR Item 7

Point	Modulus from EverCalc 5.0 (ksi)			Modulus from Modulus 5.1 (ksi)		
	AC	Subgrade	RMS Error	AC	Subgrade	RMS Error
1	16	19	21%	721	8	22%
2	18	21	19%	475	9	25%
3	9	21	23%	485	9	26%
4	12	21	23%	708	9	23%
5	12	21	18%	590	9	26%
Average	13.4	20.6	20.8%	595.8	8.8	24.4%
Std. Dev.	3.6	0.9	2.3%	117.4	0.4	1.8%
C.O.V.	26.7%	4.3%	11.0%	19.7%	5.1%	7.4%

Table B13 – Modulus Profiles from FWD Tests for FSR Item 8

Point	Modulus from EverCalc 5.0 (ksi)				Modulus from Modulus 5.1 (ksi)			
	AC	Base	Subgrade	RMS Error	AC	Base	Subgrade	RMS Error
1	750	23	14	62%	446	33	12	17%
2	411	13	14	10%	389	25	8	18%
3	490	13	14	25%	367	25	9	18%
4	635	17	14	36%	431	29	10	16%
Average	571.5	16.5	14.0	33.3%	408.3	28.0	9.8	17.3%
Std. Dev.	150.9	4.7	0.0	21.9%	36.6	3.8	1.7	1.0%
C.O.V.	26.4%	28.6%	0.0%	66.0%	9.0%	13.7%	17.5%	5.6%

Table B14 – Modulus Profiles from FWD Tests for FSR Item 9

Point	Modulus from EverCalc 5.0 (ksi)				Modulus from Modulus 5.1 (ksi)			
	AC	Base	Subgrade	RMS Error	AC	Base	Subgrade	RMS Error
1	701	51	30	10%	57	1106	24	4%
2	61	493	30	8%	57	1125	22	4%
3	59	891	29	7%	53	2116	21	3%
4	61	1581	30	8%	59	2388	24	6%
5	54	1109	28	8%	52	2061	21	5%
Average	187.2	825.0	29.4	8.2%	55.6	1759.2	22.4	4.4%
Std. Dev.	287.2	584.3	0.9	1.1%	3.0	600.6	1.5	1.1%
C.O.V.	153.4%	70.8%	3.0%	13.4%	5.3%	34.1%	6.8%	25.9%

Table B15 – Modulus Profiles from FWD Tests for FSR Item 10

Point	Modulus from EverCalc 5.0 (ksi)				Modulus from Modulus 5.1 (ksi)			
	AC	Base	Subgrade	RMS Error	AC	Base	Subgrade	RMS Error
1	803	11	21	6%	814	41.7	13.9	14%
2	874	5	14	6%	614	56.4	8.1	5%
3	1354	7	21	3%	603	120.1	12.8	9%
4	1086	21	22	12%	767	99.3	15.7	11%
5	1036	7	22	9%	835	36.8	14	9%
Average	1030.6	10.2	20.0	7.2%	726.6	70.9	12.9	9.6%
Std. Dev.	214.5	6.4	3.4	3.4%	110.7	36.9	2.9	3.3%
C.O.V.	20.8%	62.9%	17.0%	47.5%	15.2%	52.1%	22.3%	34.2%

Table B16 – Modulus Profiles from FWD Tests for FSR Item 11

Point	Modulus from EverCalc 5.0 (ksi)			Modulus from Modulus 5.1 (ksi)		
	AC	Subgrade	RMS Error	AC	Subgrade	RMS Error
1	279	24	11%	793	13	16%
2	325	19	10%	874	10	15%
3	367	26	9%	903	15	17%
4	267	21	8%	710	12	18%
5	252	22	7%	668	12	19%
Average	298.0	22.4	9.0%	789.6	12.4	17.0%
Std. Dev.	47.2	2.7	1.6%	101.4	1.8	1.6%
C.O.V.	15.9%	12.1%	17.6%	12.8%	14.6%	9.3%

Table B17 – Modulus Profiles from FWD Tests for FSR Item 12

Point	Modulus from EverCalc 5.0 (ksi)			Modulus from Modulus 5.1 (ksi)		
	AC	Subgrade	RMS Error	AC	Subgrade	RMS Error
1	546	26	5%	1771	13.9	22%
2	479	23	6%	1595	12.2	21%
3	485	28	8%	1646	14.6	20%
4	342	25	8%	1152	13.2	22%
5	301	29	12%	1079	14.7	20%
Average	430.6	26.2	8%	1448.6	13.7	21.0%
Std. Dev.	104.0	2.4	3%	311.8	1.0	1.0%
C.O.V.	24.2%	9.1%	34.4%	21.5%	7.6%	4.8%

Table B18 – Modulus Profiles from FWD Tests for Hangar 4

Point	Modulus from EverCalc 5.0 (ksi)				Modulus from Modulus 5.1 (ksi)			
	AC	Base	Subgrade	RMS Error	AC	Base	Subgrade	RMS Error
1	-	-	-	-	170	4	9	30%
2	-	-	-	-	176	4	12	73%
3	-	-	-	-	132	4	13	73%
4	-	-	-	-	107	4	13	71%
Average	-	-	-	-	146	4	12	62%
Std. Dev.	-	-	-	-	33	0	2	21%
C.O.V	-	-	-	-	22.0%	0.0%	16.1%	34.4%

APPENDIX C

MODULUS PROFILES FROM SEISMIC TESTS

Table C1 – Modulus Profiles from SASW Tests for SH 73

Point	Modulus (ksi.)					Thickness (in.)			
	AC	Base 1	Base 2	Subbase	Subgrade	AC	Base 1	Base 2	Subbase
1	1547	88.2	35.2	23.2	15.9	3.2	5.5	4.4	8.4
2	1447	72.0	36.9	24.0	14.6	3.1	4.5	5.6	8.7
3	1492	53.0	33.8	27.0	13.5	3.2	4.8	5.0	8.9
4	1395	83.9	42.1	25.2	11.3	3.1	4.8	4.7	8.9
5	1462	84.9	42.5	24.9	12.9	3.1	5.7	4.6	8.7
6	1318	87.1	40.2	37.9	13.3	3.0	5.1	4.5	9.0
7	1405	67.1	44.0	29.9	14.8	3.1	4.8	4.5	8.8
8	1422	95.5	53.4	29.6	11.7	2.9	5.9	4.3	8.1
9	1477	86.6	53.0	24.3	12.1	3.0	5.8	4.6	8.0
10	1443	54.7	36.2	44.0	11.7	3.0	5.2	4.8	8.6
11	1374	93.2	53.0	32.6	14.2	3.0	5.3	4.2	7.6
Average	1435	79	42.8	29.3	13.3	3.1	5.2	4.7	8.5
Std. Dev.	62	15	7.4	6.6	1.5	0.1	0.5	0.4	0.4
COV	4%	19%	17%	22%	11%	3%	9%	8%	5%

Table C2 – Modulus Profiles from SASW Tests for US 67

Point	Modulus (ksi.)				Thickness (in.)		
	AC	Base	Subbase	Subgrade	AC	Base	Subbase
-5	1452	1452	44	37	6.1	13.0	9.0
-4	1441	1441	42	34	5.7	13.0	9.0
-3	1432	1432	51	34	5.5	13.0	9.0
-2	1561	1561	54	36	5.7	13.0	9.0
-1	1187	1187	48	30	5.6	13.0	9.0
0	1383	1383	41	32	5.5	13.0	9.0
1	1396	1396	47	37	5.7	13.0	9.0
2	1451	1451	61	56	5.9	13.0	9.0
3	1424	1424	60	56	5.6	13.0	9.0
4	1500	1500	65	45	5.7	13.0	9.0
5	1533	1533	41	30	6.1	13.0	9.0
Average	1433	50	39	24	5.7	13.0	9.1
Std. Dev.	98	8	9	5	0.2	0.0	0.0
COV	7%	17%	24%	23%	3%	0%	0%

Table C3 – Modulus Profiles from SASW Tests for FM 2738

Point	Modulus (ksi.)			Thickness (in.)	
	AC	Base	Subgrade	AC	Base
1	1134	116	21	2.1	6.3
2	1140	126	22	1.9	6.7
3	1105	106	22	1.9	6.3
4	1174	101	25	1.8	6.0
5	1044	134	27	1.9	6.3
6	1059	121	24	2.0	6.7
7	1107	125	24	2.2	6.0
8	1063	122	18	2.3	6.7
9	1068	119	22	1.8	6.3
10	1101	111	18	1.7	6.3
Average	1099	118	22	2.0	6.3
Std. Dev.	42	10	3	0.2	0.2
COV	4%	8%	12%	10%	4%

Table C4 – Modulus Profiles from SASW Tests for FM 2415

Point	Modulus (ksi.)			Thickness (in.)	
	AC	Base	Subgrade	AC	Base
1	239	60	14	2.0	6.7
2	313	98	18	2.1	6.7
3	322	83	18	2.0	6.3
4	326	90	16	2.0	6.8
5	331	88	18	2.2	6.9
6	307	80	21	2.2	6.5
7	323	85	18	2.3	6.3
8	310	84	17	2.6	6.3
9	314	68	21	2.4	7.0
10	293	80	22	2.6	7.2
11	263	88	24	2.2	7.2
12	330	115	22	2.4	6.7
Average	306	85	19	2.2	6.7
Std. Dev.	28	14	3	0.2	0.3
COV	9%	16%	15%	9%	5%

Table C5 – Modulus Profiles from SASW Tests for FM 51

Point	Modulus (ksi.)			Thickness (in.)	
	AC	Base	Subgrade	AC	Base
1	295	149	31	1.8	7.3
2	289	116	26	1.8	7.5
3	310	114	18	1.8	6.9
4	325	151	22	1.7	7.1
5	320	**192**	31	2.2	7.1
6	316	124	21	2.0	7.3
7	327	107	28	2.0	7.3
8	288	102	28	2.2	7.3
9	302	104	33	2.0	7.3
10	318	107	30	2.3	6.9
11	312	112	31	1.9	7.5
12	306	104	29	2.0	7.3
13	293	158	28	1.8	7.5
14	315	174	32	1.9	7.3
15	274	101	18	1.7	7.5
Average	306	128	27	1.9	7.3
Std. Dev.	16	29	5	0.2	0.2
COV	5%	23%	18%	10%	3%

Table C6 – Modulus Profiles from SASW Tests for Loop 375

Point	Modulus (ksi.)			Thickness (in.)	
	AC	Base	Subgrade	AC	Base
1	1102	124.0	42	3.1	10.1
2	1120	122.0	30	3.3	10.6
3	1146	97.0	43	3.1	10.7
4	939	84.0	39	3.3	10.5
5	1004	75.0	36	2.8	10.3
6	1104	204.0	32	3.1	10.5
7	978	84.0	29	2.9	10.5
8	919	107.0	39	3.4	9.6
9	1154	174.0	36	3.1	10.2
10	1043	120.0	33	3.1	9.8
11	1078	106.0	37	3.4	10.6
12	1066	139.0	27	3.0	10.1
13	1104	124.0	33	2.8	10.4
14	1047	102.0	42	2.9	10.5
15	1039	110.0	45	3.4	10.1
16	963	98.0	34	2.9	10.4
17	991	101.0	44	2.9	10.2
18	913	145.0	44	3.2	10.5
19	911	123.0	39	3.6	9.6
20	888	129.0	35	3.1	9.9
21	1068	159.0	36	2.9	10.9
22	956	140.0	41	3.1	9.6
23	956	136.0	40	3.0	10.3
24	883	114.0	33	3.4	9.5
25	1060	90.0	36	2.9	9.8
26	906	108.0	35	2.8	10.1
27	985	81.0	31	2.8	9.8
28	1045	175.0	38	2.8	10.3
29	974	98.0	34	2.8	10.1
30	954	100.0	40	2.8	10.0
31	956	123.0	36	2.9	10.6
32	921	134.0	37	3.3	10.6
33	892	125.0	41	3.1	10.3
Average	1002	120	37	3.1	10.2
Std. Dev.	80	29	5	0.2	0.4
COV	8%	24%	12%	7%	4%

Table C7 – Modulus Profiles from SASW Tests for MLK

Point	Modulus (ksi.)			Thickness (in.)	
	AC	Base	Subgrade	AC	Base
1	1210	223.0	38.0	2.0	14.0
2	1160	254.0	39.0	2.0	15.0
3	1140	222.0	34.0	3.0	13.0
4	1179	117.0	32.0	2.0	15.0
5	1140	123.0	28.0	2.0	15.0
6	1112	132.0	35.0	2.0	15.0
7	1136	123.0	38.0	2.0	15.0
8	1082	118.0	31.0	2.0	15.0
9	1108	107.0	35.0	2.0	15.0
10	1158	146.0	36.0	2.0	15.0
11	1150	154.0	37.0	2.0	14.0
12	1072	217.0	36.0	3.0	13.0
13	1152	173.0	33.0	2.0	13.0
14	1138	161.0	30.0	2.0	14.0
15	989	103.0	28.0	2.0	15.0
16	991	109.0	32.0	3.0	13.0
17	1020	95.0	30.0	2.0	15.0
18	1035	102.0	28.0	2.0	15.0
19	993	89.0	27.0	2.0	14.0
20	974	156.0	32.0	2.0	13.0
21	1054	150.0	35.0	2.0	13.0
22	1051	171.0	36.0	2.0	14.0
23	1054	186.0	34.0	2.0	14.0
24	886	145.0	37.0	2.0	15.0
25	899	93.0	29.0	2.0	14.0
Average	1075	147	33.2	2.1	14.2
Std. Dev.	86	46	3.6	0.3	0.8
COV	8%	31%	11%	16%	6%

Table C8 – Modulus Profiles from SASW Tests for IH 20

Point	Modulus (ksi.)			Thickness (in.)	
	AC	Base	Subgrade	AC	Base
1	2082	79.3	24.6	6.5	17.7
2	2039	89.6	18.4	6.7	16.9
3	2171	91.3	25.7	6.9	16.8
4	2199	80.9	30.5	6.3	16.3
5	2230	110.1	29.6	6.5	16.8
6	1819	113.2	30.8	6.5	17.0
7	2020	115.1	38.7	6.7	17.8
8	2152	74.2	20.1	7.3	16.9
9	1770	82.0	36.0	5.7	17.3
10	1968	80.9	24.3	6.5	17.0
11	1960	91.3	29.0	6.6	17.4
12	1921	111.4	27.8	6.6	17.4
13	2114	101.4	33.2	6.7	17.2
14	2252	107.1	21.4	7.4	16.9
15	2163	105.8	24.1	7.0	17.0
16	2232	100.5	24.9	7.2	16.8
17	2176	63.5	23.1	7.3	16.9
18	2066	71.7	23.2	6.8	16.5
19	2084	60.7	26.3	6.5	16.9
20	2026	48.5	27.2	6.4	16.0
21	2095	72.2	19.6	6.7	17.8
Average	2073	88	26.6	6.7	17.0
Std. Dev.	131	19	5.3	0.4	0.5
COV	6%	22%	20%	6%	3%

Table C9 – Modulus Profiles from SASW Tests for FM 933

Point	Modulus (ksi.)			Thickness (in.)	
	AC	Base	Subgrade	AC	Base
-5	2745	346	30	2.2	15.6
-4	2751	314	26	2.1	15.3
-3	2506	375	26	2.2	16.0
-2	2442	364	27	2.2	16.0
-1	2662	276	28	1.9	16.1
0	2536	276	25	2.0	17.3
1	2457	260	24	2.0	17.8
2	2448	348	23	2.8	17.5
3	2259	335	20	2.4	16.9
4	2293	324	21	2.5	16.5
5	2536	404	26	2.5	16.3
Average	2504	327	27	2.4	16.6
Std. Dev.	150	79	3	0.3	0.8
COV	6%	24%	12%	12%	5%

Table C10 – Modulus Profiles from SASW Tests for FSR Item 5

Point	Modulus (ksi.)			Thickness (in.)	
	AC	Base	Subgrade	AC	Base
1	1380	64.2	14.8	2.2	5.9
2	1358	58.2	24.3	2.2	5.9
3	1341	156.3	21.1	2.2	5.9
4	1410	86.6	18.8	2.3	5.9
5	1404	84.9	18.5	2.4	6.3
6	1299	60.0	23.5	2.1	6.1
7	1350	48.4	27.5	2.1	6.3
8	1404	39.8	30.9	2.2	6.0
Average	1368	75	22.4	2.2	6.0
Std. Dev.	39	37	5.2	0.1	0.2
COV	3%	49%	23%	4%	3%

Table C11 – Modulus Profiles from SASW Tests for FSR Item 6

Point	Modulus (ksi.)			Thickness (in.)	
	AC	Base	Subgrade	AC	Base
1	1311	106.7	19.3	2.6	7.8
2	1330	52.1	22.9	2.2	7.8
3	1305	64.7	22.9	2.3	7.7
Average	1316	75	21.7	2.4	7.8
Std. Dev.	13	29	2.1	0.2	0.1
COV	1%	38%	10%	9%	1%

Table C12 – Modulus Profiles from SASW Tests for FSR Item 7

Point	Modulus (ksi.)		Thickness (in.)
	AC	Subgrade	AC
1	1284	24.6	4.0
2	1311	18.3	3.7
3	1228	22.4	3.8
4	1337	35.8	4.0
5	1292	28.1	4.0
Average	1291	26	3.9
Std. Dev.	40	7	0.1
COV	3%	26%	4%

Table C13 – Modulus Profiles from SASW Tests for FSR Item 8

Point	Modulus (ksi.)			Thickness (in.)	
	AC	Base	Subgrade	AC	Base
1	1428	60	22	4.0	8.0
2	1186	50	15	3.7	7.8
3	1406	58	21	3.7	7.8
Average	1340	56	19	3.8	8.0
Std. Dev.	134	6	4.0	0.1	0.2
COV	10%	10%	21%	4%	3%

Table C14 – Modulus Profiles from SASW Tests for FSR Item 9

Point	Modulus (ksi.)			Thickness (in.)	
	AC	Base	Subgrade	AC	Base
1	1382	56	40	3.8	6.0
2	1426	50	34	3.9	6.0
3	1479	54	24	4.2	6.4
4	1474	53	25	4.5	6.1
5	1470	39	28	4.2	6.1
Average	1446	50	30	4.1	6.1
Std. Dev.	42	7	7	0.3	0.2
COV	3%	14%	23%	7%	3%

Table C15 – Modulus Profiles from SASW Tests for FSR Item 10

Point	Modulus (ksi.)			Thickness (in.)	
	AC	Base	Subgrade	AC	Base
1	1563	34	27	3.8	4.1
2	1391	24	18	3.7	3.9
3	1483	28	23	4.0	3.8
4	1369	39	33	4.1	4.3
5	1450	30	23	3.7	4.0
Average	1451	31	25	3.9	4.0
Std. Dev.	77	6	6	0.2	0.2
COV	5%	19%	22%	5%	5%

Table C16 – Modulus Profiles from SASW Tests for FSR Item 11

Point	Modulus (ksi.)		Thickness (in.)
	AC	Subgrade	AC
1	1362	24	4.9
2	1318	26	5.0
3	1367	30	5.3
4	1391	29	5.0
5	1406	23	4.7
Average	1369	26	5
Std. Dev.	34	3	0.2
COV	2%	12%	5%

Table C17 – Modulus Profiles from SASW Tests for FSR Item 12

Point	Modulus (ksi.)		Thickness (in.)
	AC	Subgrade	AC
1	1481	23	4.5
2	1339	29	4.1
3	1399	33	4.5
4	1395	29	4.1
5	1470	34	4.1
Average	1417	30	4
Std. Dev.	59	4	0.2
COV	4%	15%	6%

Table C18 – Modulus Profiles from SASW Tests for Hangar 4

Point	Modulus (ksi.)			Thickness (in.)	
	AC	Base	Subgrade	AC	Base
1	674	47	25	2.2	4.2
2	652	35	24	2.0	4.0
3	684	46	26	2.2	4.0
4	655	28	21	1.9	4.4
Average	666	39	24	2.1	4.2
Std. Dev.	15	9	2	0.2	0.2
COV	2%	23%	8%	7%	4%

APPENDIX D

DEFLECTIONS FROM SEISMIC TESTS USING SMART

(Equivalent-linear Model)

Table D1 - Deflections from SMART for SH 73 under a 9000 lbs. Load

Location	Deflection (mils)							RMS Error
	0 in.	12 in.	24 in.	36 in.	48 in.	60 in.	72 in.	
1	17.3	10.3	6.0	3.8	2.6	1.9	1.4	6%
2	19.4	11.2	6.4	4.1	2.8	2.1	1.6	3%
3	20.9	12.0	6.7	4.4	3.0	2.2	1.7	4%
4	20.8	13.0	7.8	5.2	3.7	2.7	2.1	8%
5	18.5	11.4	6.9	4.6	3.2	2.4	1.8	4%
6	18.7	11.1	6.6	4.4	3.1	2.3	1.8	3%
7	19.0	10.9	6.2	4.0	2.8	2.0	1.6	3%
8	18.8	11.9	7.4	5.0	3.6	2.6	2.0	10%
9	18.9	11.8	7.3	4.9	3.5	2.5	1.9	10%
10	21.1	12.3	7.3	4.9	3.5	2.6	2.0	11%
11	17.9	10.9	6.4	4.3	3.0	2.2	1.6	5%
Average	19.2	11.5	6.8	4.5	3.2	2.3	1.8	6%
Std. Dev.	1.2	0.7	0.5	0.4	0.3	0.3	0.2	3%
COV	6%	6%	8%	10%	11%	11%	12%	51%

Table D2 - Deflections from SMART for SH 67 under a 9000 lbs. Load

Location	Deflection (mils)							RMS Error
	0 in.	12 in.	24 in.	36 in.	48 in.	60 in.	72 in.	
-5	10.3	6.5	3.9	2.6	1.9	1.4	1.1	4%
-4	10.9	6.8	3.9	2.6	1.9	1.4	1.1	4%
-3	10.5	6.5	3.8	2.6	1.9	1.4	1.1	8%
-2	10.0	6.3	3.9	2.6	1.9	1.5	1.2	12%
-1	11.0	6.5	3.7	2.5	1.8	1.3	1.0	8%
0	12.0	7.5	4.5	3.0	2.2	1.7	1.3	12%
1	10.9	6.8	4.1	2.8	2.1	1.6	1.2	5%
2	8.2	4.8	2.8	1.9	1.4	1.0	0.8	12%
3	8.1	4.5	2.5	1.6	1.2	0.9	0.7	18%
4	8.0	4.6	2.7	1.8	1.3	1.0	0.7	10%
5	10.9	7.1	4.4	2.9	2.1	1.6	1.3	10%
Average	10.1	6.2	3.7	2.4	1.8	1.3	1.0	9%
Std. Dev.	1.3	1.0	0.6	0.4	0.3	0.3	0.2	4%
COV	13%	16%	18%	18%	18%	19%	20%	45%

Table D3 - Deflections from SMART for FM 2738 under a 9000 lbs. Load

Location	Deflection (mils)							RMS Error
	0 in.	12 in.	24 in.	36 in.	48 in.	60 in.	72 in.	
1	22.28	11.72	5.48	2.85	1.91	1.38	1.05	3%
2	20.71	10.90	5.16	2.69	1.80	1.30	0.99	4%
3	23.06	11.58	5.14	2.66	1.78	1.29	0.98	4%
4	23.20	10.98	4.65	2.39	1.61	1.17	0.90	7%
5	19.18	9.75	4.34	2.24	1.50	1.09	0.83	8%
6	20.02	10.26	4.73	2.46	1.65	1.19	0.91	5%
7	20.72	10.63	4.81	2.48	1.66	1.20	0.92	8%
8	22.58	12.69	6.37	3.51	2.26	1.62	1.22	3%
9	22.88	11.77	5.36	2.77	1.85	1.34	1.02	6%
10	26.39	13.86	6.43	3.33	2.22	1.60	1.22	3%
Average	22.1	11.4	5.2	2.7	1.8	1.3	1.0	5%
Std. Dev.	2.1	1.2	0.7	0.4	0.3	0.2	0.1	2%
COV	9%	11%	13%	15%	14%	13%	13%	40%

Table D4 - Deflections from SMART for FM 2415 under a 9000 lbs. Load

Location	Deflection (mils)							RMS Error
	d0	d1	d2	d3	d4	d5	d6	
1	25.17	12.76	6.79	4.13	2.79	2.02	1.54	8%
2	26.84	12.79	6.12	3.46	2.30	1.65	1.25	12%
3	29.08	13.11	6.02	3.33	2.24	1.62	1.23	11%
4	29.39	14.04	6.74	3.83	2.53	1.82	1.38	7%
5	26.13	12.27	5.84	3.31	2.20	1.59	1.20	8%
6	25.41	11.23	5.12	2.83	1.91	1.39	1.06	12%
7	27.32	12.74	5.94	3.33	2.22	1.60	1.22	9%
8	27.77	13.40	6.36	3.60	2.39	1.72	1.31	7%
9	24.47	11.01	5.08	2.84	1.92	1.39	1.06	10%
10	22.32	10.33	4.90	2.79	1.86	1.35	1.02	14%
11	21.23	9.38	4.37	2.44	1.64	1.19	0.91	10%
12	20.85	10.05	4.85	2.75	1.83	1.32	1.00	10%
Average	25.5	11.9	5.7	3.2	2.2	1.6	1.2	10%
Std. Dev.	2.9	1.5	0.8	0.5	0.3	0.2	0.2	2%
COV	11%	12%	14%	16%	15%	15%	15%	22%

Table D5 - Deflections from SMART for FM 51 under a 9000 lbs. Load

Location	Deflection (mils)							RMS Error
	d0	d1	d2	d3	d4	d5	d6	
1	14.02	7.16	3.49	1.96	1.31	0.95	0.72	17%
2	16.58	8.36	4.08	2.29	1.54	1.12	0.85	10%
3	21.40	11.70	5.94	3.38	2.24	1.61	1.22	10%
4	17.22	9.51	4.86	2.76	1.83	1.31	1.00	11%
5	12.49	6.78	3.51	2.00	1.33	0.96	0.72	14%
6	17.81	9.69	4.99	2.87	1.90	1.37	1.04	5%
7	16.16	7.93	3.80	2.14	1.44	1.04	0.80	12%
8	16.29	7.92	3.79	2.13	1.44	1.04	0.80	10%
9	14.97	6.86	3.16	1.77	1.20	0.88	0.67	15%
10	15.41	7.46	3.52	1.97	1.33	0.97	0.74	11%
11	15.21	7.26	3.45	1.94	1.31	0.95	0.72	12%
12	15.96	7.62	3.59	2.02	1.36	0.99	0.75	13%
13	14.17	7.53	3.81	2.16	1.44	1.04	0.79	11%
14	12.76	6.73	3.36	1.90	1.27	0.91	0.70	13%
15	22.22	11.94	6.07	3.47	2.30	1.66	1.25	5%
Average	16.2	8.3	4.1	2.3	1.5	1.1	0.9	11%
Std. Dev.	2.7	1.7	0.9	0.5	0.4	0.2	0.2	3%
COV	17%	20%	23%	23%	23%	22%	22%	29%

Table D6 - Deflections from SMART for Loop 375 under a 9000 lbs. Load

Location	Deflection (mils)							RMS Error
	0 in.	12 in.	24 in.	36 in.	48 in.	60 in.	72 in.	
1	11.46	4.17	2.24	1.43	0.98	0.71	0.54	15%
2	12.71	5.39	3.06	2.01	1.40	1.01	0.76	9%
3	12.89	4.31	2.17	1.37	0.94	0.69	0.53	15%
4	14.52	4.88	2.42	1.52	1.05	0.77	0.58	12%
5	17.45	5.35	2.58	1.62	1.11	0.81	0.62	10%
6	9.82	4.67	2.88	1.94	1.36	0.98	0.74	11%
7	17.27	6.19	3.23	2.07	1.42	1.03	0.78	6%
8	12.60	4.65	2.44	1.54	1.05	0.77	0.58	13%
9	9.92	4.35	2.55	1.68	1.16	0.84	0.63	13%
10	12.89	5.16	2.84	1.83	1.26	0.91	0.69	10%
11	12.36	4.79	2.54	1.63	1.12	0.82	0.62	12%
12	13.06	5.80	3.38	2.23	1.55	1.12	0.84	8%
13	13.07	5.07	2.83	1.83	1.26	0.92	0.69	10%
14	13.16	4.33	2.21	1.40	0.96	0.70	0.53	14%
15	11.14	4.02	2.07	1.31	0.90	0.66	0.50	16%
16	14.68	5.15	2.70	1.72	1.18	0.86	0.65	10%
17	13.25	4.24	2.15	1.35	0.92	0.68	0.51	15%
18	10.30	3.83	2.12	1.36	0.94	0.68	0.52	16%
19	11.20	4.44	2.41	1.54	1.05	0.77	0.58	13%
20	12.45	4.85	2.69	1.73	1.19	0.86	0.65	11%
21	10.64	4.38	2.54	1.68	1.16	0.84	0.63	12%
22	11.03	4.22	2.32	1.47	1.01	0.73	0.55	14%
23	11.32	4.24	2.34	1.50	1.03	0.75	0.57	14%
24	13.04	5.20	2.83	1.81	1.24	0.90	0.68	10%
25	14.84	5.11	2.59	1.63	1.12	0.81	0.62	11%
26	14.32	5.00	2.67	1.70	1.16	0.84	0.64	10%
27	17.40	5.93	3.00	1.89	1.29	0.94	0.72	7%
28	10.17	4.20	2.44	1.59	1.09	0.79	0.60	14%
29	15.12	5.23	2.74	1.74	1.19	0.87	0.66	10%
30	13.96	4.57	2.35	1.48	1.01	0.74	0.56	13%
31	12.57	4.71	2.60	1.68	1.15	0.84	0.63	11%
32	11.16	4.44	2.49	1.62	1.12	0.81	0.61	13%
33	11.61	4.18	2.26	1.44	0.99	0.72	0.55	14%
Average	12.8	4.8	2.6	1.6	1.1	0.8	0.6	12%
Std. Dev.	2.1	0.6	0.3	0.2	0.2	0.1	0.1	3%
COV	16%	12%	12%	13%	14%	13%	13%	21%

Table D7 - Deflections from SMART for MLK under a 9000 lbs. Load

Location	Deflection (mils)							RMS Error
	0 in.	12 in.	24 in.	36 in.	48 in.	60 in.	72 in.	
1	8.4	3.6	2.3	1.6	1.1	0.8	0.6	18%
2	7.4	3.3	2.2	1.5	1.1	0.8	0.6	19%
3	8.9	4.1	2.6	1.8	1.3	0.9	0.7	15%
4	14.3	4.8	2.8	1.9	1.3	1.0	0.7	12%
5	13.9	5.1	3.0	2.1	1.5	1.1	0.8	10%
6	13.2	4.4	2.6	1.7	1.2	0.9	0.7	14%
7	13.5	4.2	2.4	1.6	1.1	0.8	0.6	16%
8	14.6	4.8	2.8	1.9	1.4	1.0	0.8	12%
9	15.5	4.6	2.5	1.7	1.2	0.9	0.7	14%
10	11.9	4.1	2.4	1.7	1.2	0.9	0.7	16%
11	11.2	4.0	2.4	1.6	1.2	0.8	0.6	16%
12	8.6	3.9	2.5	1.7	1.2	0.9	0.7	16%
13	10.9	4.4	2.7	1.8	1.3	0.9	0.7	14%
14	11.7	4.7	2.9	2.0	1.4	1.1	0.8	12%
15	17.6	5.5	3.1	2.1	1.5	1.1	0.8	9%
16	15.0	5.1	2.9	1.9	1.3	1.0	0.7	12%
17	17.2	5.3	2.9	2.0	1.4	1.0	0.8	11%
18	17.5	5.5	3.1	2.1	1.5	1.1	0.8	9%
19	18.8	6.0	3.3	2.2	1.6	1.1	0.9	7%
20	12.0	4.7	2.8	1.9	1.3	1.0	0.7	13%
21	11.5	4.3	2.5	1.7	1.2	0.9	0.7	15%
22	10.5	4.0	2.4	1.7	1.2	0.9	0.7	16%
23	10.1	4.2	2.6	1.8	1.3	0.9	0.7	15%
24	11.6	4.0	2.4	1.6	1.2	0.8	0.6	16%
25	18.7	5.6	3.1	2.1	1.5	1.1	0.8	9%
Average	13.0	4.6	2.7	1.8	1.3	0.9	0.7	13%
Std. Dev.	3.2	0.7	0.3	0.2	0.1	0.1	0.1	3%
COV	25%	14%	11%	11%	11%	11%	11%	23%

Table D8 - Deflections from SMART for IH 20 under a 9000 lbs. Load

Location	Deflection (mils)							RMS Error
	0 in.	12 in.	24 in.	36 in.	48 in.	60 in.	72 in.	
1	6.7	4.0	2.2	1.2	0.7	0.4	0.2	12%
2	7.0	4.4	2.6	1.6	0.9	0.5	0.3	22%
3	6.0	3.7	2.1	1.2	0.7	0.4	0.2	11%
4	6.4	3.8	2.0	1.0	0.6	0.3	0.1	13%
5	5.5	3.3	1.8	1.0	0.6	0.3	0.2	13%
6	5.7	3.2	1.7	1.0	0.6	0.3	0.2	8%
7	5.0	2.7	1.4	0.8	0.4	0.2	0.1	20%
8	6.8	4.4	2.5	1.5	0.8	0.5	0.2	10%
9	6.9	3.6	1.7	0.9	0.5	0.2	0.1	19%
10	6.9	4.1	2.2	1.3	0.7	0.4	0.2	15%
11	6.1	3.5	1.9	1.1	0.6	0.3	0.2	10%
12	5.7	3.3	1.8	1.1	0.6	0.4	0.2	9%
13	5.5	3.1	1.7	0.9	0.5	0.3	0.1	17%
14	5.6	3.6	2.2	1.3	0.8	0.5	0.3	11%
15	5.7	3.5	2.0	1.2	0.7	0.4	0.2	13%
16	5.6	3.5	2.0	1.2	0.7	0.4	0.2	24%
17	6.8	4.3	2.4	1.3	0.7	0.4	0.2	17%
18	7.0	4.4	2.4	1.3	0.7	0.4	0.2	11%
19	7.4	4.5	2.3	1.2	0.6	0.3	0.2	16%
20	8.3	5.0	2.5	1.2	0.6	0.3	0.1	12%
21	7.2	4.5	2.6	1.5	0.9	0.5	0.3	8%
Average	6.4	3.8	2.1	1.2	0.7	0.4	0.2	14%
Std. Dev.	0.8	0.6	0.3	0.2	0.1	0.1	0.1	5%
COV	13%	15%	16%	17%	18%	24%	32%	33%

Table D9 - Deflections from SMART for FM 933 under a 9000 lbs. Load

Location	Deflection (mils)							RMS Error
	0 in.	12 in.	24 in.	36 in.	48 in.	60 in.	72 in.	
-5	6.18	3.85	2.72	2.03	1.52	1.16	0.89	9%
-4	6.25	4.05	2.97	2.28	1.74	1.35	1.05	8%
-3	7.15	4.31	2.96	2.19	1.63	1.23	0.95	7%
-2	6.99	4.28	3.03	2.29	1.74	1.35	1.05	3%
-1	6.14	4.00	3.02	2.39	1.88	1.49	1.18	2%
0	7.18	4.78	3.59	2.83	2.22	1.75	1.39	15%
1	5.80	3.78	2.84	2.20	1.70	1.33	1.04	4%
2	5.19	3.24	2.36	1.80	1.38	1.06	0.83	4%
3	8.09	4.51	2.93	2.14	1.60	1.22	0.95	6%
4	5.23	3.38	2.55	1.97	1.52	1.19	0.93	3%
5	6.80	4.10	2.83	2.09	1.56	1.18	0.91	8%
Average	6.5	4.0	2.9	2.2	1.7	1.3	1.0	6%
Std .Dev.	0.8	0.4	0.3	0.3	0.2	0.2	0.1	4%
COV	13%	11%	10%	12%	13%	14%	15%	57%

Table D10 - Deflections from SMART for FSR Item 5 under a 9000 lbs. Load

Location	Deflection (mils)							RMS Error
	0 in.	12 in.	24 in.	36 in.	48 in.	60 in.	72 in.	
1	22.7	12.2	6.2	3.8	2.6	1.9	1.5	16%
2	17.2	7.9	3.7	2.3	1.6	1.2	0.9	9%
3	13.8	8.0	4.4	2.7	1.8	1.3	1.0	10%
4	17.9	9.7	5.1	3.1	2.1	1.6	1.2	9%
5	17.6	9.7	5.1	3.2	2.2	1.6	1.2	13%
6	17.4	8.0	3.8	2.3	1.6	1.2	0.9	15%
7	16.7	7.1	3.2	2.0	1.4	1.0	0.8	18%
Average	17.6	8.9	4.5	2.8	1.9	1.4	1.1	13%
Std. Dev.	2.4	1.6	1.0	0.6	0.4	0.3	0.2	3%
COV	14%	18%	21%	21%	20%	21%	21%	26%

Table D11 - Deflections from SMART for FSR Item 6 under a 9000 lbs. Load

Location	Deflection (mils)							RMS Error
	0 in.	12 in.	24 in.	36 in.	48 in.	60 in.	72 in.	
1	14.1	8.2	4.7	3.0	2.1	1.5	1.2	12%
2	17.3	8.0	4.0	2.4	1.7	1.3	1.0	12%
3	15.8	7.7	4.0	2.5	1.7	1.3	1.0	12%
Average	15.7	8.0	4.2	2.6	1.8	1.4	1.1	12%
Std. Dev.	1.3	0.2	0.3	0.3	0.2	0.1	0.1	0%
COV	8%	3%	8%	10%	10%	7%	9%	0%

Table D12 - Deflections from SMART for FSR Item 7 under a 9000 lbs. Load

Location	Deflection (mils)							RMS Error
	0 in.	12 in.	24 in.	36 in.	48 in.	60 in.	72 in.	
1	10.7	5.8	2.7	1.6	1.1	0.8	0.6	16%
2	14.2	7.9	3.6	2.1	1.4	1.1	0.8	9%
3	12.2	6.5	2.9	1.7	1.2	0.9	0.7	14%
4	8.1	4.1	1.8	1.1	0.7	0.6	0.4	21%
5	9.7	5.0	2.3	1.3	0.9	0.7	0.5	18%
Average	11.0	5.9	2.7	1.6	1.1	0.8	0.6	16%
Std. Dev.	2.1	1.3	0.6	0.3	0.2	0.2	0.1	4%
COV	19%	22%	23%	22%	23%	21%	24%	26%

Table D13 - Deflections from SMART for FSR Item 8 under a 9000 lbs. Load

Location	Deflection (mils)							RMS Error
	0 in.	12 in.	24 in.	36 in.	48 in.	60 in.	72 in.	
1	13.1	7.9	4.4	2.7	1.9	1.4	1.1	8%
2	18.4	11.3	6.3	4.0	2.8	2.0	1.6	8%
3	14.1	8.2	4.5	2.8	1.9	1.4	1.1	14%
4	10.6	5.6	2.7	1.7	1.2	0.9	0.7	21%
Average	14.1	8.3	4.5	2.8	2.0	1.4	1.1	13%
Std. Dev.	2.8	2.0	1.3	0.8	0.6	0.4	0.3	5%
COV	20%	25%	28%	29%	29%	27%	28%	42%

Table D14 - Deflections from SMART for FSR Item 9 under a 9000 lbs. Load

Location	Deflection (mils)							RMS Error
	0 in.	12 in.	24 in.	36 in.	48 in.	60 in.	72 in.	
1	10.5	5.2	2.4	1.4	1.0	0.7	0.6	13%
2	11.9	6.2	2.9	1.7	1.2	0.9	0.7	11%
3	13.2	7.7	4.1	2.5	1.7	1.2	1.0	6%
4	12.6	7.5	4.0	2.4	1.7	1.2	0.9	9%
5	13.0	7.3	3.5	2.1	1.4	1.1	0.8	10%
Average	12.2	6.8	3.4	2.0	1.4	1.0	0.8	10%
Std. Dev.	1.0	0.9	0.6	0.4	0.3	0.2	0.1	2%
COV	8%	14%	19%	21%	20%	19%	18%	24%

Table D15 - Deflections from SMART for FSR Item 10 under a 9000 lbs. Load

Location	Deflection (mils)							RMS Error
	0 in.	12 in.	24 in.	36 in.	48 in.	60 in.	72 in.	
1	21.9	11.9	5.5	3.3	2.2	1.7	1.3	13%
2	30.7	17.4	8.2	4.8	3.3	2.4	1.9	14%
3	23.9	13.6	6.5	3.8	2.6	1.9	1.5	10%
4	18.1	9.5	4.4	2.6	1.8	1.3	1.0	14%
5	24.5	13.3	6.1	3.6	2.5	1.9	1.4	8%
Average	23.8	13.1	6.1	3.6	2.5	1.8	1.4	12%
Std. Dev.	4.1	2.6	1.2	0.7	0.5	0.4	0.3	2%
COV	17%	20%	20%	20%	20%	19%	21%	20%

Table D16 - Deflections from SMART for FSR Item 11 under a 9000 lbs. Load

Location	Deflection (mils)							RMS Error
	0 in.	12 in.	24 in.	36 in.	48 in.	60 in.	72 in.	
1	14.4	8.5	4.2	2.5	1.7	1.2	1.0	8%
2	13.5	7.8	3.8	2.2	1.5	1.1	0.9	15%
3	11.7	6.8	3.4	2.0	1.3	1.0	0.8	11%
4	12.3	7.1	3.5	2.1	1.4	1.0	0.8	16%
5	15.3	9.1	4.5	2.6	1.8	1.3	1.0	10%
Average	13.4	7.9	3.9	2.3	1.5	1.1	0.9	12%
Std. Dev.	1.3	0.9	0.4	0.2	0.2	0.1	0.1	3%
COV	10%	11%	11%	10%	12%	10%	10%	25%

Table D17 - Deflections from SMART for FSR Item 12 under a 9000 lbs. Load

Location	Deflection (mils)							RMS Error
	0 in.	12 in.	24 in.	36 in.	48 in.	60 in.	72 in.	
1	15.8	9.1	4.4	2.5	1.7	1.3	1.0	5%
2	14.4	7.3	3.2	1.9	1.3	1.0	0.8	13%
3	12.2	6.4	3.0	1.7	1.2	0.9	0.7	11%
4	14.5	7.4	3.3	2.0	1.4	1.0	0.8	12%
5	12.4	6.3	2.8	1.7	1.2	0.9	0.7	12%
Average	13.9	7.3	3.3	2.0	1.4	1.0	0.8	11%
Std. Dev.	1.4	1.0	0.6	0.3	0.2	0.1	0.1	3%
COV	10%	14%	17%	15%	14%	14%	14%	27%

Table D18 - Deflections from SMART for Hangar 4 under a 9000 lbs. Load

Location	Deflection (mils)							RMS Error
	d0	d1	d2	d3	d4	d5	d6	
1	18.82	8.11	3.53	2.16	1.51	1.13	0.87	20%
2	21.93	8.56	3.65	2.25	1.58	1.18	0.91	35%
3	18.87	8.09	3.50	2.15	1.50	1.12	0.87	33%
4	25.74	9.92	4.18	2.58	1.81	1.35	1.05	32%
Average	21.3	8.7	3.7	2.3	1.6	1.2	0.9	30%
Std. Dev.	3.3	0.9	0.3	0.2	0.1	0.1	0.1	7%
COV	15%	10%	9%	9%	9%	9%	9%	22%

APPENDIX E

DEFLECTIONS FROM SEISMIC TESTS USING SMART

(PI Model)

Table E1 - Deflections from SMART for SH 73 under a 9000 lbs. Load

Location	Deflection (mils)							RMS Error
	0 in.	12 in.	24 in.	36 in.	48 in.	60 in.	72 in.	
1	22.05	9.46	5.4	3.59	2.54	1.87	1.42	8%
2	25.08	10.17	5.75	3.86	2.75	2.04	1.55	6%
3	26.3	10.73	6.03	4.1	2.95	2.2	1.68	6%
4	24.56	11.29	7.01	4.9	3.56	2.66	2.03	8%
5	22.3	10.14	6.21	4.32	3.13	2.33	1.78	6%
6	22	9.46	5.86	4.13	3.03	2.27	1.74	6%
7	22.67	9.44	5.55	3.78	2.72	2.02	1.54	7%
8	21.19	10.19	6.61	4.72	3.47	2.6	1.99	10%
9	22.15	10.4	6.57	4.62	3.36	2.51	1.91	9%
10	25.47	10.56	6.4	4.59	3.41	2.58	1.99	10%
11	20.04	9.19	5.74	3.99	2.88	2.14	1.63	7%
Average	23.1	10.1	6.1	4.2	3.1	2.3	1.8	8%
Std. Dev.	2.0	0.6	0.5	0.4	0.3	0.3	0.2	2%
COV	9%	6%	8%	10%	11%	12%	12%	20%

Table E2 - Deflections from SMART for SH 67 under a 9000 lbs. Load

Location	Deflection (mils)							RMS Error
	0 in.	12 in.	24 in.	36 in.	48 in.	60 in.	72 in.	
-5	11.38	6.63	3.81	2.57	1.87	1.41	1.1	5%
-4	12.35	6.98	3.9	2.6	1.88	1.42	1.1	5%
-3	11.76	6.61	3.8	2.59	1.9	1.44	1.12	8%
-2	11.01	6.44	3.81	2.64	1.94	1.48	1.15	11%
-1	12.62	6.72	3.69	2.45	1.76	1.32	1.02	8%
0	13.63	7.73	4.4	2.99	2.19	1.66	1.3	13%
1	12.14	6.98	4.08	2.82	2.08	1.59	1.24	5%
2	8.86	4.79	2.72	1.84	1.35	1.03	0.8	11%
3	8.88	4.55	2.48	1.64	1.19	0.9	0.7	17%
4	8.71	4.67	2.62	1.75	1.26	0.95	0.74	10%
5	12.14	7.4	4.32	2.93	2.12	1.61	1.25	10%
Average	11.2	6.3	3.6	2.4	1.8	1.3	1.0	9%
Std. Dev.	1.7	1.1	0.7	0.5	0.4	0.3	0.2	4%
COV	15%	18%	19%	20%	20%	20%	20%	41%

Table E3 - Deflections from SMART for FM 2738 under a 9000 lbs. Load

Location	Deflection (mils)							RMS Error
	0 in.	12 in.	24 in.	36 in.	48 in.	60 in.	72 in.	
1	20.52	8.60	4.61	2.79	1.88	1.36	1.04	6%
2	19.18	8.04	4.34	2.63	1.77	1.29	0.98	7%
3	20.68	8.25	4.31	2.6	1.76	1.28	0.98	6%
4	20.12	7.71	3.89	2.34	1.59	1.16	0.89	10%
5	16.85	6.95	3.64	2.19	1.48	1.08	0.82	11%
6	18.23	7.48	3.98	2.41	1.63	1.18	0.9	5%
7	18.35	7.67	4.03	2.43	1.64	1.19	0.91	10%
8	22.01	9.74	5.4	3.32	2.23	1.61	1.22	6%
9	20.7	8.51	4.5	2.71	1.83	1.33	1.01	9%
10	25.43	10.10	5.39	3.25	2.19	1.59	1.21	5%
Average	20.2	8.3	4.4	2.7	1.8	1.3	1.0	8%
Std. Dev.	2.4	1.0	0.6	0.4	0.2	0.2	0.1	2%
COV	12%	12%	14%	14%	14%	13%	13%	30%

Table E4 - Deflections from SMART for FM 2415 under a 9000 lbs. Load

Location	Deflection (mils)							RMS Error
	d0	d1	d2	d3	d4	d5	d6	
1	25.08	12.75	6.79	4.13	2.79	2.02	1.54	8%
2	25.25	10.14	5.51	3.37	2.27	1.64	1.25	13%
3	27.03	10.28	5.41	3.27	2.21	1.61	1.23	13%
4	28.15	11.13	6.07	3.72	2.5	1.81	1.37	9%
5	24.07	9.75	5.27	3.22	2.18	1.58	1.2	10%
6	23.33	8.88	4.6	2.79	1.89	1.38	1.05	14%
7	25.39	10.05	5.34	3.24	2.19	1.59	1.21	11%
8	25.81	10.62	5.72	3.5	2.36	1.71	1.30	9%
9	23.88	8.84	4.57	2.79	1.90	1.38	1.06	12%
10	21.16	8.33	4.43	2.72	1.84	1.34	1.02	16%
11	20.07	7.51	3.94	2.4	1.63	1.19	0.90	11%
12	18.71	8.02	4.38	2.68	1.81	1.31	0.99	12%
Average	24.0	9.7	5.2	3.2	2.1	1.5	1.2	11%
Std. Dev.	2.8	1.5	0.8	0.5	0.3	0.2	0.2	2%
COV	12%	15%	16%	16%	16%	15%	15%	19%

Table E5 - Deflections from SMART for FM 51 under a 9000 lbs. Load

Location	Deflection (mils)							RMS Error
	d0	d1	d2	d3	d4	d5	d6	
1	14.17	5.91	3.18	1.93	1.3	0.94	0.72	18%
2	17.27	6.91	3.71	2.26	1.53	1.11	0.85	11%
3	24.07	9.84	5.39	3.29	2.21	1.6	1.21	10%
4	18.37	8.04	4.42	2.7	1.81	1.31	0.99	12%
5	12.87	5.78	3.2	1.96	1.31	0.95	0.72	15%
6	19.23	8.2	4.55	2.8	1.88	1.36	1.03	6%
7	16.78	6.53	3.46	2.1	1.43	1.04	0.79	13%
8	16.99	6.55	3.45	2.1	1.43	1.04	0.79	11%
9	15.43	5.61	2.88	1.75	1.19	0.87	0.67	16%
10	15.71	6.14	3.2	1.95	1.32	0.96	0.74	12%
11	15.72	5.98	3.14	1.91	1.29	0.94	0.72	13%
12	16.53	6.26	3.27	1.99	1.35	0.98	0.75	14%
13	14.59	6.31	3.47	2.12	1.42	1.03	0.78	12%
14	12.95	5.61	3.06	1.87	1.25	0.91	0.69	14%
15	25.39	10.03	5.52	3.39	2.28	1.65	1.25	6%
Average	17.1	6.9	3.7	2.3	1.5	1.1	0.8	12%
Std. Dev.	3.6	1.4	0.8	0.5	0.3	0.2	0.2	3%
COV	21%	21%	23%	23%	23%	22%	22%	27%

Table E6 - Deflections from SMART for Loop 375 under a 9000 lbs. Load

Location	Deflection (mils)							RMS Error
	0 in.	12 in.	24 in.	36 in.	48 in.	60 in.	72 in.	
1	10.98	4.49	2.28	1.42	0.98	0.71	0.54	14%
2	13.97	6.12	3.20	2.01	1.39	1.01	0.76	7%
3	11.49	4.50	2.20	1.37	0.94	0.69	0.53	15%
4	13.31	5.16	2.47	1.52	1.05	0.76	0.58	12%
5	16.16	5.73	2.65	1.61	1.11	0.81	0.62	10%
6	12.45	5.54	2.99	1.94	1.36	0.98	0.74	9%
7	17.87	6.90	3.36	2.07	1.42	1.03	0.78	5%
8	12.45	5.03	2.50	1.54	1.05	0.77	0.58	12%
9	11.06	4.93	2.62	1.68	1.16	0.84	0.63	12%
10	13.90	5.79	2.93	1.83	1.26	0.91	0.69	9%
11	12.01	5.10	2.60	1.63	1.12	0.82	0.62	11%
12	16.19	6.96	3.55	2.23	1.55	1.12	0.84	6%
13	13.76	5.70	2.91	1.83	1.26	0.92	0.69	9%
14	11.95	4.57	2.25	1.40	0.96	0.70	0.53	14%
15	10.31	4.21	2.10	1.31	0.90	0.66	0.50	16%
16	14.29	5.60	2.78	1.72	1.18	0.86	0.65	9%
17	11.90	4.51	2.18	1.35	0.92	0.68	0.51	15%
18	9.77	4.11	2.15	1.36	0.94	0.68	0.52	16%
19	11.28	4.81	2.46	1.53	1.05	0.77	0.58	13%
20	13.13	5.41	2.77	1.73	1.18	0.86	0.65	10%
21	11.18	4.89	2.61	1.67	1.16	0.84	0.63	12%
22	11.16	4.61	2.37	1.47	1.01	0.73	0.55	14%
23	11.08	4.60	2.39	1.50	1.03	0.75	0.57	14%
24	13.98	5.81	2.91	1.81	1.24	0.90	0.68	9%
25	14.48	5.54	2.66	1.63	1.12	0.81	0.62	10%
26	14.25	5.51	2.75	1.69	1.16	0.84	0.64	10%
27	17.71	6.59	3.11	1.89	1.29	0.94	0.72	6%
28	10.95	4.72	2.50	1.59	1.09	0.79	0.60	13%
29	15.06	5.76	2.82	1.74	1.19	0.87	0.66	9%
30	13.03	4.93	2.40	1.47	1.01	0.74	0.56	13%
31	12.52	5.16	2.66	1.67	1.15	0.84	0.63	11%
32	11.22	4.83	2.55	1.62	1.12	0.81	0.61	12%
33	11.00	4.50	2.30	1.44	0.99	0.72	0.55	14%
Average	12.9	5.2	2.6	1.6	1.1	0.8	0.6	11%
Std. Dev.	2.1	0.7	0.4	0.2	0.2	0.1	0.1	3%
COV	16%	14%	13%	13%	14%	13%	13%	26%

Table E7 - Deflections from SMART for MLK under a 9000 lbs. Load

Location	Deflection (mils)							RMS Error
	0 in.	12 in.	24 in.	36 in.	48 in.	60 in.	72 in.	
1	8.45	4	2.33	1.58	1.13	0.82	0.62	17%
2	7.57	3.72	2.22	1.54	1.11	0.82	0.62	18%
3	9.98	4.72	2.69	1.81	1.29	0.94	0.71	14%
4	12.13	5.06	2.86	1.88	1.34	0.98	0.74	13%
5	12.64	5.57	3.15	2.09	1.49	1.1	0.83	10%
6	11.2	4.68	2.65	1.74	1.23	0.9	0.68	14%
7	10.89	4.37	2.43	1.59	1.12	0.82	0.62	16%
8	12.17	5.06	2.88	1.9	1.35	0.99	0.75	12%
9	12.11	4.7	2.6	1.71	1.2	0.88	0.67	14%
10	10.19	4.39	2.49	1.66	1.17	0.86	0.65	16%
11	9.76	4.27	2.44	1.63	1.15	0.84	0.64	16%
12	9.34	4.39	2.55	1.71	1.22	0.89	0.67	16%
13	11.14	5	2.79	1.83	1.29	0.94	0.7	14%
14	11.63	5.29	3	2	1.43	1.05	0.79	12%
15	14.74	5.85	3.25	2.1	1.48	1.08	0.82	9%
16	13.6	5.49	2.92	1.88	1.31	0.95	0.72	12%
17	14.17	5.55	3.03	1.96	1.38	1.01	0.77	11%
18	14.87	5.91	3.28	2.12	1.5	1.1	0.83	9%
19	16.51	6.44	3.46	2.21	1.55	1.14	0.86	7%
20	12.08	5.3	2.93	1.9	1.33	0.97	0.73	12%
21	10.58	4.63	2.59	1.71	1.21	0.88	0.66	15%
22	9.54	4.32	2.5	1.67	1.18	0.86	0.65	16%
23	10.05	4.69	2.69	1.8	1.28	0.94	0.71	14%
24	9.87	4.26	2.43	1.62	1.15	0.84	0.64	16%
25	15.82	6	3.24	2.07	1.45	1.06	0.8	9%
Average	11.6	4.9	2.8	1.8	1.3	0.9	0.7	13%
Std. Dev.	2.3	0.7	0.3	0.2	0.1	0.1	0.1	3%
COV	20%	14%	12%	10%	10%	10%	10%	22%

Table E8 - Deflections from SMART for IH 20 under a 9000 lbs. Load

Location	Deflection (mils)							RMS Error
	0 in.	12 in.	24 in.	36 in.	48 in.	60 in.	72 in.	
1	7.14	3.78	1.95	1.13	0.66	0.37	0.19	13%
2	7.44	4.18	2.35	1.46	0.9	0.53	0.29	20%
3	6.29	3.43	1.84	1.09	0.64	0.36	0.19	12%
4	6.74	3.48	1.73	0.96	0.54	0.28	0.14	14%
5	5.75	2.99	1.61	0.96	0.57	0.32	0.17	14%
6	5.95	2.92	1.55	0.92	0.54	0.3	0.16	9%
7	5.21	2.5	1.28	0.74	0.43	0.24	0.12	20%
8	7.09	4.13	2.29	1.37	0.82	0.46	0.24	10%
9	7.46	3.28	1.5	0.81	0.44	0.23	0.11	20%
10	7.25	3.83	1.99	1.16	0.67	0.37	0.19	16%
11	6.44	3.27	1.68	0.98	0.56	0.31	0.16	10%
12	6	3.05	1.64	1	0.6	0.34	0.18	9%
13	5.71	2.88	1.49	0.86	0.5	0.28	0.14	17%
14	5.84	3.38	1.97	1.24	0.77	0.46	0.26	10%
15	5.91	3.28	1.84	1.13	0.69	0.4	0.22	12%
16	5.79	3.26	1.82	1.11	0.67	0.38	0.21	22%
17	7.1	4.11	2.18	1.25	0.71	0.38	0.19	16%
18	7.35	4.08	2.14	1.23	0.71	0.38	0.19	12%
19	7.85	4.21	2.05	1.11	0.61	0.32	0.15	16%
20	8.87	4.73	2.17	1.11	0.57	0.28	0.12	12%
21	7.74	4.35	2.33	1.39	0.82	0.47	0.25	7%
Average	6.7	3.6	1.9	1.1	0.6	0.4	0.2	14%
Std. Dev.	0.9	0.6	0.3	0.2	0.1	0.1	0.0	4%
COV	14%	16%	16%	17%	19%	22%	26%	31%

Table E9 - Deflections from SMART for FM 933 under a 9000 lbs. Load

Location	Deflection (mils)							RMS Error
	0 in.	12 in.	24 in.	36 in.	48 in.	60 in.	72 in.	
-5	6.71	3.77	2.57	1.95	1.49	1.15	0.89	9%
-4	7.39	4.05	2.84	2.19	1.71	1.33	1.05	8%
-3	7.52	4.24	2.79	2.1	1.6	1.22	0.95	7%
-2	7.56	4.31	2.89	2.21	1.72	1.34	1.05	2%
-1	7.31	4.13	2.94	2.31	1.85	1.47	1.17	2%
0	8.74	4.97	3.49	2.74	2.18	1.74	1.38	15%
1	6.84	3.82	2.73	2.13	1.68	1.32	1.04	4%
2	5.73	3.21	2.26	1.74	1.35	1.06	0.83	5%
3	7.87	4.13	2.74	2.06	1.57	1.21	0.95	5%
4	6.33	3.38	2.45	1.91	1.5	1.17	0.92	4%
5	7.12	4.02	2.66	2.01	1.53	1.17	0.91	9%
Average	7.2	4.0	2.8	2.1	1.7	1.3	1.0	6%
Std .Dev.	0.8	0.5	0.3	0.3	0.2	0.2	0.2	4%
COV	11%	12%	11%	12%	13%	15%	15%	59%

Table E10 - Deflections from SMART for FSR Item 5 under a 9000 lbs. Load

Location	Deflection (mils)							RMS Error
	0 in.	12 in.	24 in.	36 in.	48 in.	60 in.	72 in.	
1	27.86	11.69	6.15	3.79	2.6	1.92	1.48	16%
2	20.36	7.59	3.68	2.27	1.57	1.17	0.91	8%
3	16.65	7.86	4.34	2.7	1.84	1.34	1.03	9%
4	20.85	9.34	4.98	3.08	2.11	1.55	1.19	8%
5	20.68	9.32	5.04	3.13	2.15	1.58	1.21	12%
6	20.85	7.68	3.78	2.33	1.62	1.2	0.93	15%
7	21.43	6.41	2.83	1.76	1.24	0.92	0.72	19%
Average	21.2	8.6	4.4	2.7	1.9	1.4	1.1	13%
Std. Dev.	3.3	1.7	1.1	0.7	0.5	0.3	0.2	4%
COV	16%	20%	25%	25%	24%	24%	23%	33%

Table E11 - Deflections from SMART for FSR Item 6 under a 9000 lbs. Load

Location	Deflection (mils)							RMS Error
	0 in.	12 in.	24 in.	36 in.	48 in.	60 in.	72 in.	
1	17.09	8.07	4.64	3	2.07	1.51	1.15	11%
2	22.03	7.8	3.89	2.42	1.68	1.25	0.96	11%
3	19.38	7.53	3.92	2.45	1.7	1.25	0.97	12%
Average	19.5	7.8	4.2	2.6	1.8	1.3	1.0	11%
Std. Dev.	2.5	0.3	0.4	0.3	0.2	0.2	0.1	0%
COV	13%	3%	10%	12%	12%	11%	10%	3%

Table E12 - Deflections from SMART for FSR Item 7 under a 9000 lbs. Load

Location	Deflection (mils)							RMS Error
	0 in.	12 in.	24 in.	36 in.	48 in.	60 in.	72 in.	
1	10.23	5.63	2.64	1.54	1.07	0.8	0.62	17%
2	13.54	7.62	3.59	2.09	1.44	1.07	0.83	9%
3	11.63	6.27	2.89	1.7	1.17	0.88	0.68	14%
4	7.69	3.93	1.79	1.06	0.74	0.55	0.43	22%
5	9.19	4.86	2.24	1.32	0.91	0.68	0.53	18%
Average	10.5	5.7	2.6	1.5	1.1	0.8	0.6	16%
Std. Dev.	2.2	1.4	0.7	0.4	0.3	0.2	0.2	5%
COV	21%	25%	26%	25%	25%	25%	25%	30%

Table E13 - Deflections from SMART for FSR Item 8 under a 9000 lbs. Load

Location	Deflection (mils)							RMS Error
	0 in.	12 in.	24 in.	36 in.	48 in.	60 in.	72 in.	
1	14.96	7.85	4.29	2.72	1.88	1.38	1.06	7%
2	21.53	11.31	6.25	3.99	2.75	2.02	1.55	8%
3	16.19	8.17	4.38	2.76	1.91	1.4	1.08	14%
4	12.38	5.57	2.69	1.65	1.15	0.85	0.66	20%
Average	16.3	8.2	4.4	2.8	1.9	1.4	1.1	12%
Std. Dev.	3.9	2.4	1.5	1.0	0.7	0.5	0.4	6%
COV	24%	29%	33%	34%	34%	34%	33%	50%

Table E14 - Deflections from SMART for FSR Item 9 under a 9000 lbs. Load

Location	Deflection (mils)							RMS Error
	0 in.	12 in.	24 in.	36 in.	48 in.	60 in.	72 in.	
1	11.88	5.01	2.33	1.41	0.99	0.74	0.57	13%
2	13.47	6.03	2.84	1.72	1.19	0.89	0.69	11%
3	14.59	7.64	4	2.45	1.68	1.24	0.96	7%
4	13.78	7.46	3.93	2.4	1.65	1.21	0.93	10%
5	14.75	7.28	3.48	2.07	1.43	1.06	0.82	11%
Average	13.7	6.7	3.3	2.0	1.4	1.0	0.8	10%
Std. Dev.	1.1	1.1	0.7	0.4	0.3	0.2	0.2	2%
COV	8%	17%	22%	22%	21%	21%	21%	22%

Table E15 - Deflections from SMART for FSR Item 10 under a 9000 lbs. Load

Location	Deflection (mils)							RMS Error
	0 in.	12 in.	24 in.	36 in.	48 in.	60 in.	72 in.	
1	24.09	11.82	5.45	3.22	2.23	1.66	1.29	13%
2	35.53	17.57	8.14	4.76	3.28	2.44	1.89	14%
3	26.83	13.71	6.44	3.76	2.58	1.92	1.49	10%
4	19.86	9.44	4.33	2.56	1.78	1.33	1.03	14%
5	27.85	13.27	6.09	3.59	2.48	1.85	1.44	8%
Average	26.8	13.2	6.1	3.6	2.5	1.8	1.4	12%
Std. Dev.	5.8	3.0	1.4	0.8	0.5	0.4	0.3	3%
COV	21%	23%	23%	23%	22%	22%	22%	22%

Table E16 - Deflections from SMART for FSR Item 11 under a 9000 lbs. Load

Location	Deflection (mils)							RMS Error
	0 in.	12 in.	24 in.	36 in.	48 in.	60 in.	72 in.	
1	13.78	8.24	4.19	2.45	1.66	1.23	0.95	9%
2	12.88	7.58	3.82	2.23	1.52	1.12	0.87	16%
3	11.16	6.6	3.37	1.98	1.34	0.99	0.77	12%
4	11.75	6.92	3.49	2.04	1.39	1.03	0.8	16%
5	14.67	8.81	4.46	2.6	1.76	1.3	1.01	10%
Average	12.8	7.6	3.9	2.3	1.5	1.1	0.9	12%
Std. Dev.	1.4	0.9	0.5	0.3	0.2	0.1	0.1	3%
COV	11%	12%	12%	12%	12%	12%	11%	27%

Table E17 - Deflections from SMART for FSR Item 12 under a 9000 lbs. Load

Location	Deflection (mils)							RMS Error
	0 in.	12 in.	24 in.	36 in.	48 in.	60 in.	72 in.	
1	15.13	8.78	4.32	2.52	1.72	1.28	0.99	5%
2	13.76	7.07	3.22	1.91	1.33	0.99	0.77	13%
3	11.64	6.23	2.93	1.72	1.19	0.89	0.69	12%
4	13.87	7.2	3.29	1.95	1.35	1.01	0.79	12%
5	11.84	6.08	2.78	1.65	1.15	0.86	0.67	13%
Average	13.2	7.1	3.3	2.0	1.3	1.0	0.8	11%
Std. Dev.	1.5	1.1	0.6	0.3	0.2	0.2	0.1	3%
COV	11%	15%	18%	18%	17%	16%	16%	31%

Table E18 - Deflections from SMART for Hangar 4 under a 9000 lbs. Load

Location	Deflection (mils)							RMS Error
	d0	d1	d2	d3	d4	d5	d6	
1	21.5	7.76	3.49	2.15	1.51	1.12	0.87	20%
2	25.87	8.28	3.61	2.24	1.57	1.18	0.91	34%
3	21.39	7.73	3.46	2.13	1.49	1.12	0.87	32%
4	33.07	9.53	4.12	2.57	1.81	1.35	1.05	31%
Average	25.5	8.3	3.7	2.3	1.6	1.2	0.9	29%
Std. Dev.	5.5	0.8	0.3	0.2	0.1	0.1	0.1	6%
COV	22%	10%	8%	9%	9%	9%	9%	22%

APPENDIX F

DEFLECTIONS FROM SEISMIC TESTS USING SMART

(Linear Model)

Table F1 - Deflections from SMART for SH 73 under a 9000 lbs. Load

Location	Deflection (mils)							RMS Error
	0 in.	12 in.	24 in.	36 in.	48 in.	60 in.	72 in.	
1	15.1	9.0	5.4	3.6	2.5	1.9	1.4	8%
2	17.0	9.6	5.7	3.9	2.8	2.0	1.6	5%
3	18.2	10.2	6.0	4.1	3.0	2.2	1.7	5%
4	17.6	10.8	7.0	4.9	3.6	2.7	2.0	7%
5	16.0	9.7	6.2	4.3	3.1	2.3	1.8	5%
6	15.8	9.2	5.9	4.1	3.0	2.3	1.7	5%
7	16.3	9.1	5.5	3.8	2.7	2.0	1.5	4%
8	15.9	9.9	6.6	4.7	3.5	2.6	2.0	9%
9	16.3	10.0	6.6	4.6	3.4	2.5	1.9	9%
10	17.9	10.1	6.4	4.6	3.4	2.6	2.0	9%
11	15.0	8.9	5.7	4.0	2.9	2.1	1.6	7%
Average	16.5	9.7	6.1	4.2	3.1	2.3	1.7	7%
Std. Dev.	1.0	0.6	0.5	0.4	0.3	0.3	0.2	2%
COV	6%	6%	8%	9%	11%	12%	12%	29%

Table F2 - Deflections from SMART for SH 67 under a 9000 lbs. Load

Location	Deflection (mils)							RMS Error
	0 in.	12 in.	24 in.	36 in.	48 in.	60 in.	72 in.	
-5	10.0	6.3	3.8	2.6	1.9	1.4	1.1	4%
-4	10.7	6.6	3.9	2.6	1.9	1.4	1.1	4%
-3	10.2	6.3	3.8	2.6	1.9	1.4	1.1	8%
-2	9.7	6.1	3.8	2.6	1.9	1.5	1.2	12%
-1	10.8	6.4	3.7	2.5	1.8	1.3	1.0	8%
0	11.7	7.3	4.4	3.0	2.2	1.7	1.3	12%
1	10.6	6.6	4.1	2.8	2.1	1.6	1.2	5%
2	8.0	4.7	2.7	1.8	1.4	1.0	0.8	12%
3	7.9	4.4	2.5	1.6	1.2	0.9	0.7	18%
4	7.8	4.5	2.6	1.8	1.3	1.0	0.7	10%
5	10.6	7.0	4.3	2.9	2.1	1.6	1.3	10%
Average	9.8	6.0	3.6	2.4	1.8	1.3	1.0	9%
Std. Dev.	1.3	1.0	0.6	0.5	0.3	0.3	0.2	4%
COV	13%	16%	18%	19%	18%	19%	20%	45%

Table F3 - Deflections from SMART for FM 2738 under a 9000 lbs. Load

Location	Deflection (mils)							RMS Error
	0 in.	12 in.	24 in.	36 in.	48 in.	60 in.	72 in.	
1	15.83	8.53	4.62	2.8	1.88	1.36	1.04	7%
2	14.84	7.97	4.35	2.64	1.77	1.29	0.98	9%
3	16.14	8.23	4.32	2.60	1.76	1.28	0.98	7%
4	15.93	7.70	3.91	2.34	1.59	1.16	0.89	11%
5	13.51	6.94	3.65	2.19	1.48	1.08	0.82	12%
6	14.35	7.45	3.99	2.42	1.63	1.18	0.90	6%
7	14.53	7.64	4.04	2.43	1.64	1.19	0.91	11%
8	16.49	9.48	5.4	3.33	2.23	1.61	1.22	7%
9	16.06	8.47	4.51	2.71	1.83	1.33	1.01	10%
10	18.47	10.02	5.41	3.26	2.19	1.59	1.21	7%
Average	15.6	8.2	4.4	2.7	1.8	1.3	1.0	9%
Std. Dev.	1.4	0.9	0.6	0.4	0.2	0.2	0.1	2%
COV	9%	11%	13%	14%	14%	13%	13%	25%

Table F4 - Deflections from SMART for FM 2415 under a 9000 lbs. Load

Location	Deflection (mils)							RMS Error
	d0	d1	d2	d3	d4	d5	d6	
1	25.08	12.75	6.79	4.13	2.79	2.02	1.54	8%
2	18.24	9.98	5.52	3.38	2.27	1.64	1.25	14%
3	19.66	10.2	5.42	3.28	2.21	1.61	1.23	14%
4	19.86	10.93	6.08	3.73	2.51	1.81	1.37	10%
5	18.03	9.61	5.28	3.23	2.18	1.58	1.2	11%
6	17.85	8.84	4.61	2.79	1.89	1.38	1.05	15%
7	18.68	9.93	5.35	3.26	2.19	1.59	1.21	12%
8	18.93	10.43	5.74	3.51	2.36	1.71	1.3	10%
9	17.98	8.75	4.58	2.8	1.9	1.38	1.06	13%
10	16.25	8.22	4.44	2.72	1.84	1.34	1.02	16%
11	15.5	7.47	3.95	2.4	1.63	1.19	0.9	12%
12	14.53	7.91	4.38	2.69	1.81	1.31	0.99	13%
Average	18.4	9.6	5.2	3.2	2.1	1.5	1.2	12%
Std. Dev.	2.7	1.5	0.8	0.5	0.3	0.2	0.2	2%
COV	14%	15%	16%	16%	16%	15%	15%	18%

Table F5 - Deflections from SMART for FM 51 under a 9000 lbs. Load

Location	Deflection, mils							RMS Error
	d0	d1	d2	d3	d4	d5	d6	
1	11.51	5.89	3.18	1.93	1.3	0.94	0.72	19%
2	13.66	6.87	3.72	2.26	1.53	1.11	0.85	12%
3	17.4	9.67	5.4	3.3	2.22	1.6	1.21	11%
4	14.05	7.88	4.42	2.7	1.81	1.31	0.99	13%
5	10.31	5.69	3.2	1.96	1.31	0.95	0.72	16%
6	14.67	8.07	4.55	2.81	1.88	1.36	1.03	8%
7	13.3	6.5	3.46	2.11	1.43	1.04	0.79	14%
8	13.46	6.52	3.46	2.11	1.43	1.04	0.79	12%
9	12.35	5.6	2.89	1.75	1.19	0.87	0.67	16%
10	12.64	6.12	3.21	1.95	1.32	0.96	0.74	13%
11	12.57	5.97	3.15	1.91	1.29	0.94	0.72	14%
12	13.13	6.24	3.28	1.99	1.35	0.98	0.75	15%
13	11.71	6.25	3.47	2.12	1.42	1.03	0.78	13%
14	10.52	5.57	3.06	1.87	1.25	0.91	0.69	15%
15	18.21	9.87	5.53	3.4	2.28	1.65	1.25	8%
Average	13.3	6.8	3.7	2.3	1.5	1.1	0.8	13%
Std. Dev.	2.2	1.4	0.8	0.5	0.3	0.2	0.2	3%
COV	17%	20%	23%	23%	23%	22%	22%	23%

Table F6 - Deflections from SMART for Loop 375 under a 9000 lbs. Load

Location	Deflection (mils)							RMS Error
	0 in.	12 in.	24 in.	36 in.	48 in.	60 in.	72 in.	
1	8.14	3.96	2.23	1.42	0.98	0.71	0.54	16%
2	9.18	5.02	3.05	2.01	1.39	1.01	0.76	11%
3	8.77	4.02	2.16	1.37	0.94	0.69	0.53	16%
4	9.81	4.52	2.41	1.52	1.05	0.76	0.58	14%
5	11.21	4.93	2.57	1.61	1.11	0.81	0.62	12%
6	7.51	4.42	2.87	1.94	1.36	0.98	0.74	12%
7	11.54	5.71	3.22	2.07	1.42	1.03	0.78	9%
8	8.98	4.38	2.43	1.54	1.05	0.77	0.58	14%
9	7.44	4.12	2.55	1.68	1.16	0.84	0.63	14%
10	9.25	4.86	2.84	1.83	1.26	0.91	0.69	11%
11	8.79	4.45	2.53	1.63	1.12	0.82	0.62	13%
12	9.51	5.41	3.37	2.23	1.55	1.12	0.84	10%
13	9.18	4.76	2.82	1.83	1.26	0.92	0.69	12%
14	8.90	4.07	2.21	1.40	0.96	0.70	0.53	16%
15	7.95	3.79	2.06	1.31	0.90	0.66	0.50	17%
16	9.96	4.81	2.70	1.72	1.18	0.86	0.65	12%
17	8.93	4.00	2.14	1.35	0.92	0.68	0.51	16%
18	7.44	3.65	2.12	1.36	0.94	0.68	0.52	17%
19	8.24	4.19	2.40	1.53	1.05	0.77	0.58	15%
20	8.92	4.59	2.69	1.73	1.18	0.86	0.65	13%
21	7.74	4.14	2.54	1.67	1.16	0.84	0.63	14%
22	8.02	4.03	2.31	1.47	1.01	0.73	0.55	16%
23	8.08	4.02	2.33	1.50	1.03	0.75	0.57	15%
24	9.42	4.89	2.82	1.81	1.24	0.90	0.68	12%
25	10.10	4.78	2.58	1.63	1.12	0.81	0.62	13%
26	9.76	4.72	2.66	1.69	1.16	0.84	0.64	12%
27	11.58	5.50	2.99	1.89	1.29	0.94	0.72	9%
28	7.50	4.00	2.43	1.59	1.09	0.79	0.60	15%
29	10.21	4.91	2.74	1.74	1.19	0.87	0.66	12%
30	9.41	4.31	2.34	1.47	1.01	0.74	0.56	15%
31	8.82	4.44	2.59	1.67	1.15	0.84	0.63	13%
32	8.09	4.19	2.48	1.62	1.12	0.81	0.61	14%
33	8.20	3.97	2.25	1.44	0.99	0.72	0.55	16%
Average	9.0	4.5	2.6	1.6	1.1	0.8	0.6	14%
Std. Dev.	1.1	0.5	0.3	0.2	0.2	0.1	0.1	2%
COV	12%	11%	12%	13%	14%	13%	13%	16%

Table F7 - Deflections from SMART for MLK under a 9000 lbs. Load

Location	Deflection (mils)							RMS Error
	0 in.	12 in.	24 in.	36 in.	48 in.	60 in.	72 in.	
1	6.3	3.4	2.3	1.6	1.1	0.8	0.6	19%
2	5.7	3.2	2.2	1.5	1.1	0.8	0.6	19%
3	6.7	3.9	2.6	1.8	1.3	0.9	0.7	16%
4	9.1	4.4	2.8	1.9	1.3	1.0	0.7	14%
5	9.1	4.7	3.0	2.1	1.5	1.1	0.8	13%
6	8.5	4.1	2.6	1.7	1.2	0.9	0.7	16%
7	8.5	3.9	2.4	1.6	1.1	0.8	0.6	17%
8	9.2	4.4	2.8	1.9	1.4	1.0	0.8	14%
9	9.4	4.2	2.5	1.7	1.2	0.9	0.7	16%
10	7.9	3.8	2.4	1.7	1.2	0.9	0.7	17%
11	7.6	3.8	2.4	1.6	1.2	0.8	0.6	17%
12	6.6	3.7	2.5	1.7	1.2	0.9	0.7	17%
13	7.7	4.2	2.7	1.8	1.3	0.9	0.7	16%
14	8.1	4.4	2.9	2.0	1.4	1.1	0.8	14%
15	10.6	5.0	3.1	2.1	1.5	1.1	0.8	12%
16	9.8	4.7	2.8	1.9	1.3	1.0	0.7	14%
17	10.5	4.8	2.9	2.0	1.4	1.0	0.8	13%
18	10.6	5.0	3.1	2.1	1.5	1.1	0.8	11%
19	11.4	5.4	3.3	2.2	1.6	1.1	0.9	10%
20	8.4	4.4	2.8	1.9	1.3	1.0	0.7	15%
21	7.9	4.0	2.5	1.7	1.2	0.9	0.7	17%
22	7.3	3.7	2.4	1.7	1.2	0.9	0.7	17%
23	7.2	3.9	2.6	1.8	1.3	0.9	0.7	16%
24	7.8	3.8	2.4	1.6	1.2	0.8	0.6	17%
25	11.2	5.1	3.1	2.1	1.5	1.1	0.8	12%
Average	8.5	4.2	2.7	1.8	1.3	0.9	0.7	15%
Std. Dev.	1.5	0.5	0.3	0.2	0.1	0.1	0.1	2%
COV	18%	13%	11%	11%	11%	11%	11%	16%

Table F8 - Deflections from SMART for IH 20 under a 9000 lbs. Load

Location	Deflection (mils)							RMS Error
	0 in.	12 in.	24 in.	36 in.	48 in.	60 in.	72 in.	
1	6.0	3.5	2.0	1.1	0.7	0.4	0.2	14%
2	6.3	3.9	2.3	1.5	0.9	0.5	0.3	20%
3	5.4	3.2	1.8	1.1	0.6	0.4	0.2	12%
4	5.8	3.3	1.7	1.0	0.5	0.3	0.1	13%
5	5.0	2.8	1.6	1.0	0.6	0.3	0.2	15%
6	5.2	2.8	1.6	0.9	0.5	0.3	0.2	8%
7	4.6	2.4	1.3	0.7	0.4	0.2	0.1	21%
8	6.1	3.8	2.3	1.4	0.8	0.5	0.2	8%
9	6.2	3.1	1.5	0.8	0.4	0.2	0.1	20%
10	6.1	3.6	2.0	1.2	0.7	0.4	0.2	16%
11	5.5	3.1	1.7	1.0	0.6	0.3	0.2	10%
12	5.2	2.9	1.6	1.0	0.6	0.3	0.2	8%
13	4.9	2.7	1.5	0.9	0.5	0.3	0.1	18%
14	5.1	3.2	2.0	1.2	0.8	0.5	0.3	8%
15	5.2	3.1	1.8	1.1	0.7	0.4	0.2	10%
16	5.1	3.1	1.8	1.1	0.7	0.4	0.2	21%
17	6.1	3.8	2.2	1.3	0.7	0.4	0.2	13%
18	6.3	3.8	2.1	1.2	0.7	0.4	0.2	9%
19	6.6	3.9	2.0	1.1	0.6	0.3	0.2	12%
20	7.3	4.3	2.2	1.1	0.6	0.3	0.1	9%
21	6.5	4.0	2.3	1.4	0.8	0.5	0.3	7%
Average	5.7	3.3	1.9	1.1	0.6	0.4	0.2	13%
Std. Dev.	0.7	0.5	0.3	0.2	0.1	0.1	0.1	5%
COV	12%	15%	16%	18%	20%	25%	32%	37%

Table F9 - Deflections from SMART for FM 933 under a 9000 lbs. Load

Location	Deflection (mils)							RMS Error
	0 in.	12 in.	24 in.	36 in.	48 in.	60 in.	72 in.	
-5	5.28	3.38	2.55	1.95	1.49	1.15	0.89	11%
-4	5.42	3.61	2.81	2.19	1.71	1.33	1.05	9%
-3	6.06	3.73	2.77	2.10	1.60	1.22	0.95	8%
-2	6.05	3.76	2.85	2.21	1.72	1.34	1.05	4%
-1	5.45	3.64	2.88	2.31	1.85	1.47	1.17	3%
0	6.27	4.29	3.42	2.74	2.18	1.74	1.38	14%
1	5.09	3.43	2.69	2.13	1.68	1.32	1.04	2%
2	4.58	2.92	2.23	1.74	1.35	1.06	0.83	5%
3	6.92	3.87	2.74	2.06	1.57	1.21	0.95	3%
4	4.63	3.08	2.42	1.91	1.50	1.17	0.92	4%
5	5.79	3.57	2.65	2.01	1.53	1.17	0.91	10%
Average	5.6	3.6	2.7	2.1	1.7	1.3	1.0	7%
Std .Dev.	0.7	0.4	0.3	0.2	0.2	0.2	0.1	4%
COV	12%	10%	11%	12%	13%	14%	15%	57%

Table F10 - Deflections from SMART for FSR Item 5 under a 9000 lbs. Load

Location	Deflection (mils)							RMS Error
	0 in.	12 in.	24 in.	36 in.	48 in.	60 in.	72 in.	
1	20.9	11.5	6.2	3.8	2.6	1.9	1.5	16%
2	16.2	7.6	3.7	2.3	1.6	1.2	0.9	10%
3	12.7	7.6	4.3	2.7	1.8	1.3	1.0	11%
4	16.5	9.2	5.0	3.1	2.1	1.6	1.2	10%
5	16.3	9.2	5.1	3.1	2.2	1.6	1.2	13%
6	16.4	7.6	3.8	2.3	1.6	1.2	0.9	15%
7	16.3	6.4	2.8	1.8	1.2	0.9	0.7	20%
Average	16.5	8.4	4.4	2.7	1.9	1.4	1.1	14%
Std. Dev.	2.2	1.5	1.0	0.6	0.4	0.3	0.2	3%
COV	13%	18%	23%	23%	23%	22%	23%	25%

Table F11 - Deflections from SMART for FSR Item 6 under a 9000 lbs. Load

Location	Deflection (mils)							RMS Error
	0 in.	12 in.	24 in.	36 in.	48 in.	60 in.	72 in.	
1	13.1	7.8	4.6	3.0	2.1	1.5	1.2	12%
2	16.5	7.7	3.9	2.4	1.7	1.3	1.0	12%
3	14.9	7.4	3.9	2.5	1.7	1.3	1.0	13%
Average	14.8	7.6	4.1	2.6	1.8	1.4	1.1	12%
Std. Dev.	1.4	0.2	0.3	0.3	0.2	0.1	0.1	0%
COV	9%	2%	8%	10%	10%	7%	9%	4%

Table F12 - Deflections from SMART for FSR Item 7 under a 9000 lbs. Load

Location	Deflection (mils)							RMS Error
	0 in.	12 in.	24 in.	36 in.	48 in.	60 in.	72 in.	
1	10.2	5.6	2.6	1.5	1.1	0.8	0.6	17%
2	13.5	7.6	3.6	2.1	1.4	1.1	0.8	9%
3	11.6	6.3	2.9	1.7	1.2	0.9	0.7	14%
4	7.7	3.9	1.8	1.1	0.7	0.6	0.4	22%
5	9.2	4.9	2.2	1.3	0.9	0.7	0.5	18%
Average	10.4	5.7	2.6	1.5	1.1	0.8	0.6	16%
Std. Dev.	2.0	1.3	0.6	0.3	0.2	0.2	0.1	4%
COV	19%	22%	23%	22%	23%	21%	24%	27%

Table F13 - Deflections from SMART for FSR Item 8 under a 9000 lbs. Load

Location	Deflection (mils)							RMS Error
	0 in.	12 in.	24 in.	36 in.	48 in.	60 in.	72 in.	
1	0 in.	12 in.	24 in.	36 in.	48 in.	60 in.	72 in.	
2	12.5	7.5	4.3	2.7	1.9	1.4	1.1	9%
3	17.3	10.7	6.2	4.0	2.8	2.0	1.6	9%
4	13.3	7.9	4.4	2.8	1.9	1.4	1.1	15%
Average	10.2	5.4	2.7	1.7	1.2	0.9	0.7	21%
Std. Dev.	13.3	7.9	4.4	2.8	2.0	1.4	1.1	14%
COV	2.6	1.9	1.2	0.8	0.6	0.4	0.3	5%

Table F14 - Deflections from SMART for FSR Item 9 under a 9000 lbs. Load

Location	Deflection (mils)							RMS Error
	0 in.	12 in.	24 in.	36 in.	48 in.	60 in.	72 in.	
1	10.1	5.0	2.3	1.4	1.0	0.7	0.6	14%
2	11.4	5.9	2.8	1.7	1.2	0.9	0.7	11%
3	12.5	7.4	4.0	2.5	1.7	1.2	1.0	6%
4	12.0	7.2	3.9	2.4	1.7	1.2	0.9	8%
5	12.5	7.0	3.5	2.1	1.4	1.1	0.8	10%
Average	11.7	6.5	3.3	2.0	1.4	1.0	0.8	10%
Std. Dev.	0.9	0.9	0.7	0.4	0.3	0.2	0.1	3%
COV	8%	14%	20%	21%	20%	19%	18%	28%

Table F15 - Deflections from SMART for FSR Item 10 under a 9000 lbs. Load

Location	Deflection (mils)							RMS Error
	0 in.	12 in.	24 in.	36 in.	48 in.	60 in.	72 in.	
1	21.0	11.5	5.5	3.2	2.2	1.7	1.3	14%
2	29.4	16.8	8.1	4.8	3.3	2.4	1.9	14%
3	23.0	13.2	6.4	3.8	2.6	1.9	1.5	10%
4	17.4	9.2	4.3	2.6	1.8	1.3	1.0	15%
5	23.5	12.8	6.1	3.6	2.5	1.9	1.4	8%
Average	22.9	12.7	6.1	3.6	2.5	1.8	1.4	12%
Std. Dev.	3.9	2.5	1.2	0.7	0.5	0.4	0.3	3%
COV	17%	20%	20%	20%	20%	19%	21%	22%

Table F16 - Deflections from SMART for FSR Item 11 under a 9000 lbs. Load

Location	Deflection (mils)							RMS Error
	0 in.	12 in.	24 in.	36 in.	48 in.	60 in.	72 in.	
1	13.8	8.2	4.2	2.5	1.7	1.2	1.0	9%
2	12.9	7.6	3.8	2.2	1.5	1.1	0.9	16%
3	11.2	6.6	3.4	2.0	1.3	1.0	0.8	12%
4	11.8	6.9	3.5	2.0	1.4	1.0	0.8	16%
5	14.7	8.8	4.5	2.6	1.8	1.3	1.0	10%
Average	12.9	7.6	3.9	2.3	1.5	1.1	0.9	13%
Std. Dev.	1.3	0.8	0.4	0.2	0.2	0.1	0.1	3%
COV	10%	11%	11%	11%	12%	10%	10%	23%

Table F17 - Deflections from SMART for FSR Item 12 under a 9000 lbs. Load

Location	Deflection (mils)							RMS Error
	0 in.	12 in.	24 in.	36 in.	48 in.	60 in.	72 in.	
1	15.1	8.8	4.3	2.5	1.7	1.3	1.0	5%
2	13.8	7.1	3.2	1.9	1.3	1.0	0.8	13%
3	11.6	6.2	2.9	1.7	1.2	0.9	0.7	12%
4	13.9	7.2	3.3	2.0	1.4	1.0	0.8	12%
5	11.8	6.1	2.8	1.7	1.2	0.9	0.7	13%
Average	13.2	7.1	3.3	2.0	1.4	1.0	0.8	11%
Std. Dev.	1.3	1.0	0.5	0.3	0.2	0.1	0.1	3%
COV	10%	14%	16%	15%	14%	14%	14%	28%

Table F18 - Deflections from SMART for Hangar 4 under a 9000 lbs. Load

Location	Deflection, mils							RMS Error
	d0	d1	d2	d3	d4	d5	d6	
1	17.91	7.74	3.51	2.15	1.51	1.12	0.87	20%
2	20.88	8.23	3.63	2.24	1.57	1.18	0.91	35%
3	17.95	7.71	3.48	2.14	1.49	1.12	0.87	32%
4	24.55	9.46	4.15	2.57	1.81	1.35	1.05	32%
Average	20.3	8.3	3.7	2.3	1.6	1.2	0.9	30%
Std. Dev.	3.1	0.8	0.3	0.2	0.1	0.1	0.1	7%
COV	15%	10%	8%	9%	9%	9%	9%	22%

APPENDIX G

COMPARISON OF DEFLECTIONS CALCULATED BY ESTIMATION OF NONLINEAR PARAMETERS WITH FWD DEFLECTIONS

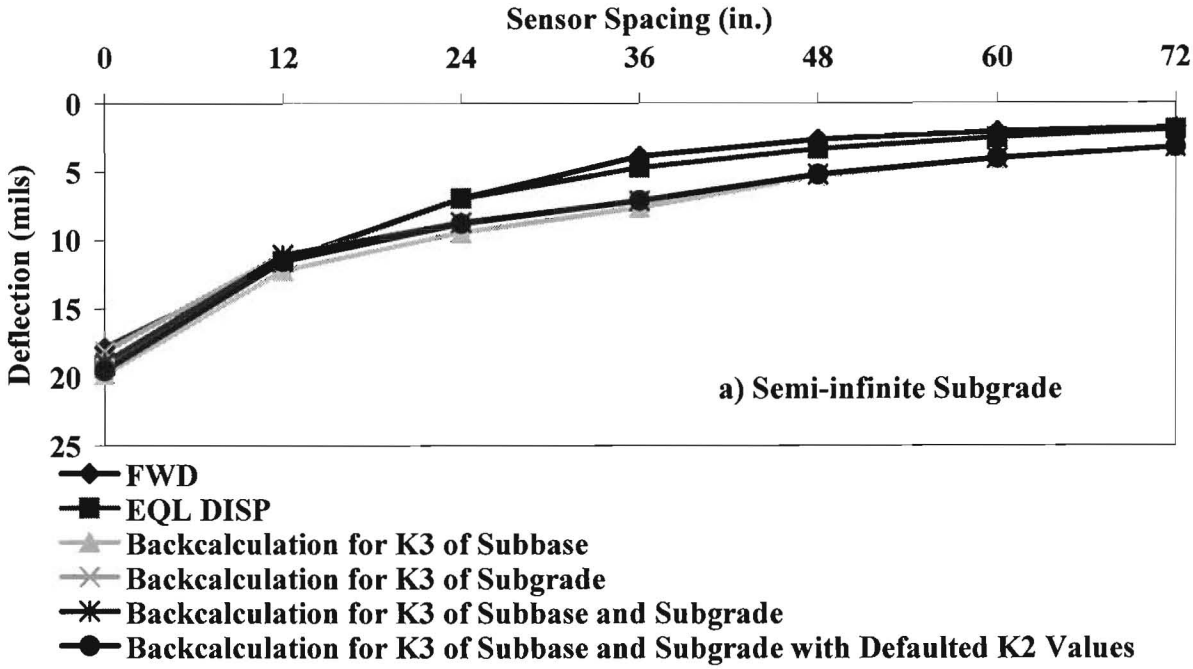

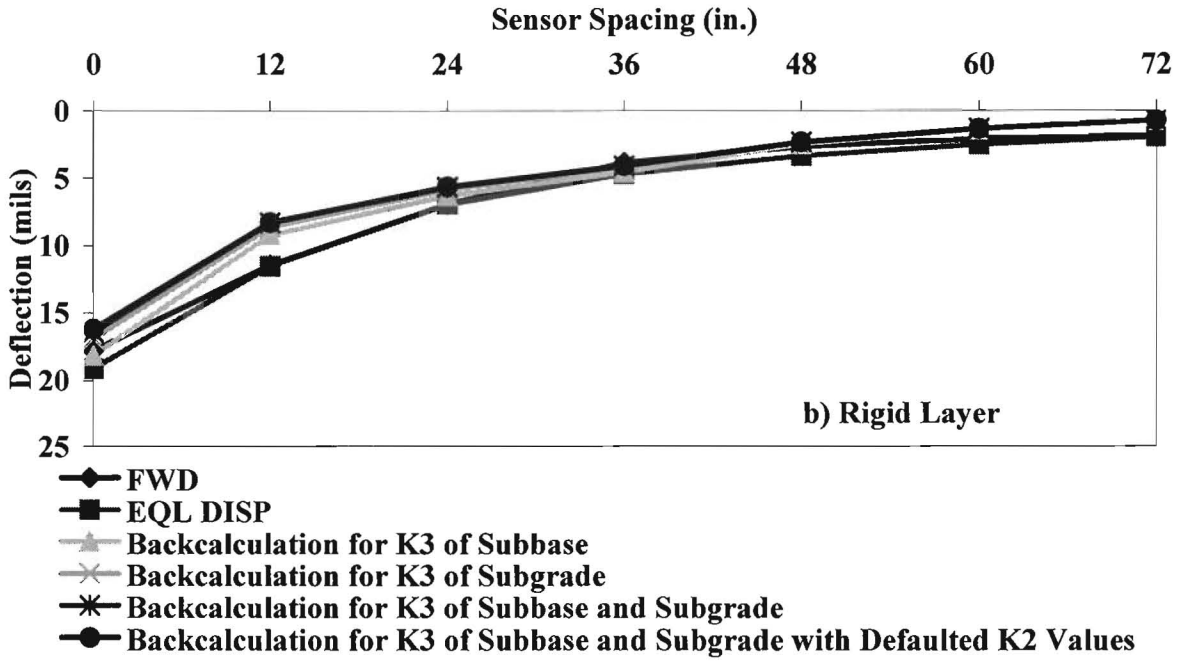

Figure G1 – Comparison of Deflections Calculated Based on Estimation of Non-linear Parameters and FWD Deflections for SH 73

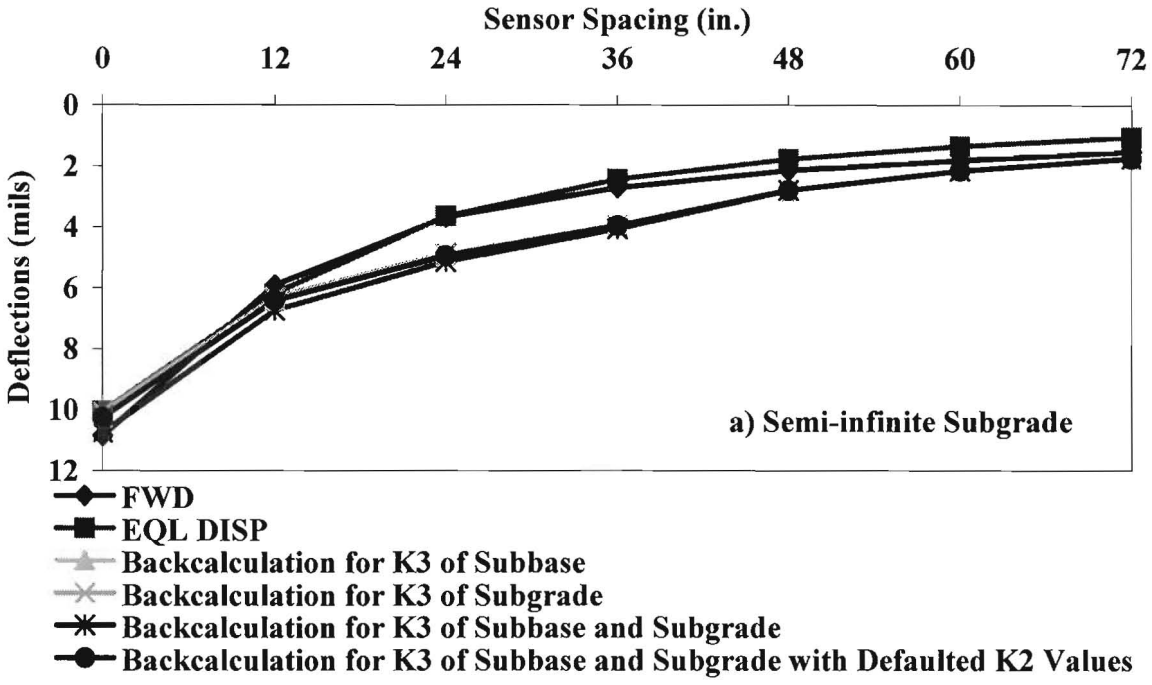

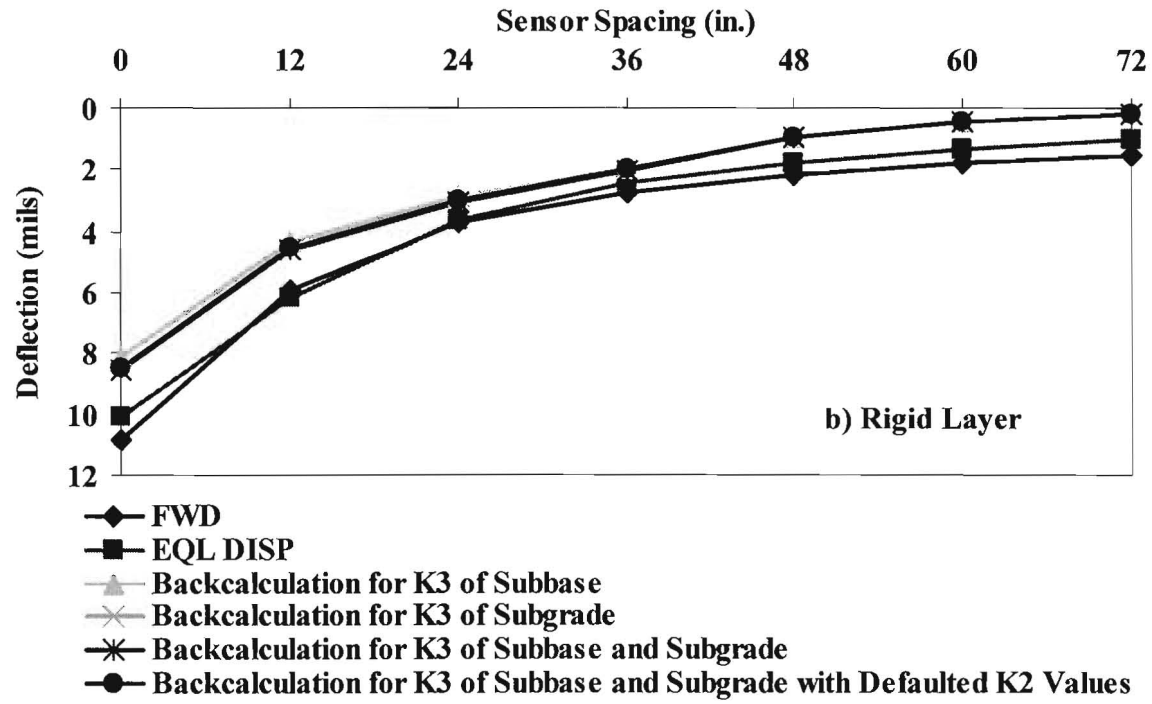

Figure G2 – Comparison of Deflections Calculated Based on Estimation of Non-linear Parameters and FWD Deflections for US 67

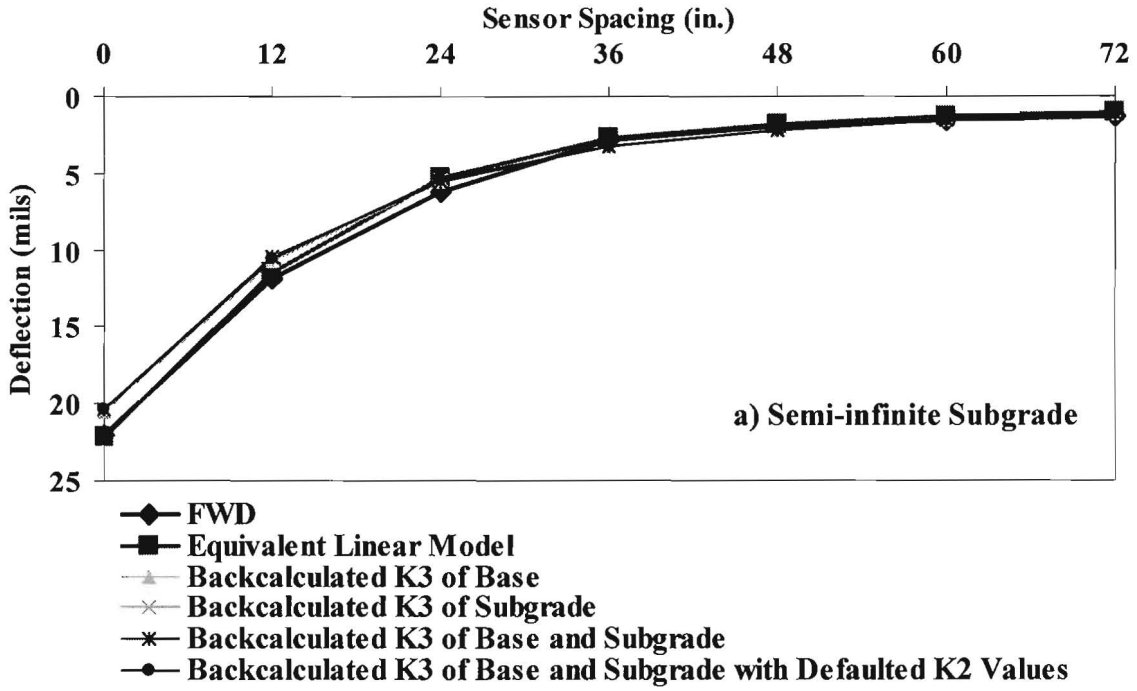

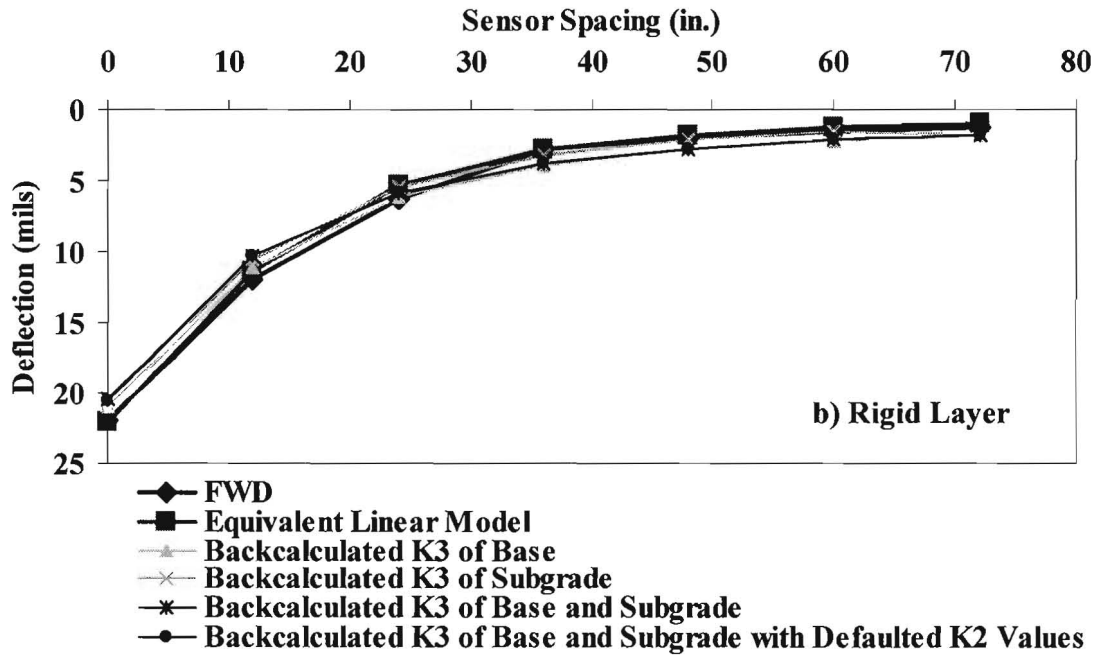

Figure G3 – Comparison of Deflections Calculated Based on Estimation of Non-linear Parameters and FWD Deflections for FM 2738

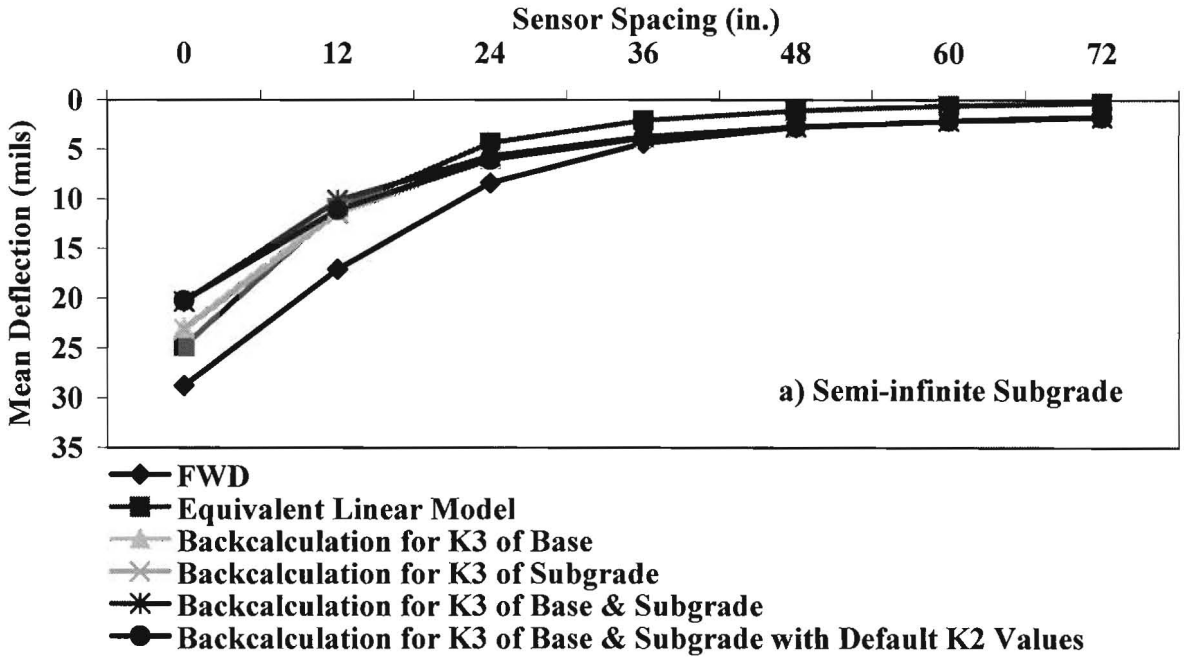

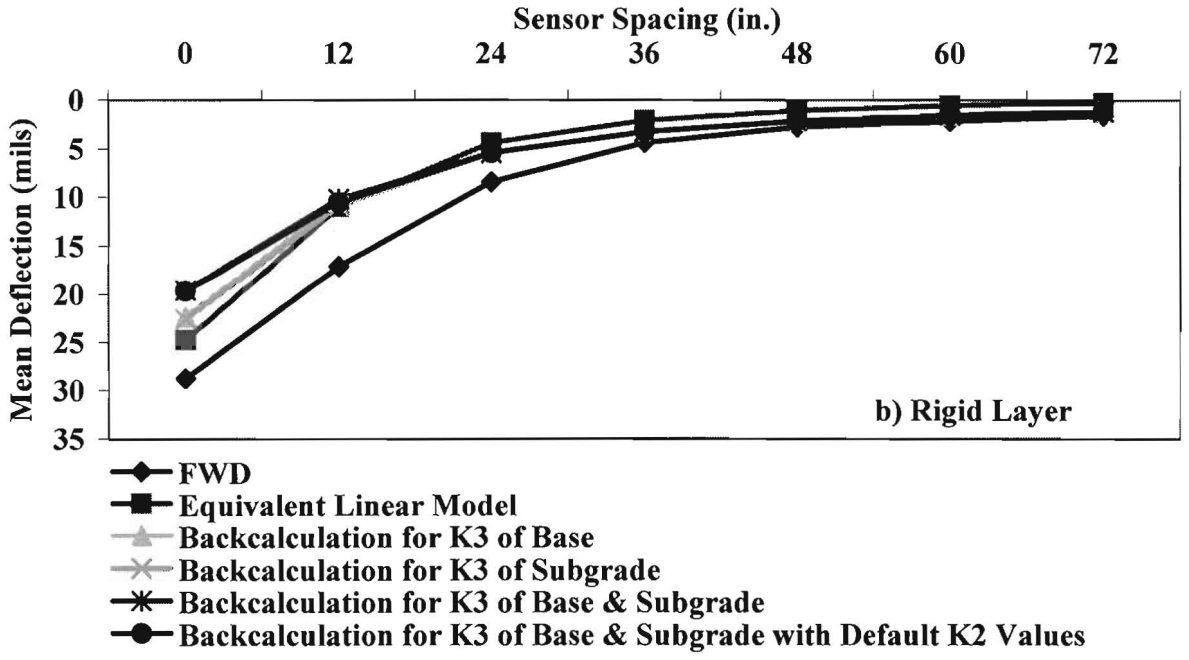

Figure G4 – Comparison of Deflections Calculated Based on Estimation of Non-linear Parameters and FWD Deflections for FM 2415

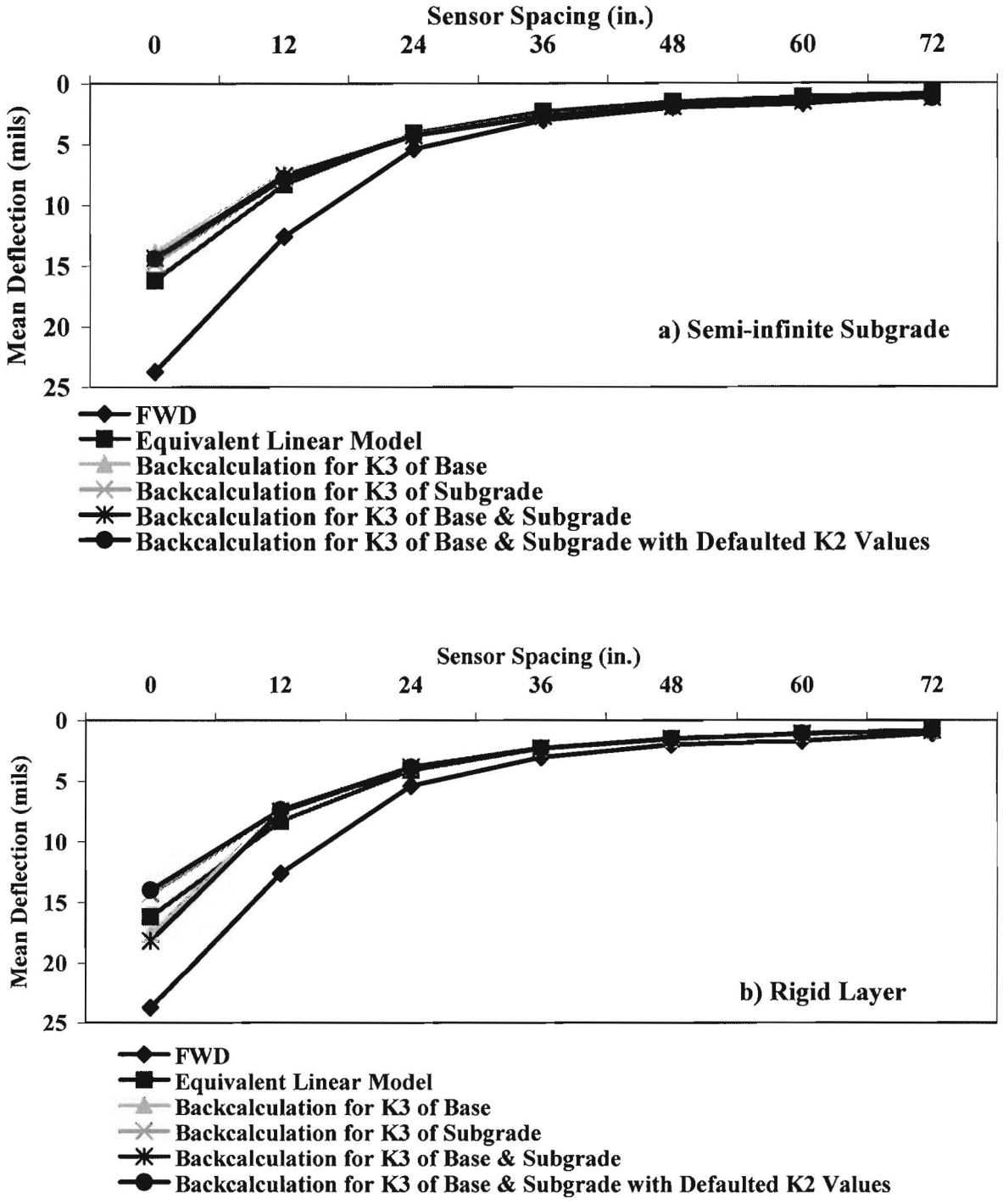

Figure G5 – Comparison of Deflections Calculated Based on Estimation of Non-linear Parameters and FWD Deflections for FM 51

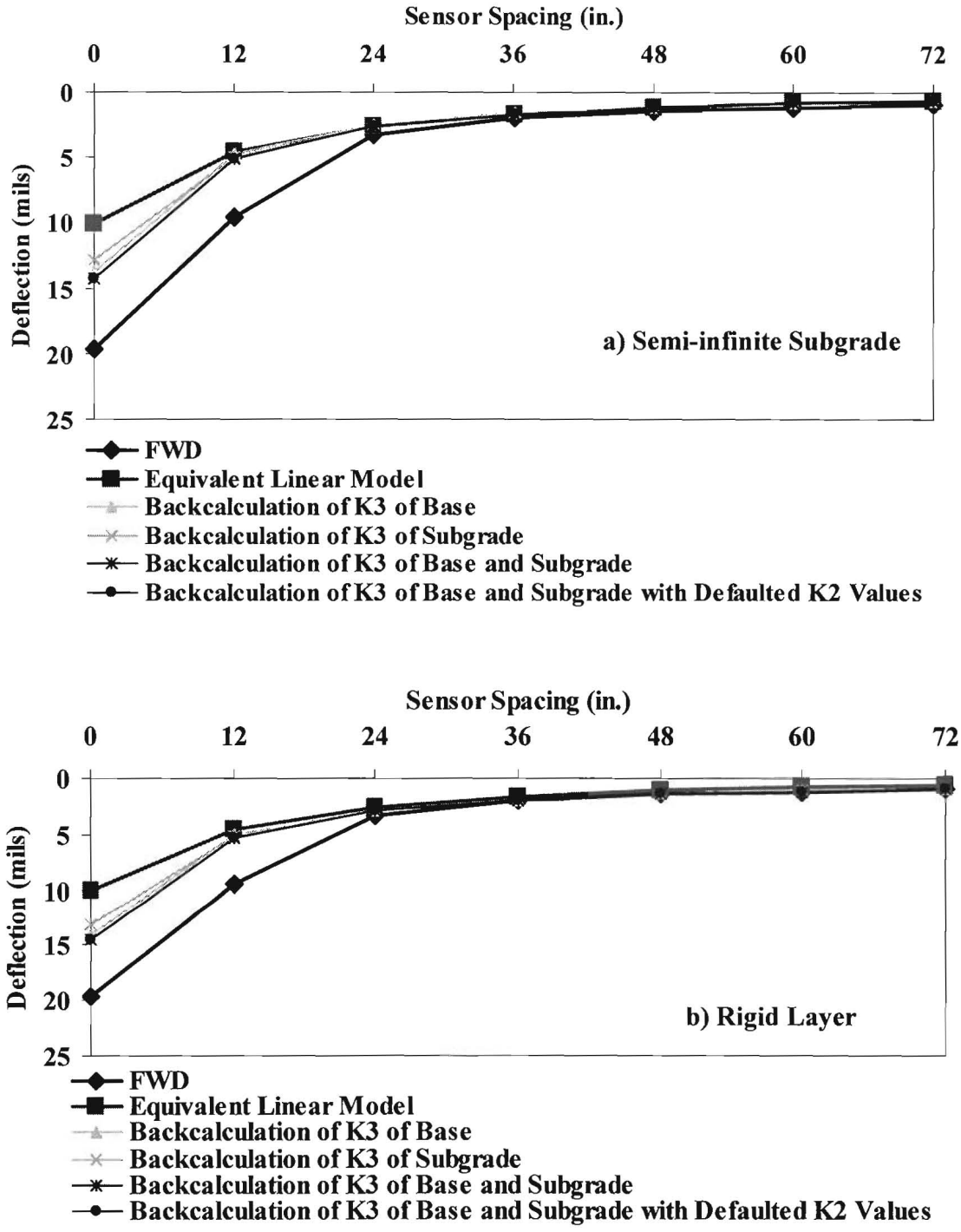

Figure G6 – Comparison of Deflections Calculated Based on Estimation of Non-linear Parameters and FWD Deflections for Loop 375

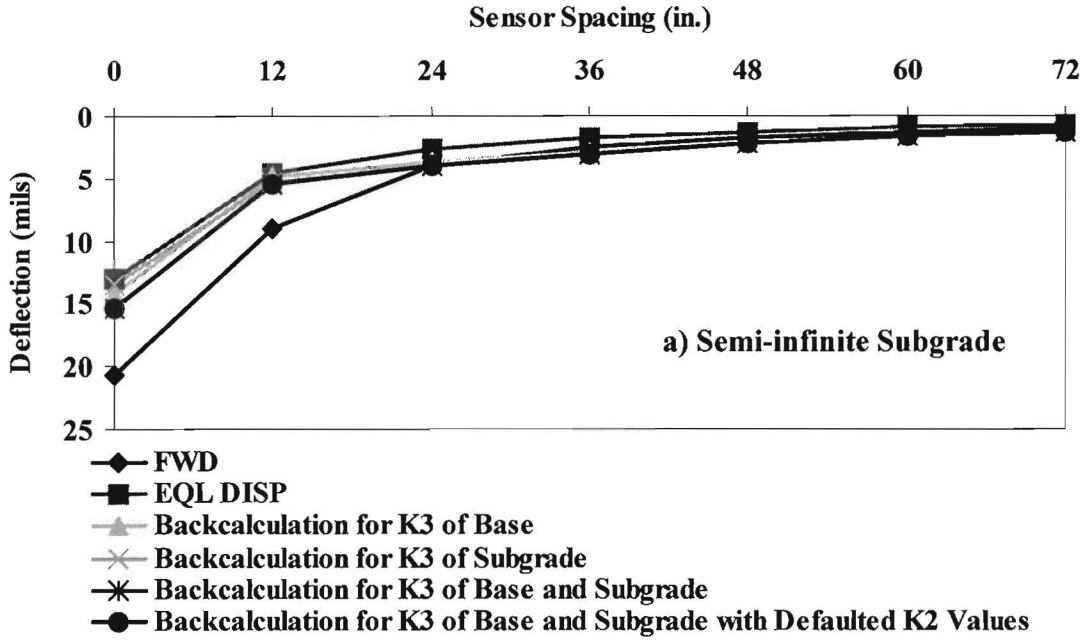

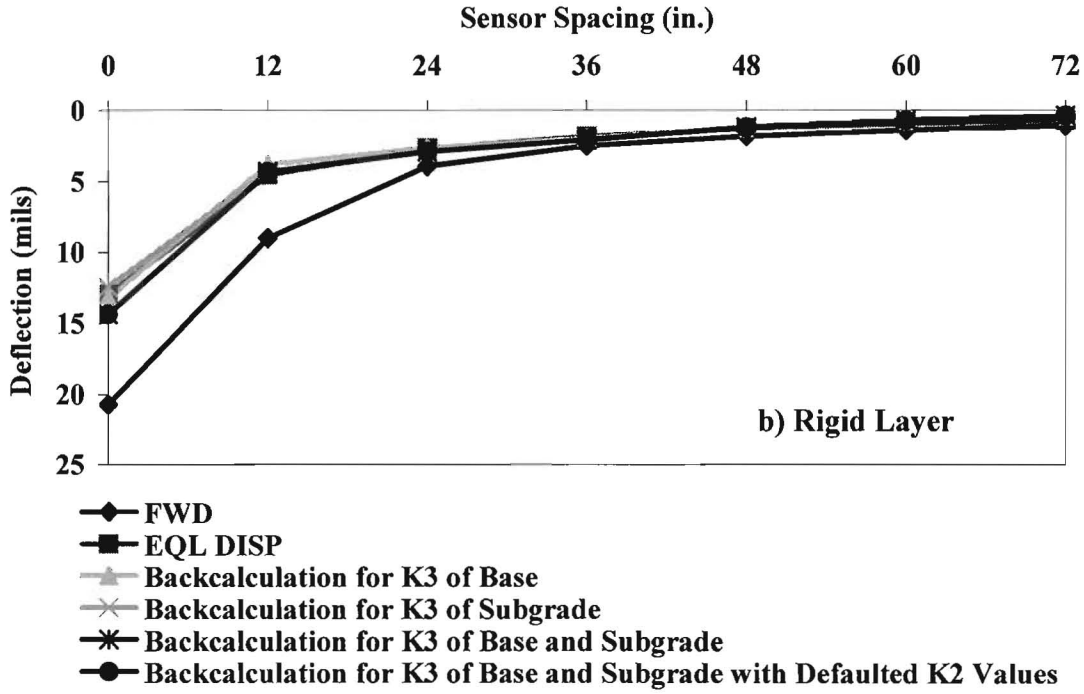

Figure G7 – Comparison of Deflections Calculated Based on Estimation of Non-linear Parameters and FWD Deflections for MLK

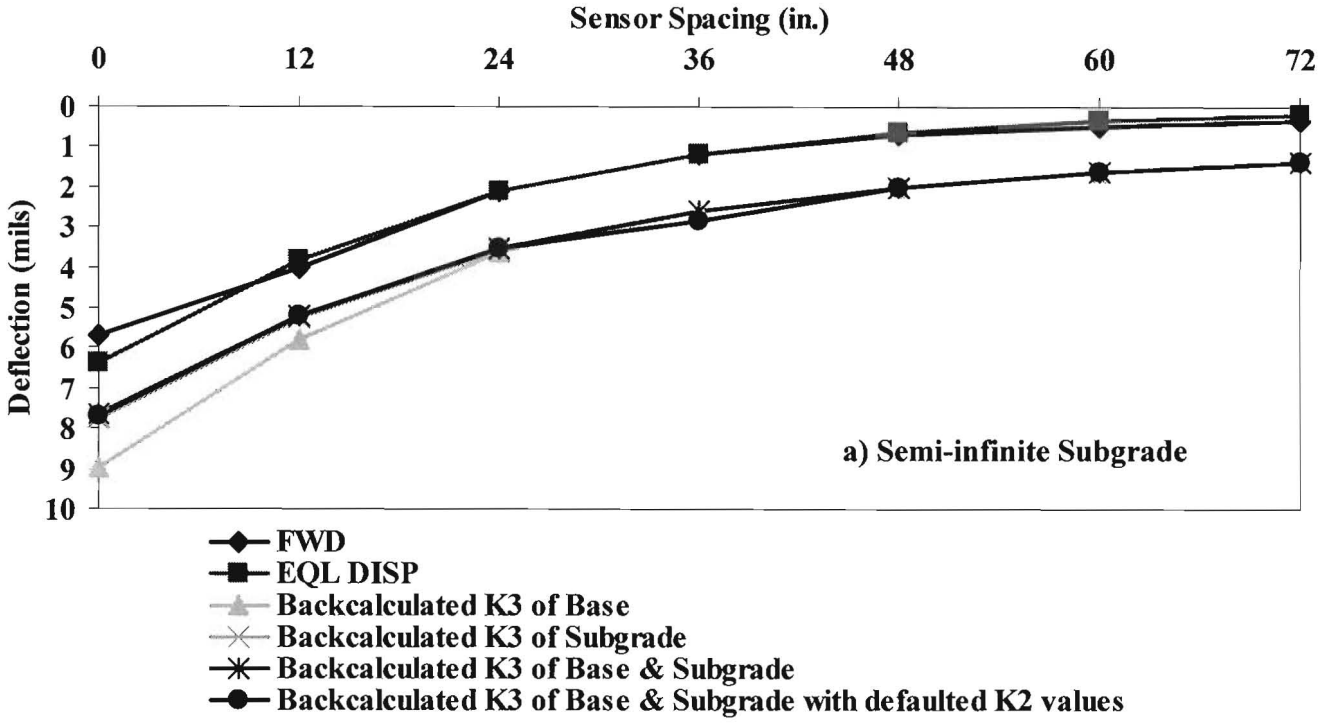

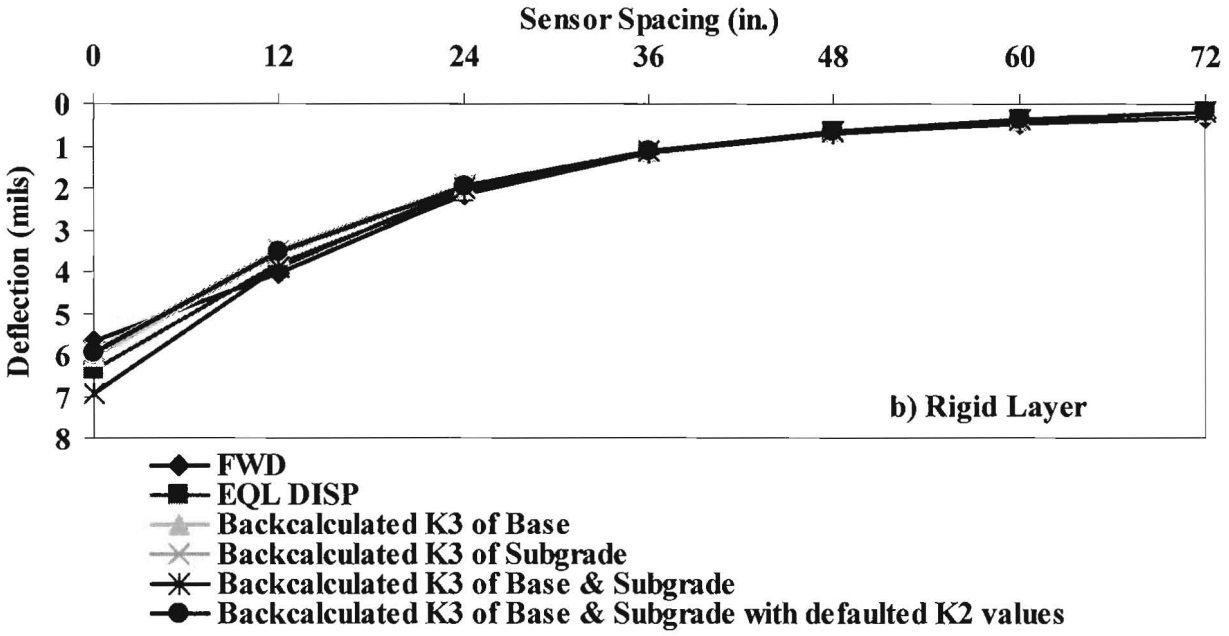

Figure G8 – Comparison of Deflections Calculated Based on Estimation of Non-linear Parameters and FWD Deflections for IH 20

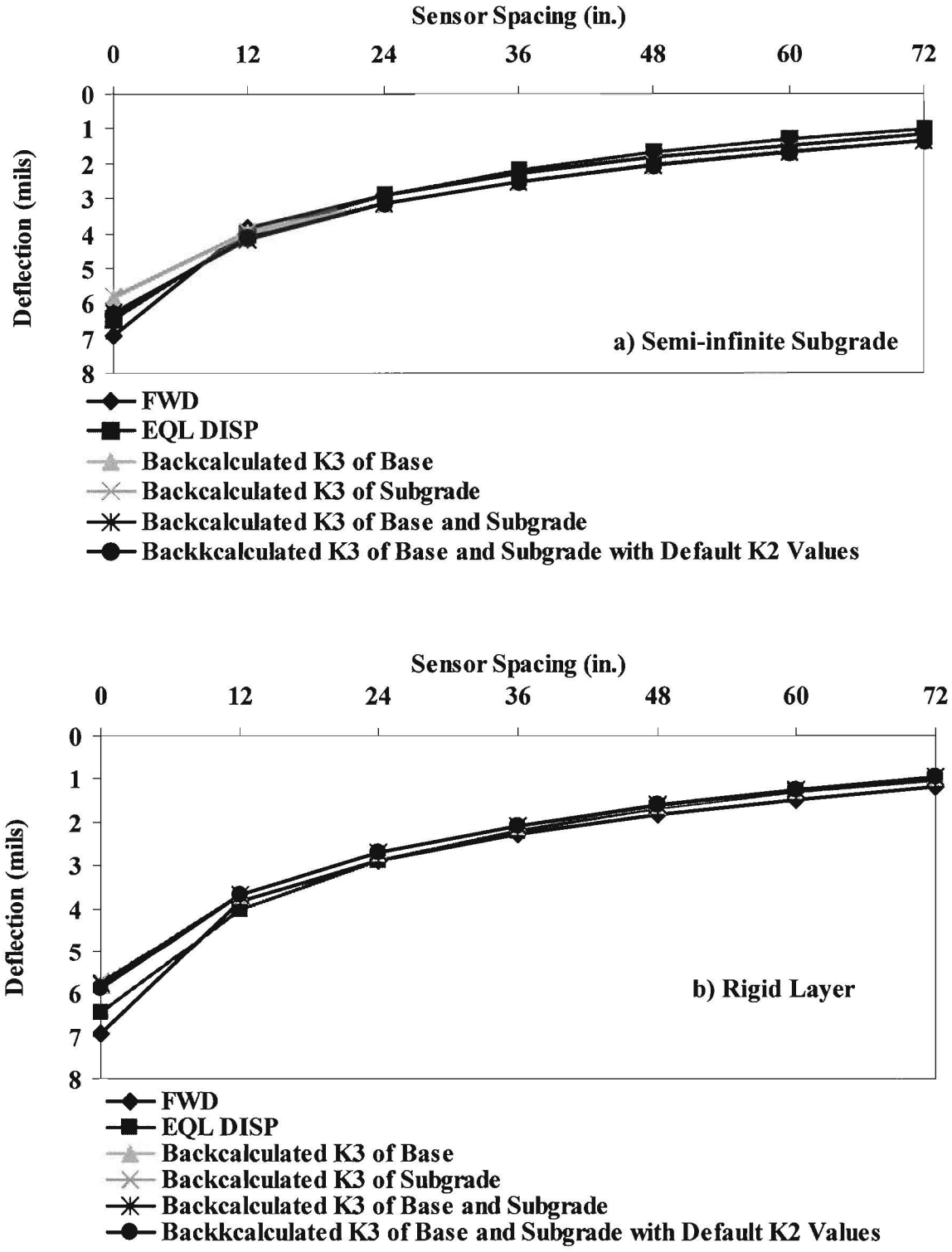

Figure G9 – Comparison of Deflections Calculated Based on Estimation of Non-linear Parameters and FWD Deflections for FM 933

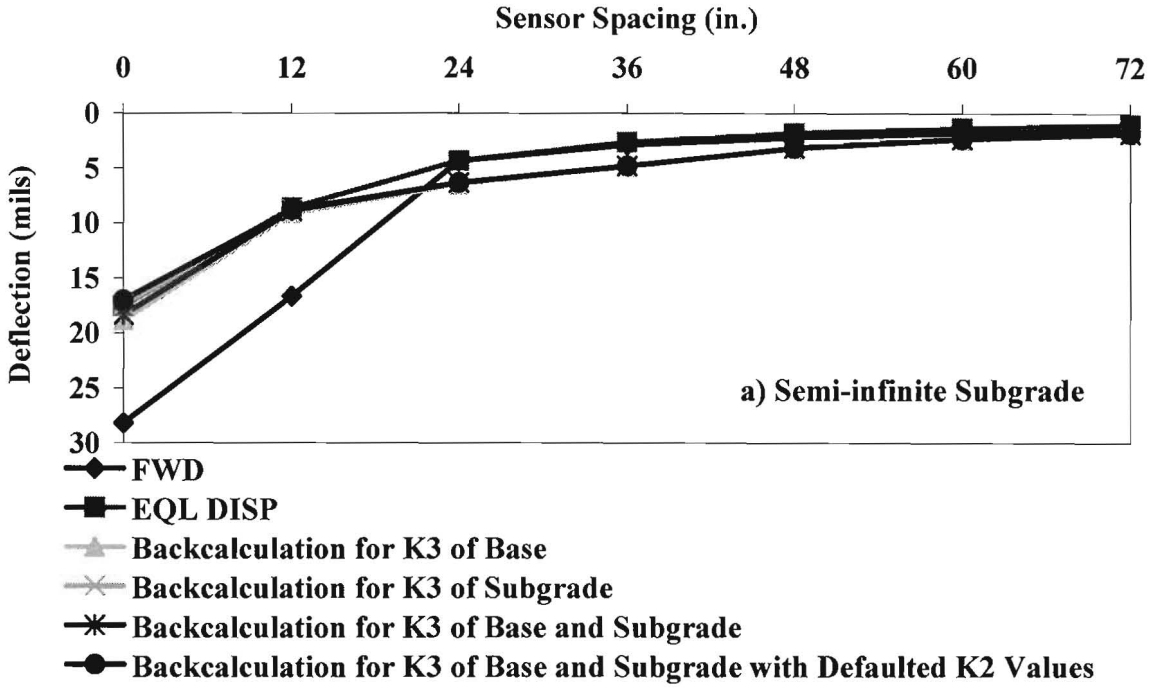

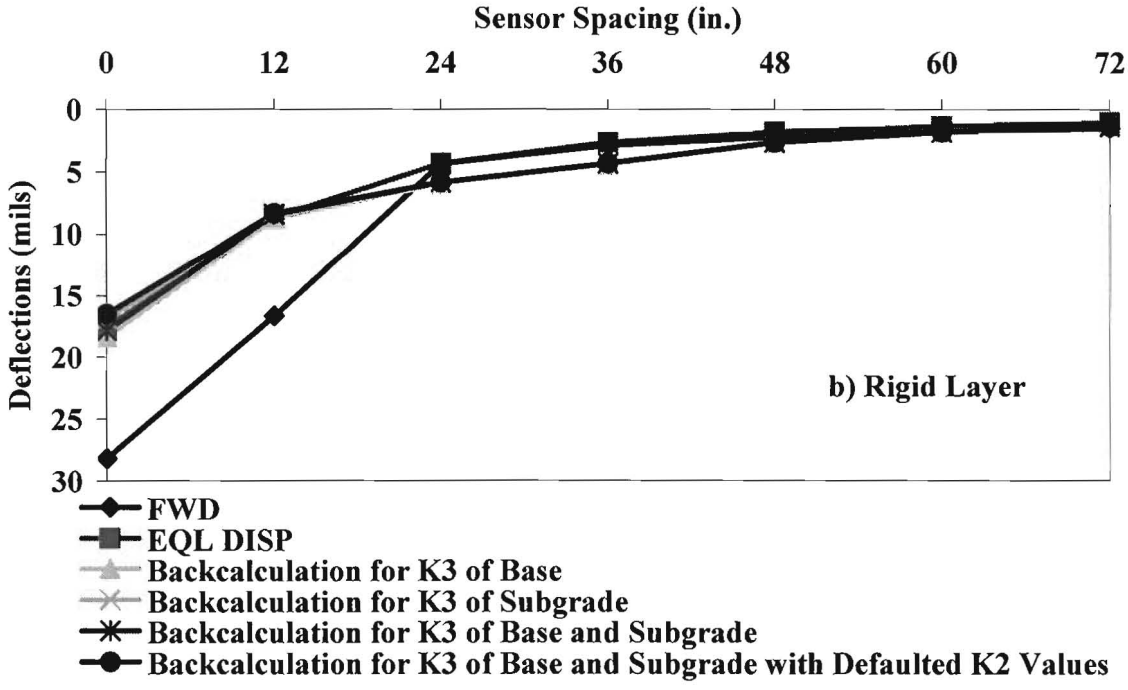

Figure G10 – Comparison of Deflections Calculated Based on Estimation of Non-linear Parameters and FWD Deflections for FSR Item 5

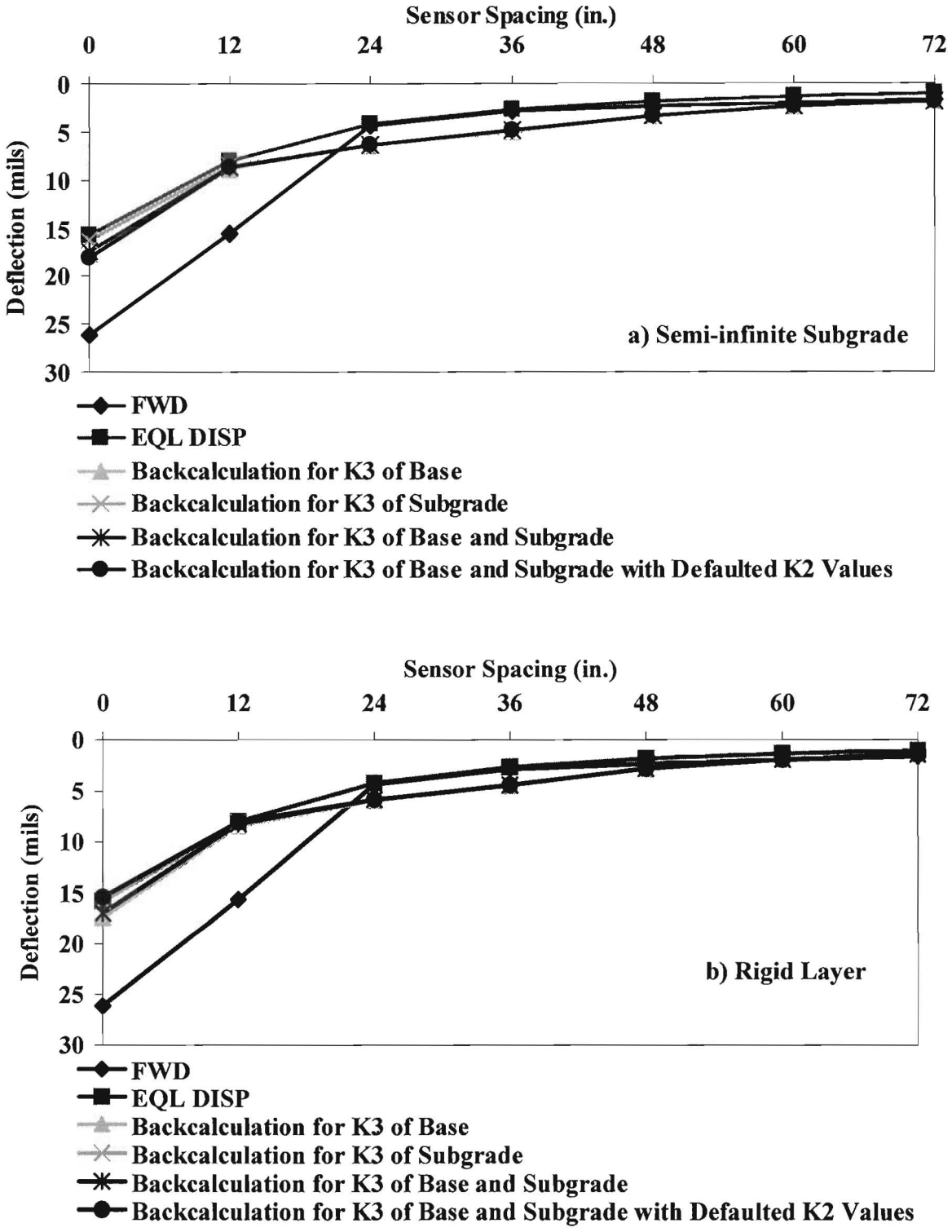

Figure G11 – Comparison of Deflections Calculated Based on Estimation of Non-linear Parameters and FWD Deflections for FSR Item 6

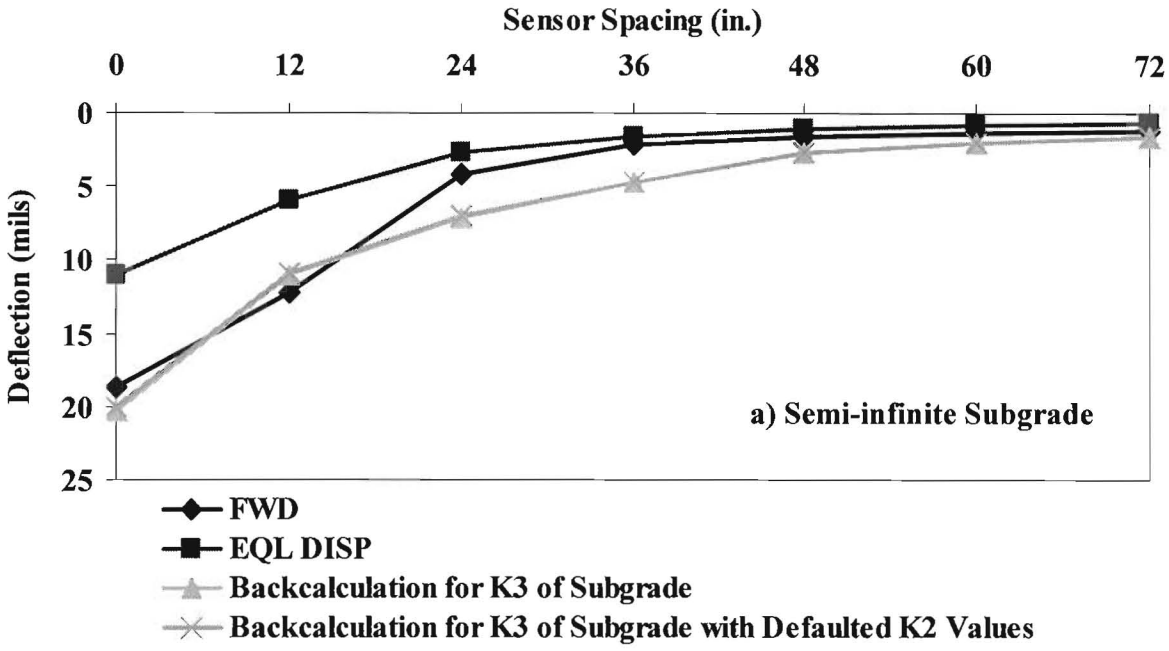

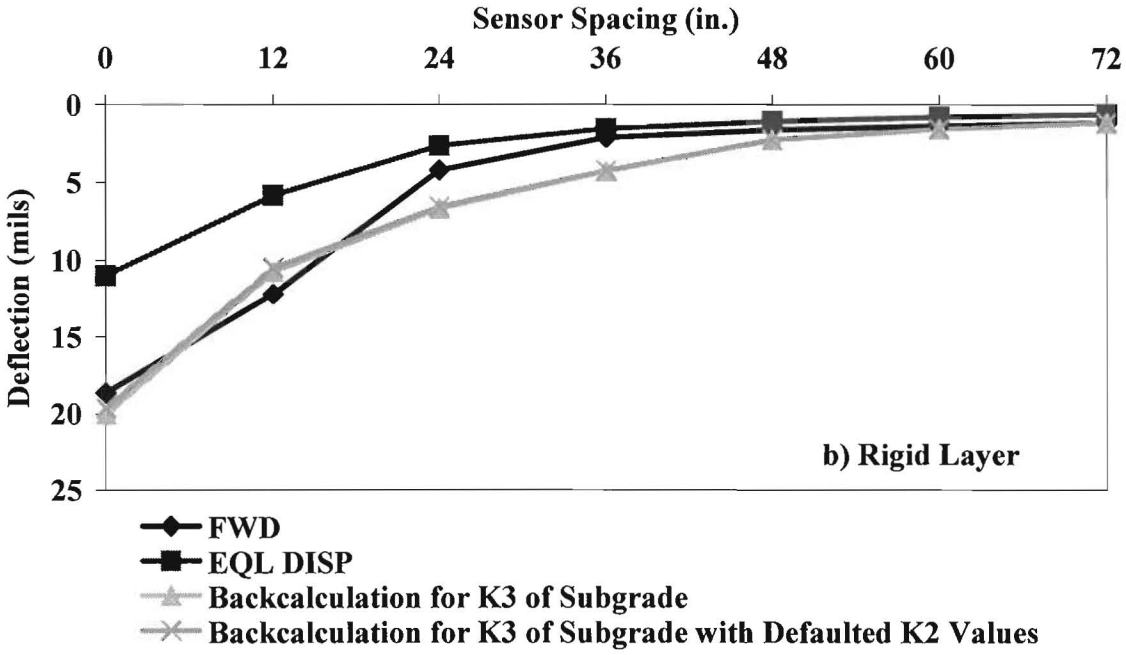

Figure G12 – Comparison of Deflections Calculated Based on Estimation of Non-linear Parameters and FWD Deflections for FSR Item 7

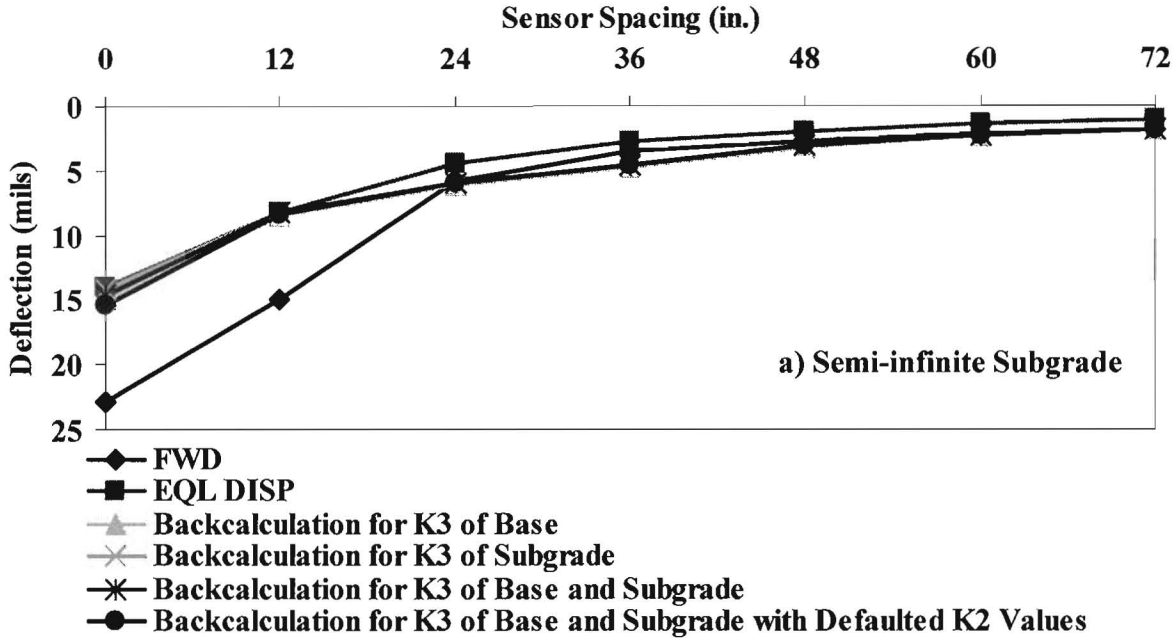

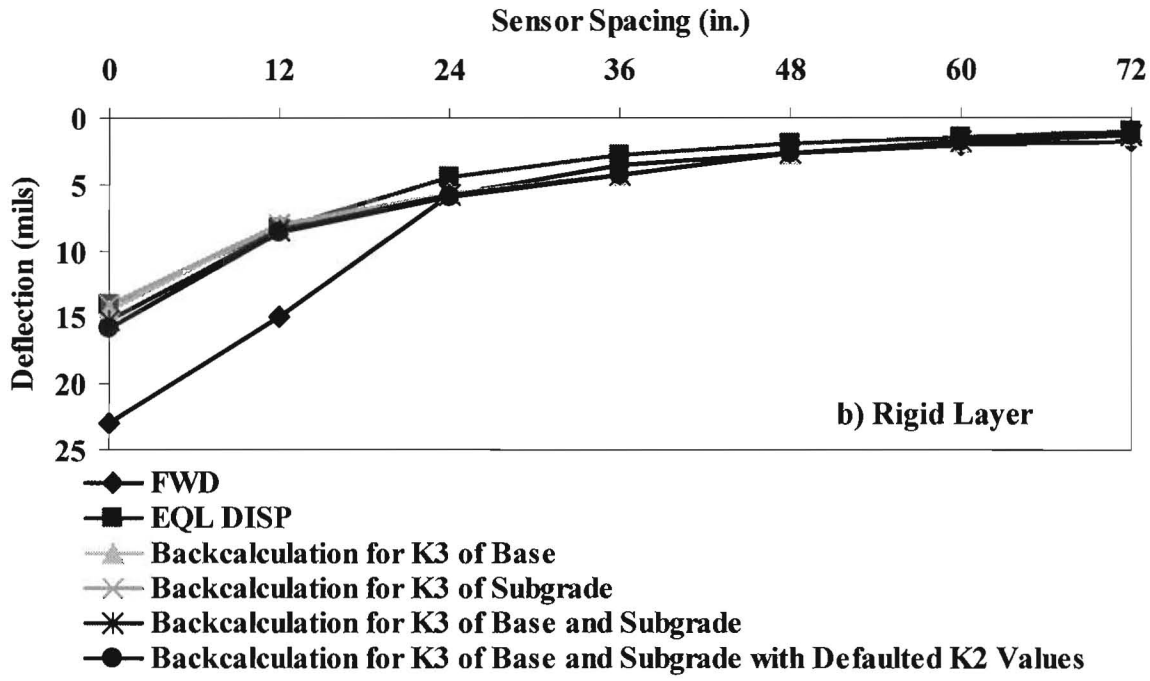

Figure G13 – Comparison of Deflections Calculated Based on Estimation of Non-linear Parameters and FWD Deflections for FSR Item 8

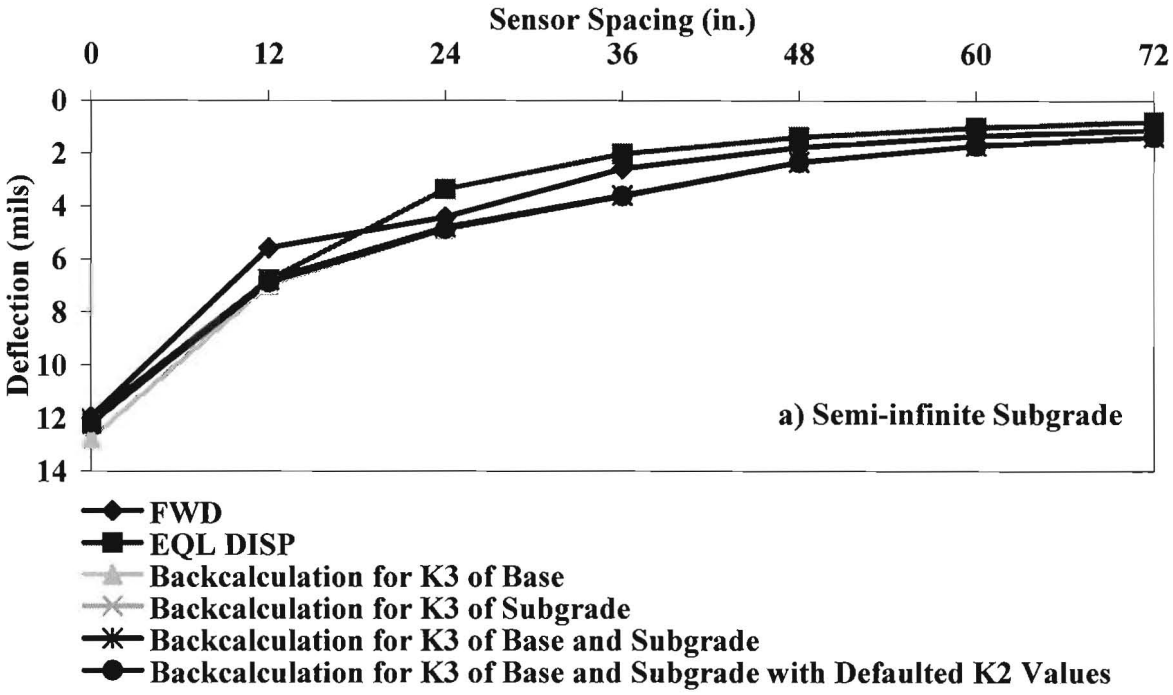

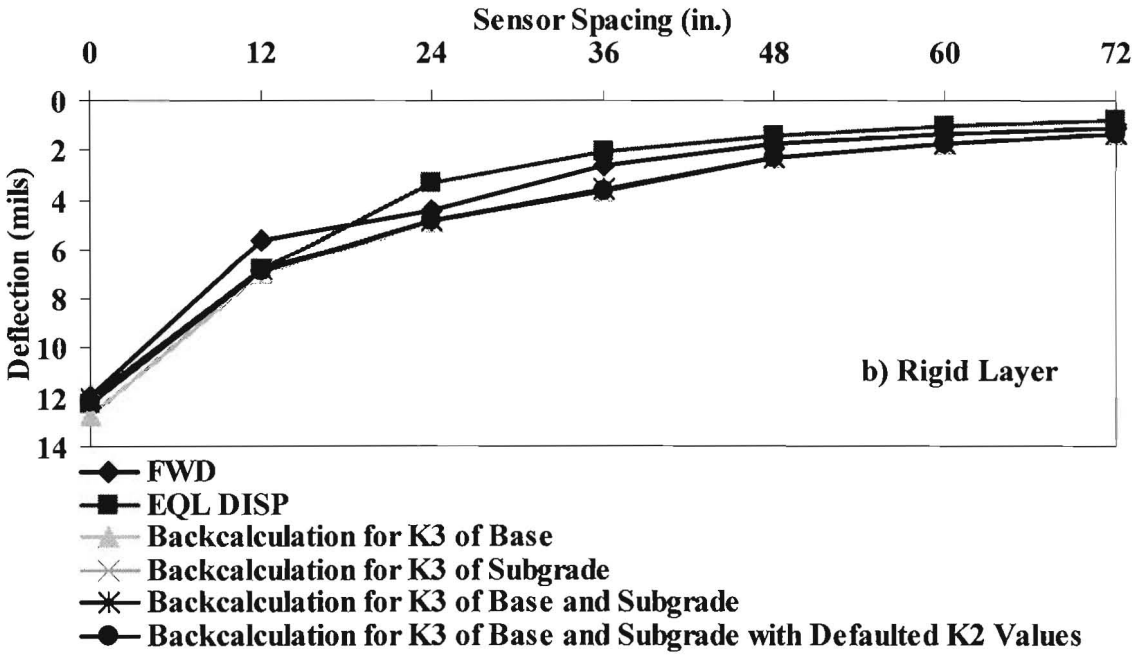

Figure G14 – Comparison of Deflections Calculated Based on Estimation of Non-linear Parameters and FWD Deflections for FSR Item 9

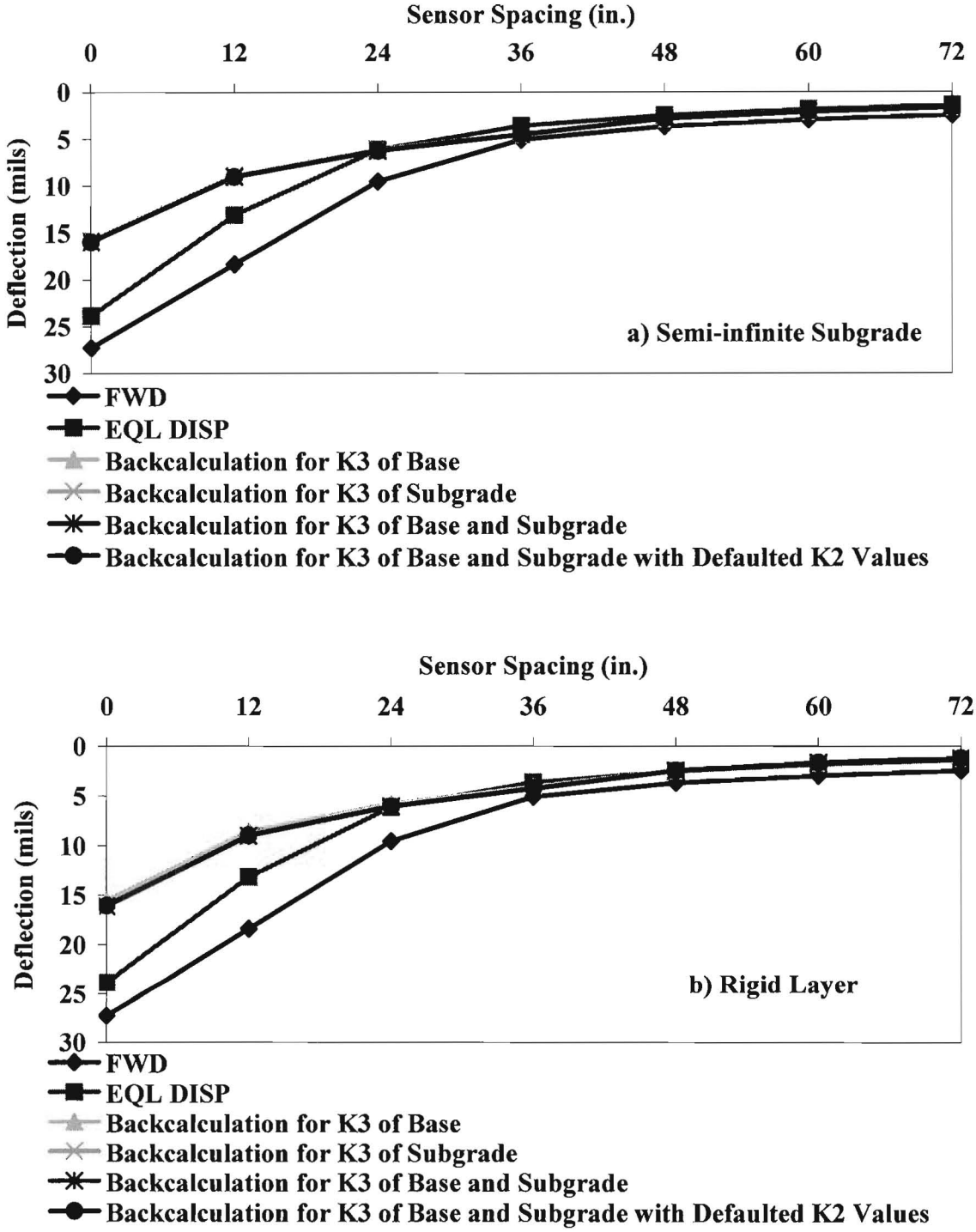

Figure G15 – Comparison of Deflections Calculated Based on Estimation of Non-linear Parameters and FWD Deflections for FSR Item 10

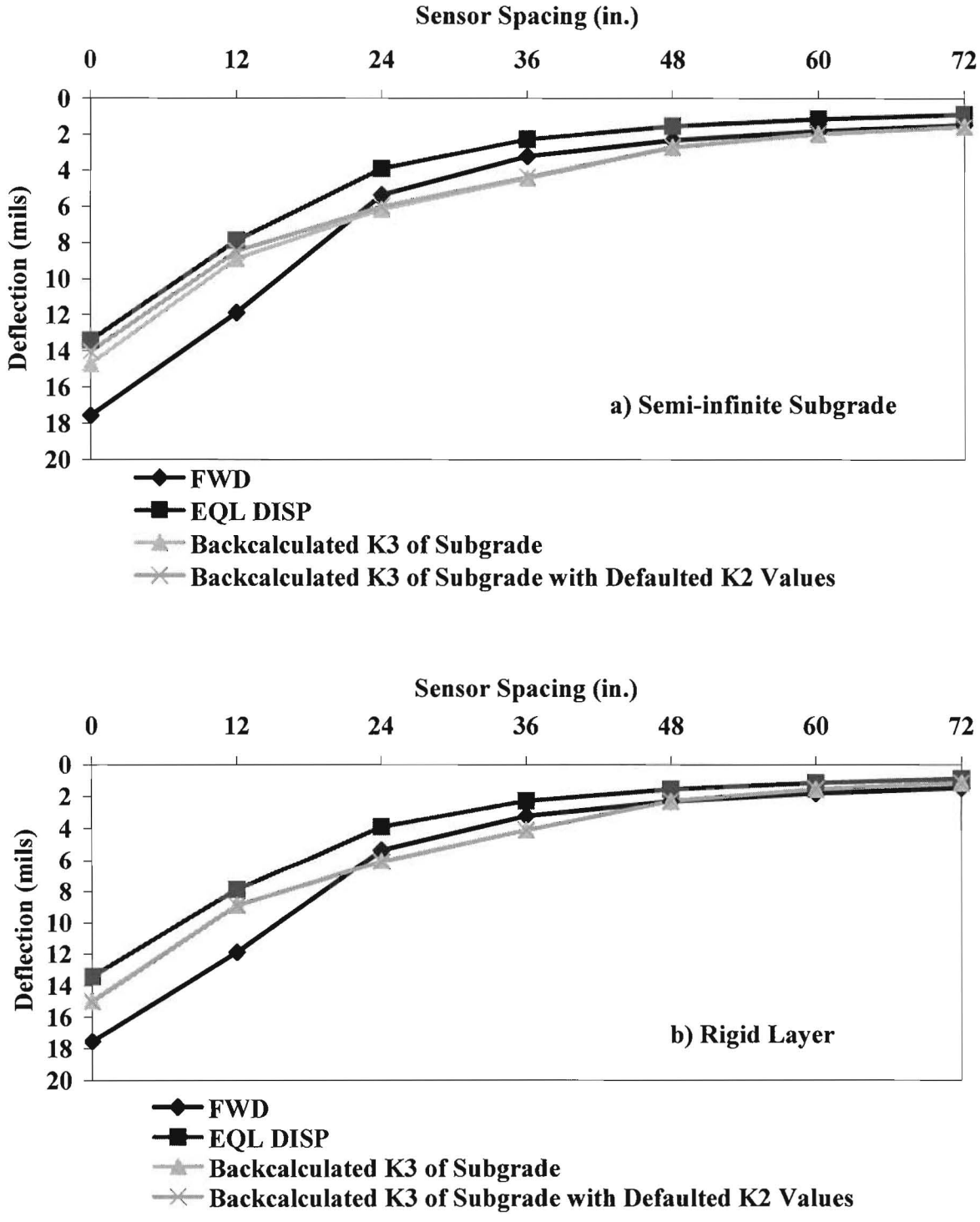

Figure G16 – Comparison of Deflections Calculated Based on Estimation of Non-linear Parameters and FWD Deflections for FSR Item 11

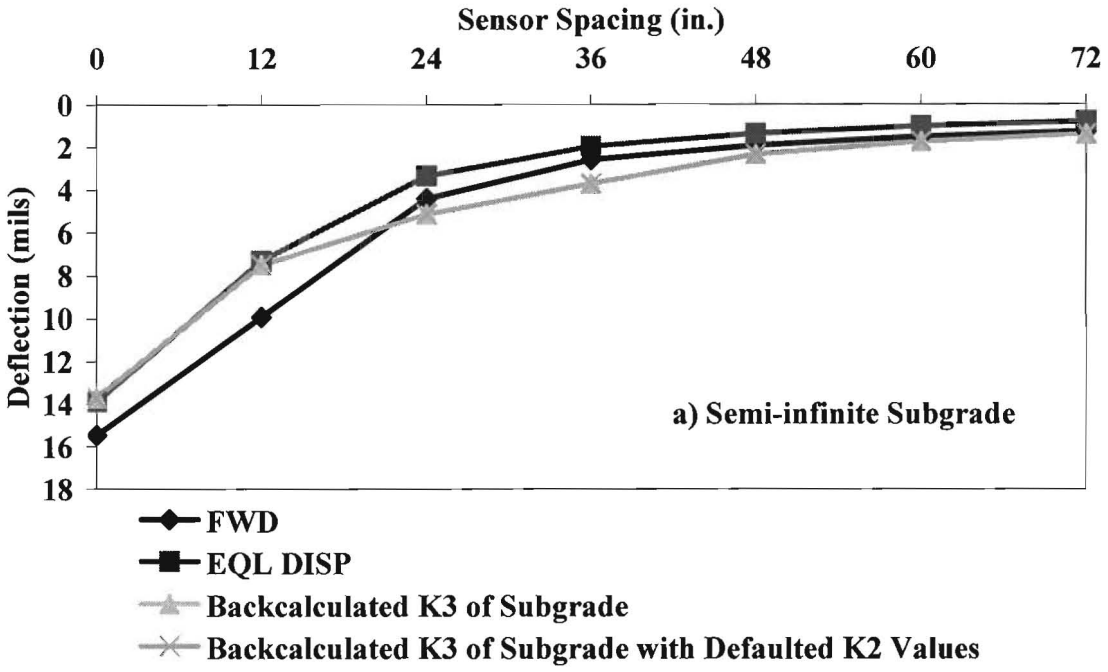

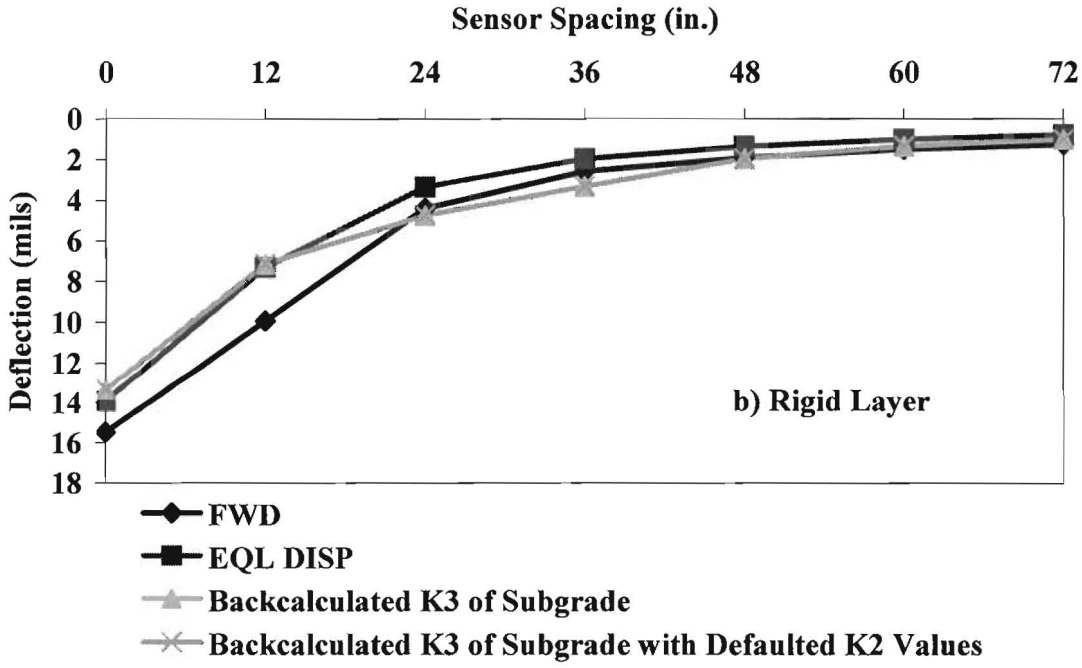

Figure G17 – Comparison of Deflections Calculated Based on Estimation of Non-linear Parameters and FWD Deflections for FSR Item 12

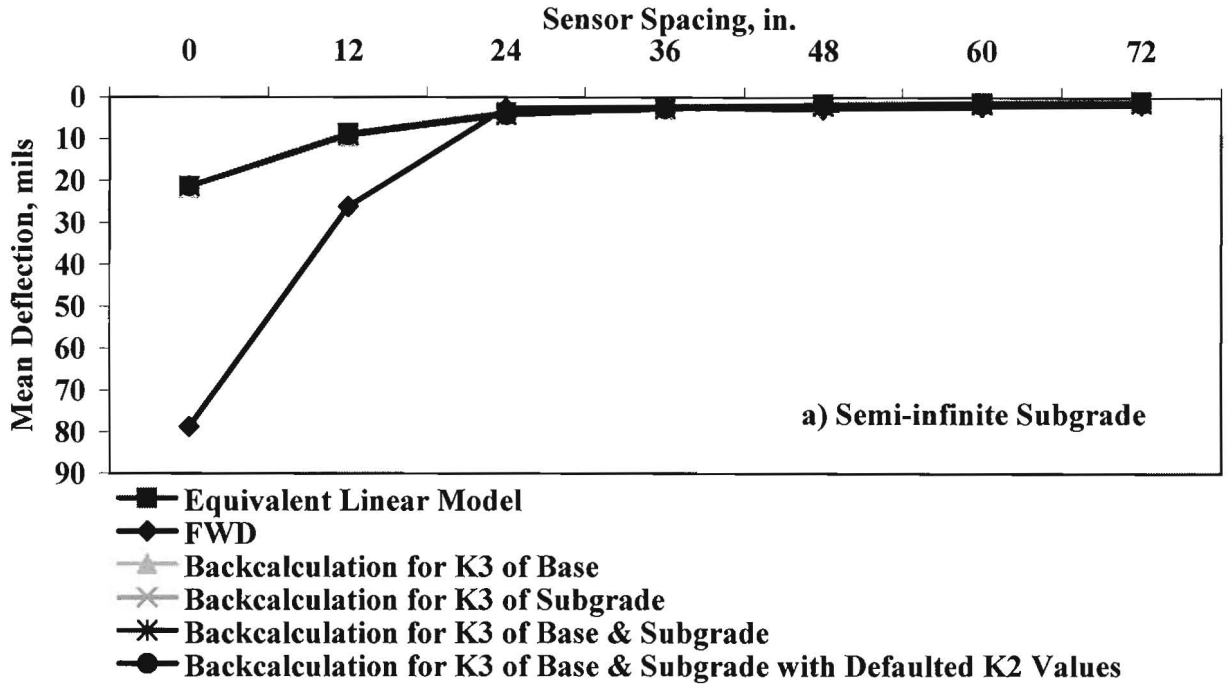

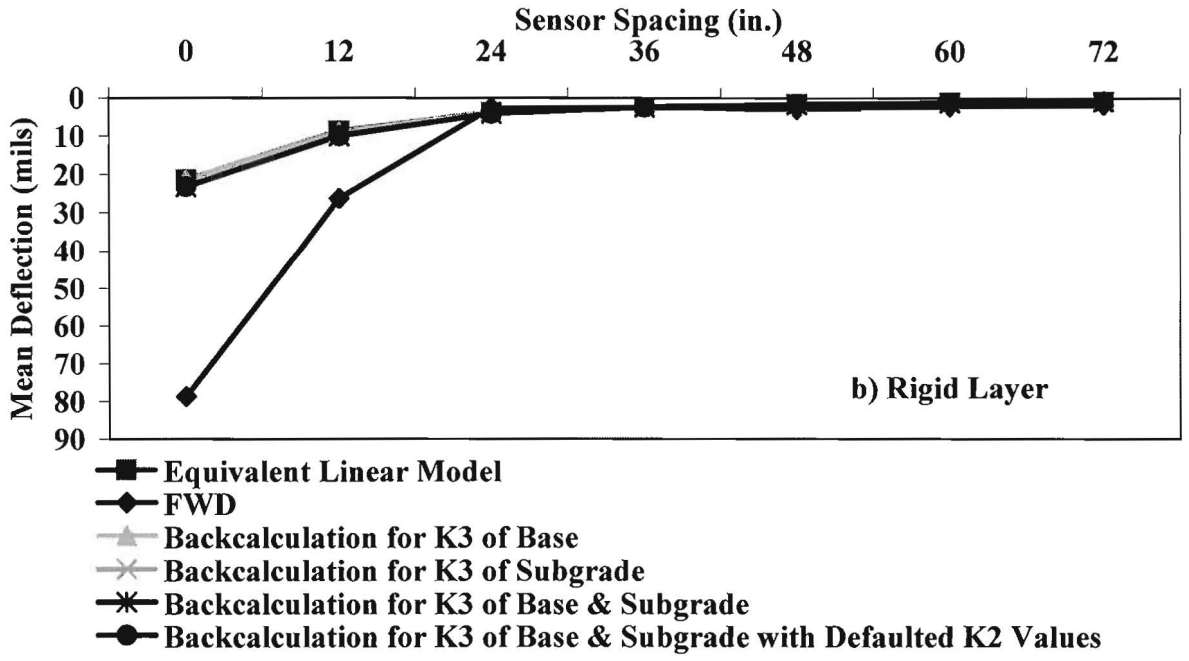

Figure G18 – Comparison of Deflections Calculated Based on Estimation of Non-linear Parameters and FWD Deflections for Hangar 4